OXAZOLOPYRIDINES TOWARDS THE TREATMENT OF HUMAN AFRICAN SLEEPING SICKNESS

Basmah Almohaywi

A thesis submitted in total fulfillment of the requirement degree of Master of Science

November 2014

School of Chemistry

University of Tasmania

“The first thing you have to know is yourself. Someone who knows himself can step outside himself and watch his own reactions like an observer.”
— Adam Smith

DECLARATION

This Thesis entitled “Oxazolopyridine towards the treatment of Human African sleeping sickness” is a piece of original work and contains no material that has, to the best of my knowledge, been previously submitted for a degree or diploma in any university, nor does contain material published or written by another person, except where due reference is made. I certify that every effort has been made to acknowledge previously published material. Diagrams from electronic resources have been referenced.

Basmah Mohammed Khelewi

November 2014

Copyright declaration

This thesis may be made available for loan. Copying of any part of this thesis is prohibited for two years from the date this statement was signed; after that time limited copying and communication is permitted in accordance with the Copyright Act 1968.

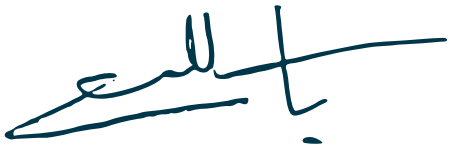

Basmah Almohaywi

November 2014

Abstract

This thesis describes the synthesis and structure activity relationship (SAR) of oxazolopyridine and related analogues against *Trypanosoma brucei*, the causative agent of Human African Trypanosomiasis, a neglected, fatal parasitic disease that is a major cause of death and disability affecting many sub-Saharan African countries.

Collaborators at Monash Institute of Pharmaceutical Science (MIPs), and ESKITIS institute found eight compounds as potential candidates *via* high throughput screening (HTS) of a large library of compounds against the disease. Amongst the compounds screened, an oxazolo[4,5-*b*]pyridine compound was of particular interest. In collaboration with MIPS, this work aimed to modify certain regions of the lead compounds and to develop a SAR against *T. brucei*, aiming for the synthesis of better analogues of the lead compound, as discussed in Chapter 2 and Chapter 3. A number of compounds have been made through modification around the central phenyl ring and the heterocyclic oxazolopyridine core. Modification at the central phenyl ring revealed the intolerance of that position for substitution, while the best compounds remained either the lead compound itself or its analogues, with the chlorine being replaced by either a hydrogen or substituting the 2-furyl amide for its 3-furyl counterpart. Modification of the heterocyclic core has resulted in a number of active compounds. We suggested that the modification and substitutions on oxazolopyridine core is more favourable for better activity.

In addition to the anti-trypanosomal activities, these compounds are similar to heterocyclic amine derivatives found in cooked meat and fish, which has the potential to cause cancer. This has prompted us to investigate the potential for DNA damage activity of these compounds and the amine precursors, as discussed in Chapter 4.

Acknowledgements

First and foremost I would like to thank the best main supervisor in the whole world, Dr Jason Smith, for his guidance and never-ending generous support, and patience during this degree. I also thank my co-supervisor A/prof A/Prof Michael Gardiner. I also would like to thank my previous supervisors Christian Narckowicz and Chris Hyland for their guidance and support.

Thanks to everyone, current and previous students, in "Jason's lab" for your advice and support.

Also thanks to everyone else in Chemistry, in particular to A/Prof Noel Davis and our beloved laboratory manager Murray Frith.

From my deep heart I thank my parents, my sibling and my husband, without whom I wouldn't be inspired, and for their endless support, patience and caring.

A Big thanks to my ever-best friends, Aliaa Shallan and Hajerr Al-shaman, whom I have shared gossip, laughter and tears with during my study at UTAS.

Abbreviation

DMF Dimethyl formamide

DMAP Dimethylaminopyridine

DNDi Drugs for Neglected Diseases initiative

HTS High throughput screening

MS Mass spectrometry

NMR Nuclear Magnetic resonance

PPA Polyphosphoric acid

SAR Structure activity relationship

EDCI 1-ethyl-3-(3-dimethylaminopropyl) carbodiimide

T. Brucei *Trypanosoma brucei*

TLC Thin layer chromatography

Author's Contribution

As part of this thesis, the author contributed to the synthesis and structural characterisation to library of compounds. These compounds were synthesised by the author and were sent to collaborators in Professor Jonathan Baell's group (Monash University) to add to a larger library where the screening against *T. brucei* were conducted at the ESKITIS institute at Griffith University. These compounds and their hetrocyclic-amine precursors were also assessed for DNA damage activity, by Associate Professor Nuri Guven (Pharmacy School at UTAS).

Publication (Co-author)

Ferrins, L.; Rahmani, R.; Sykes, M. L.; Jones, A.; Avery, V. M.; Teston, E.; Almohaywi, B.; Yin, J.; Smith, J.; Hyland, C.; White, K. L.; Ryan, E.; AU - Campbell, M.; Charman, S. A.; Kaiser, M.; Baell, J. B., 3-(Oxazolo[4,5-*b*]pyridin-2-yl)anilides as a novel class of potent inhibitors for the kinetoplastid Trypanosoma brucei, the causative agent for human African trypanosomiasis. *European Journal of Medicinal Chemistry* **2013**, (http://dx.doi.org/10.1016/j.ejmech.2013.05.007) [1].

TABLE OF CONTENT

CHAPTER 1 – Insights towards the treatment of Human African Trypanosomiasis

1.1 Background of Human African Trypanosoma (HAT) and current treatment

Tropical diseases are especially endemic among low-income populations in the developing regions of Africa, Asia and the Americas, resulting in mass mortality and devastating economic consequences. Such diseases are also often neglected by the major pharmaceutical companies despite their significant global impact, where the world's poorest populations have been primarily and disproportionately neglected [2]. It is often accepted that the process of drug development is no simple task, being costly and time-consuming. Therefore, pharmaceutical companies tend to invest their money in viable target markets for diseases that would recoup their investments [3]. This is frequently the case with less prevalent diseases that are more widespread in the developed world of Europe and North America, which demonstrate that the matter is largely economic [2].

Over the past few years, interest in neglected diseases has been revived by the emerging support and funding from major philanthropy sources and focused-support from some pharmaceutical industries, including the Institute for One World Health (iOWH), Gates Foundations, Wellcome Trust, and the Sandler Family supporting foundation, World Health Organisation (WHO) and the Drugs for Neglected Diseases Initiatives (DNDi), the last two having embarked on the provision of financial support [2].

Diseases associated with parasitic infections that are caused by the so-called tritryps (three common protozoan) are among the most important diseases invading poorer regions as problematic as malaria, which is caused by *plasmodium* species (Table 1, [2]). These three protozoan pathogens belong to the family of Trypanosomatidae and the genus *Trypanosoma*: *Leishmania major*, which is responsible for leishmaniasis; *Trypanosoma brucei* (*T. brucei*), responsible for African trypanosomiasis (African sleeping sickness); and *Trypanosoma Cruzi* (*T. cruzi*), responsible for Chagas disease (American trypanosomiasis) [4].

Table 1. Selection of neglected diseases with high prevalence impact

Disease	Organism	Scope of infection	Treatment Needs
Malaria	Plasmodium spp.	500 million	Circumvent resistance to medications
Leishmaniasis	Leishmania spp.	2 million	Be Safe, orally bioavailable, particularly for the visceral form
Trypanosomiasis	T. brucei (Sleeping sickness) T. cruzi (chagas disease)	HAT: According to WHO, 30 000 cases have been currently estimated and 7 million people are at risk[5]. Chagas: 16 million existing cases of infections[2]	Be safe and orally bioavailable particularly for the chronic stages

Human African trypanosomiasis (HAT), or sleeping sickness is a fatal neglected disease that is a major cause of death and disability and is endemic over 10 million square kilometres of sub-Saharan Africa (around 36 countries are affected) [5]. It is estimated by the World Health Organisation that 7 million people are at risk as well as

all livestock, with tens of thousands of new cases reported every year. The disease is caused by two subspecies recognised as causing infection in humans [6].

These are *Trypanosoma brucei rhodesiense* (*T.b. rhodesience*), responsible for East African sleeping sickness and *Trypanosoma brucei gambiense*, responsible for West African sleeping sickness. *T.b. rhodesience* has the ability to protect itself from lysis (destruction of cells by lysins antibodies) by the immune system's defences due to its expression of lytic resistance associated genes. *T.b. gambience* is also protected from the host owing to resistance to the trypanosome lytic factor, which is present in human serum [7].

Other subspecies of trypanosomes are *trypanosoma brucei brucei (T.b. brucei), trypanosoma brucei golense (T.b. golense)* and *trypanosoma brucei evansi (T.b. evansi)*, which are responsible for infection to domestic and wild animals but do not harm humans [7] due to their inability to survive under the human immune system as maintained by the presence of trypanosome lytic factors in human serum. However, there have been reports of humans being infected with *T.b. brucei* [6].

The disease is transmitted to humans and animals *via* the bite of the bloodsucking tsetse fly, host of any of these parasite subspecies. Of the two types of the disease, East African HAT tends to develop more rapidly, leading to acute infection and lasting less than six months from the indication of symptoms to death, while the West African disease progresses slowly, leading to chronic infection followed by death in 1-5 years [5,6].

T. brucei replicates in the blood, leading to the observed early haemolymphatic stage of disease involving fever, headache, weight loss, vomiting and malaise [7]. Ultimately these parasites migrate to the central nervous system in the later stages, associated with a wide range of neurological features including neuropsychiatric, motor sleeping disorders, motor weakness, visual and sensory abnormalities. This breakdown of neurological function can lead to death if untreated [7].

1.2 Life cycle of parasites

The agent of HAT, the trypanosome, is transmitted by the Tstse fly, which has a cyclic life cycle (Figure 1) [8]. The parasite undergoes morphological and biochemical stages between vector insect and human host. When a blood meal from an infected host is taken by the tsetse fly, trypanosomes migrate through the blood stream into the stomach of the fly and procyclic trypomastigotes transformation occurs. These then migrate to the salivary glands (transformation called epimastigote) where they become infectious in the saliva [8]. When the fly subsequently bites human, metacyclic trypomastigotes are injected into the skin where they undergo differentiation process into the long-slender bloodstream form. This form of the parasite is entirely dependent on glycolysis for energy while harvesting glucose from an infected host. This process is then followed by extracellular multiplication in the bloodstream (at the bite site) followed by invasion of lymphatics of the new host [8]. There, the parasites are transformed into the stumpy, short and non-proliferating form, while limiting the number, prolonging the survival and increasing the risk of transmission of infection [8]. The cycle of the fly takes between 3-7 weeks, depending on the species type and environmental conditions, and each fly can inject up to 40000

metacyclic forms when feeding [8]. There are many reasons why HAT is a difficult disease to eradicate. Principally, African trypanosomes are capable of changing their surface coat proteins, known as variant surface glycoproteins (VSGs) [9].

Upon doing so, they can escape the host's immune system (i.e. the lytic factors and circulating antibodies in the host's plasma) in a very sophisticated process called antigenic variation [10]. Trypanosomes have two distinct life cycle stages: a) the infectious bloodstream form, where cells are extracellular and most vulnerable to the host's immune system and b) the insect procyclic form where cells are covered with a sheet of 10_7 VSG homodimers [9]. The parasites in the later stage are thereby protected from antigens produced by the host immune response, since they are able to switch between hundreds of antigenically diverse VSG coats. As a consequence this process render the host antibody-mediated lysis useless [9].

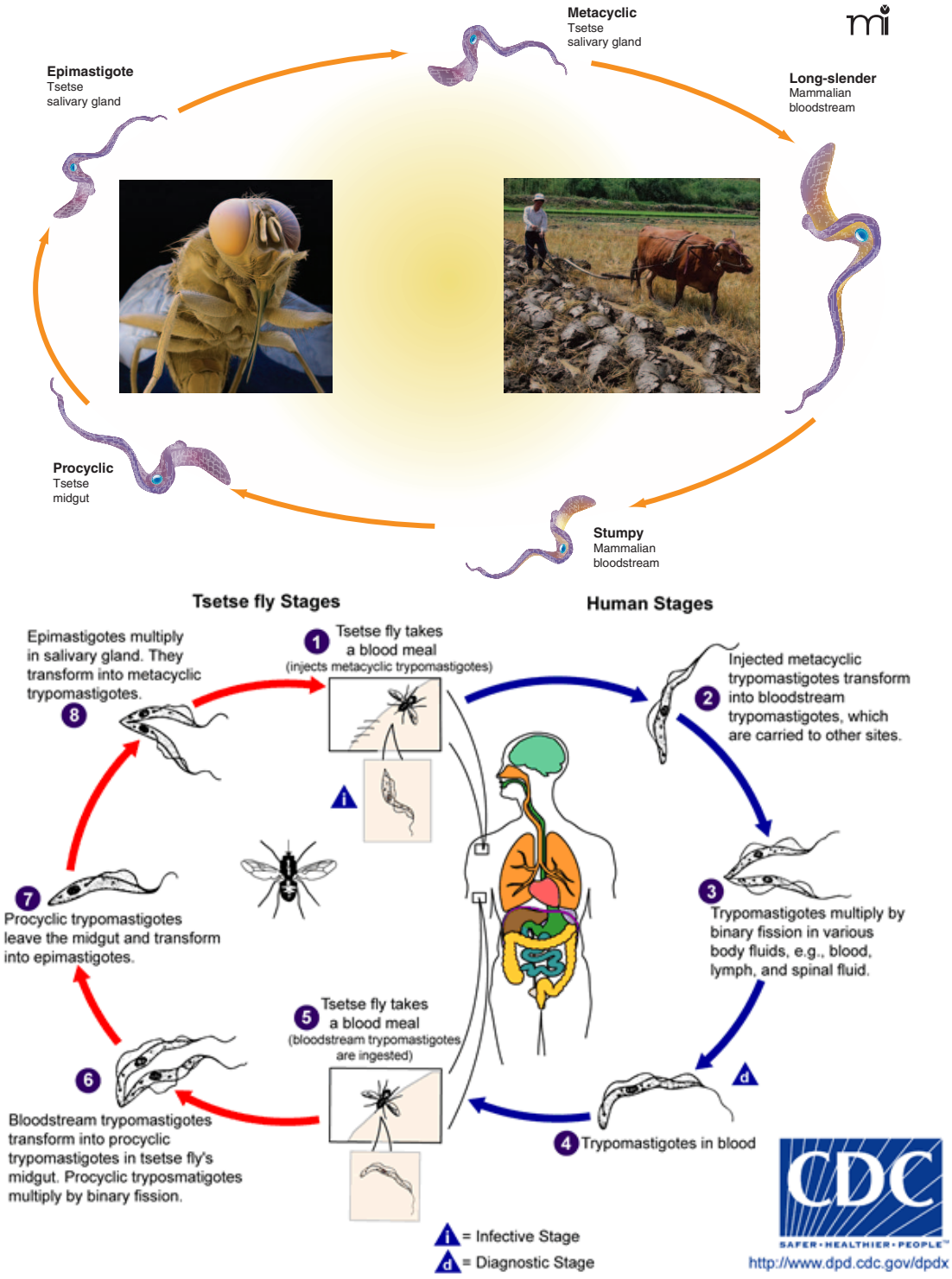

Figure 1 Top and bottom is a representation of Lifecycle of *T.brucei* [6].

.

Protective and preventive measures such as the use of insecticides, protective clothing and insect repellent can reduce the incidence of this disease. However, HAT also infects hosts apart from humans, and even the most successful and sophisticated insect irradiation (method for biological control and sterilisation by radiation) could not destroy all the parasites reservoirs [11]. The use of these measures may be effective for visitors to endemic regions but not for those living in the area. Therefore, for such individuals early diagnosis and drug therapy is the treatment approach [11] [12].

Conventional vaccines might not be effective for trypanosomes, but novel vaccines are being tested targeting VSGs [13]. Normal human serum contains apoliprotein L-21 (apoL-1) that lyses all African trypanosomes except those that causes HAT, for example, apoL-1 resistant *T. b. rhodesiense* [13]. This subspecies circumvents the human defense system through the expression of apoL-1 serum's resistant protein, and thus endowing these parasites with a superior ability to infect humans. The development of synthetic immunotoxin led to the synthesis of an engineered copy of apol-1 that lacks the protein's domain responsible for resistance. This new modified apol-1 was effective in eradicating *T. b. rhodesiense* acute infection. Although it was not completely curative for the chronic form of the infection [13].

1.3 Current medication for treatment of HAT

Despite the availability of certain drugs for the treatment of HAT (Figure 1), those on the market are confronted with issues including the potential for toxicity, limited effectiveness, difficult administration regimes and the need for hospitalisation [7] More problematic is the fact that four out of five of the key drugs are either

administered intramuscularly or intravenously. These non-oral forms of the drug administration are not only inconvenient but have resulted in poor patient compliance since most disease victims live in developing countries where medical access is either limited or difficult [12].

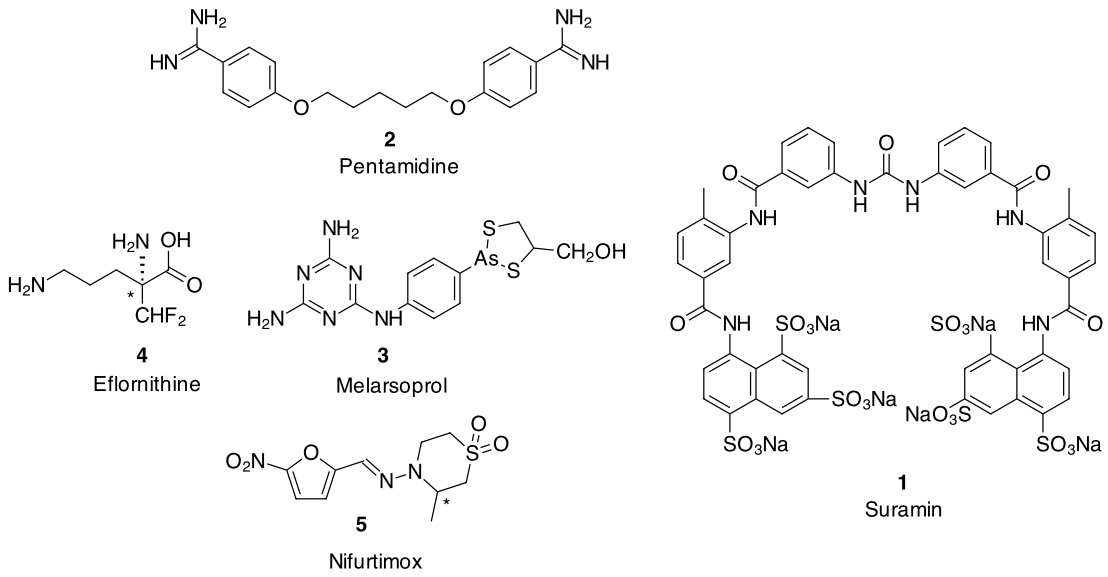

Figure 2. Clinical compounds for treatment of HAT

Treatment of early-stage HAT

Suramin

Suramin (Figure 2) is only used for the treatment of stage 1 HAT. It was first synthesised during German dye manufacturing as part of Ehrlich's work on the naphthalene-based dyes Trypan red and blue. The observation of the antitrypanosomal activity of those symmetrical dyes led to the development of suramin, which was introduced for the treatment of HAT in the 1920s [6] [5]. It is a large and highly-charged molecule at physiological pH, which consists of a urea group with poly-sulfonated naphthylamine and benzamide functions [6] .

Suramin binds with blood proteins, leading to its prolonged half-life and prophylactic activity. However, due to its highly charged nature, it does not penetrate the blood brain barrier (BBB) and hence is not used for cases where the disease has developed to a late stage [5].

In addition, suramin's ability to form complexes with serum proteins and LDLs retards its absorption from the gastric intestinal tract. As a result it is only administered as a series of five intravenous infusions within three weeks [7]. However, Suramin is also limited by its side effects, including nephrotoxicity, neuropathy, rash, fatigue and in some cases renal failure [6]. Furthermore, there have been reports of *T. brucei* developing resistance to suramin [6].

Pentamidine

Aromatic diamidines, a class to which pentamidine isothionate belongs, was synthesised in 1938 and displayed promising activity against HAT. It is effective when used prophylactically against *T.b. gambiense* (the causative agent of the West African sleeping sickness), including the hemolymphatic stage of the disease. Pentamidine was synthesised from work on synthalin, a medication used to control the blood sugar levels in the 1930s [5]. Since the 1940s, it has been given mainly for early-stage *T.b. gambiense* infection as intramuscular injections over 7-10 days, causing pain at the injection site. Evidence for clinical resistance to pentamidine is uncommon due to its long half-life and the presence of various uptake transporters in parasites, but most of the reported clinical failures arise from inaccurate dosing or the presence of CNS disease [5]. It is currently still used to treat patients with early-stage *T.b. gambiense*. Similar to suramin, it is not used for the late-stage owing to its

highly-charged nature at physiological pH, leading to slow diffusion rates across the biological membranes which prevent it from crossing BBB [6]. The exact mechanism of action of pentamidine and related compounds remain unclear but the available evidence indicates is they bind to DNA, particularly to extrachromosomal DNA found in the kinetoplasts of the organism, thereby inhibiting replication of the kinetoplast DNA. At high concentration, they can impair oxygen consumption. Inhibitory activity may also depend on the uptake rate of the parasite to pentamidine and whether innate or acquired resistance arises from altered transport [14]. However, its administration (intramuscularly or slow intravenous infusion) remains an issue, requiring medical supervision. Moreover, toxicity and adverse effects including diabetes mellitus, hypotension and nephrotoxicity are other major issues that limit the use of pentamidine [7].

Treatment of the late-stage HAT

Melarsoprol

In the mid 1940s, Ernst Feiedheim began a project on organic arsenic-based compounds at the Rockefeller University. In 1947 he introduced melarsoprol, 'a melanophenyl-based aresenical' compound (Figure 2) and commenced clinical trials on patients with late-stage West African trypanosomiasis [5]. At the time, Patients were successfully treated for late stage CNS of HAT using melarsoprol which remains the first choice medication for such patients [6]. However, toxicity has been of concern, especially with the occurrence of post-treatment reactive encephalopathy (PTRE) in about one-fifth of patients on the medication, while about 5% die from complications of PTRE [5]. Melarsoprol is given by intravenous injection, which is

also painful and patients also develop vein thrombophlebitis and atrophy, which is common with melarsprol administration [5].

Eflornithin (difluromethylornithine)

Eflornithin is a known inhibitor of ornithine decarboxylase and was initially developed as an antitumor agent but failed clinical trials [5]. It was licenced for clinical use in the CNS stage of HAT 23 years ago, and it was considered to be the first treatment for late stage *trypanosomal* infection in forty years. However, clinical use of eflornithin suffers from a difficult therapeutic regimen of four intravenous-injections daily over two weeks, as a result of its short half-life. Furthermore, it is not effective for treatment of patients with *T.b. rhodesiense* [5].

Nifurtimox-eflornithine combination therapy

The latest clinical use of eflornithin is accompanied by nifurtimox, a nitroimidazole compound used in relapsed diseases. This led to the development of a composite regimen containing a combination of eflornithin, in a reduced dose of s 200 mg/kg in slow intravenous infusions twice daily for one week, and nifurtimox (15 mg/kg/day) taken orally every eight hours for ten days [15]. This therapy is 96 % curative with fewer adverse effects and is now the standard clinical therapy. The main advantage of this regimen is the reduction of eflornithin intravenous from four daily doses for two weeks to two doses a day once weekly [15]. Although the doses have been reduced this is still perceived as a serious issue due to problematic conditions in rural areas where patients require a clinical setting, dose monitoring and supervision in hospitals, which often lack modern medical equipment [7].

1.4 Current research towards the discovery of new treatment for HAT

As evident in the preceding discussion, a number of serious considerations surround the use of these medications. Fortunately, over the last decades, the need for new drug candidates for neglected tropical diseases including HAT has been recognised, and there is a renewed interest in the current environment, given the establishment of private-public partnerships including Drugs for Neglected Diseases Initiative and philanthropic support such as Bill and Melinda Gates foundations [5].

Approaches toward the discovery of new treatments for HAT are diverse, including the design and synthesis of new derivatives based on a well-known drugs (e.g. analogues to pentamidine), targeting metabolic pathways (e.g. glycolysis) and high throughout screening of compound libraries. The following section discusses new discoveries and the resurgence in the investigation of novel treatments over the last 20 years.

1.4.1 Amidine compounds

Pentamidine-based derivative

Diamidines, analogues of pentamidine, are one of the most widely explored classes of compounds found to inhibit *T. brucei* spp. The mechanism of action is unclear but their anti-parasitic action may be partly due to their ability to bind strongly to AT-rich sequences in the minor groove of DNA, which has evolved as a useful target for the design of new anti-parasitic agents [16]. As a result of the binding of amidine compounds with DNA, it is suggested that this event eventually triggers the inhibition of one or more of a number of DNA-dependent enzymes such as topoisomerases and nucleases or leads to direct inhibition of transcription [16].

Aromatic diamidines have been extensively studied for half a century. However, only pentamidine has been broadly used clinically in humans, despite unfavorable side effects [16]. Nevertheless, the high flexibility nature renders it a suitable molecule for further medicinal chemistry investigations. In this regard, with the intention to improve efficacy and reduce unwanted side effects associated with pentamidine use, several independent research groups have carried out the design and synthesis of newer analogues of pentamidine with similar or enhanced pharmacological activity [17,18]. For instance, Tidwell RR and co-workers [17] have synthesised and studied the SAR of many structurally-related analogues of pentamidine. They have used a number of strategies for modification including the introduction of substituents on the amidine moiety, varying the position from *para*- to *meta-substitution*, varying the length of the aliphatic chain in the middle of two aromatic moieties and introducing substituents on the aromatic groups at *ortho* or *meta* positions (some of these examples are shown in Figure 3). They have also made some analogues, which replace the oxygen atom in the alkyl linker with the isosteric sulfur or nitrogen counterparts (Figure 3). However, only a few compounds demonstrated activity similar or superior to pentamidine and/or melarsoprol.

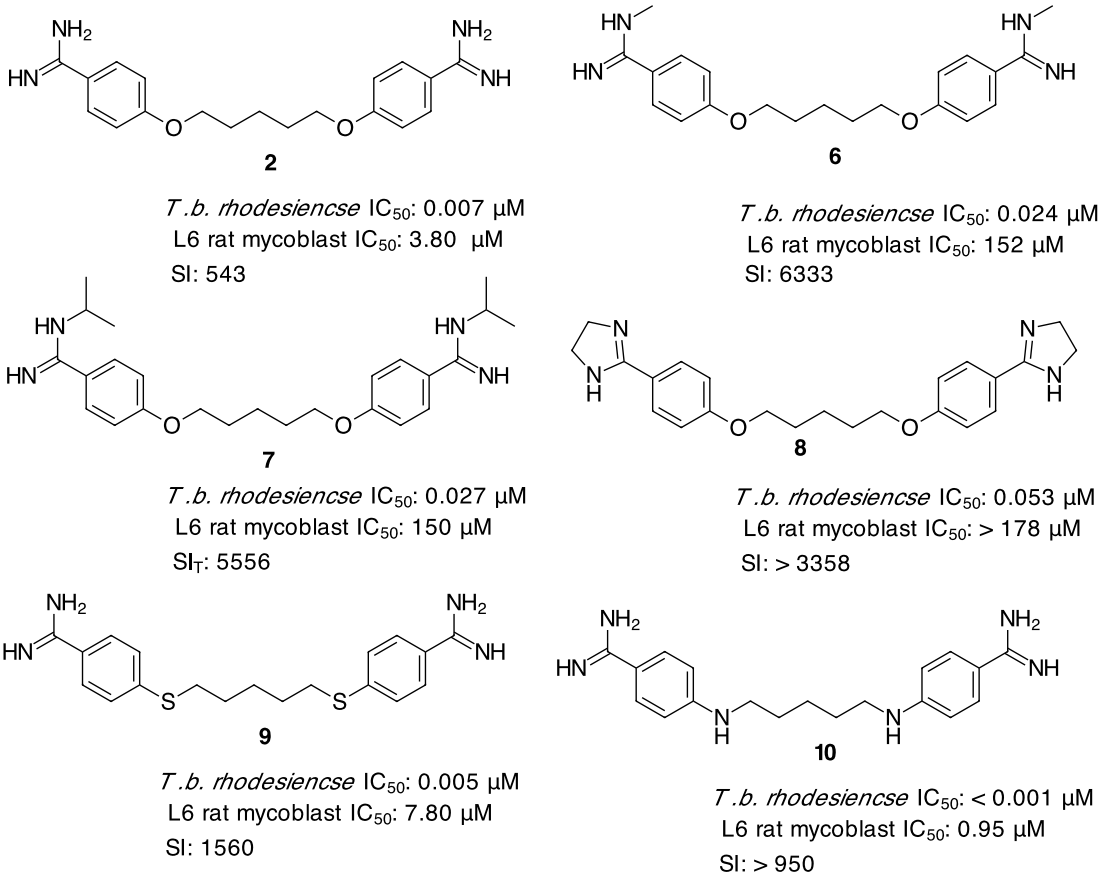

Figure 3. The effect of amidine nature on the activity of pentamidine.

Earlier work by the same group found that the nature of the amidine group is critical for *in-vitro* activity against *T.b. rhodesiences* where the mono-substituted amidine moiety, as in pentamidine, is the best in the series (Figure 3). In contrast, the *N*-alkylation of the amidine moiety as in compound **6**, **7** and the imidazoline **8** resulted in less activity against *T.b. rhodesience*, although these compounds were less cytotoxic compared to pentamidine **2**, with high selectivity to *T.b. rhodesience*. The oxygen in the carbon linker was described as important for recognition of the P2 transporter (in the trypanosoma species) of pentamidine, and thus they suggested that substitution of oxygen for other isosteric atoms might optimise the activity.

For example, the Tidwell group [17] found that the presence of sulfur and a secondary amino group (Figure 3) in place of the oxygen atom (in the carbon linker chain) led to compounds **9** and **10** with higher antitrypanosomal activity with an IC_{50} of 0.005 µM and 0.001 against *T. b. rhodesiense* and a selectivity profile almost twice that of pentamidine. However, these compounds were even more cytotoxic than pentamidine [17].

Tidwell also investigated the presence of pyridine analogues as in Figure 4 finding that compound **11** inhibits *T.b rhodesience* at 0.019 µM and is less cytotoxic, with the advantage of being highly selective over mammalian cells amongst other screened compounds in the series. In contrast, compound **12** with the NH group of analogue **11** replaced by an oxygen atom was more active against the same parasite in *in-vitro* testing, but was much more cytotoxic (4.90 µM) and less selective relative to **11** [19].

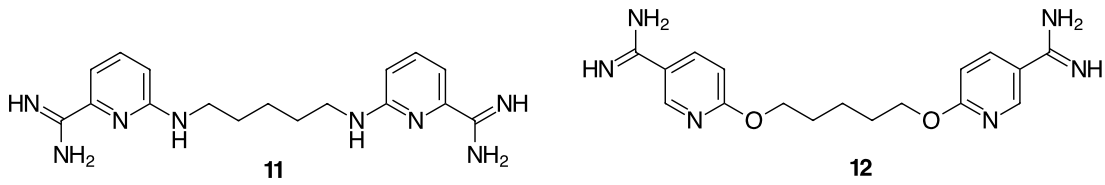

T.b. rhodesiencse IC_{50}: 0.019 µM
L6 rat mycoblast IC_{50}: 114 µM
SI: 6000

T.b. rhodesiencse IC_{50}: 0.001 µM
L6 rat mycoblast IC_{50}: 4.90 µM
SI: 4900

Figure 4. Pyridyl analogous of pentamidine

Furamidine compounds

There are a number of recently developed amidine agents based on pentamidines which have either been entered or are remain under assessment for entry into clinical trials [6]. In the 1980s, furamidine **13,** DB75 (Figure 5) was initially identified as part of the US-government's anti-trypanosomal screening campaign, but was terminated

from further clinical trials because it displayed fewer clinical benefits compared to pentamidine [6]. With the finding of 2,5-bis[4-(*N*-methoxy)amidinophenyl]furan (pafuramidine), the methoxy prodrug of furmamidine **(13)**, or the so-called pafuramidine **(14)**, was considered to have clinical benefits superior to pentamidine, and was successfully progressed to clinical trials. Pafuramidine **(14)** was also progressed into phase 3 clinical trials for treatment of first-stage HAT but this was halted after evidence of nephrotoxicity and hepatotoxicity [20].

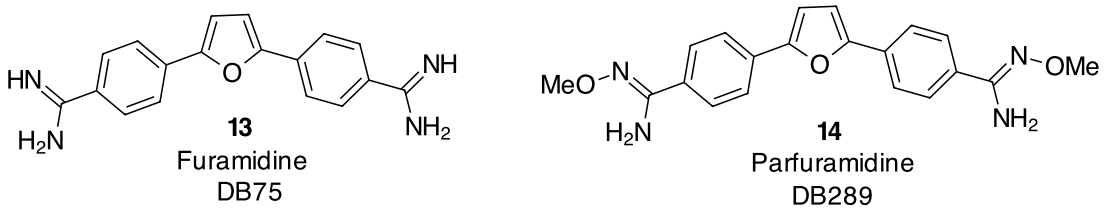

Figure 5. Recent diamidine compounds developed for treatment of HAT

Although furamidine, pafuramidine and related derivatives from earlier work have resulted in interesting activity, none of these series of compounds has been suitable for clinical studies into stage 2 of HAT [12], presumably due to the cationic nature of the amidine group at physiological pH that leads to poor membrane permeability and limited access to the CNS [21]. As explained earlier, oral administration is generally the preferred dosing regimen for treatment of HAT as recommended by Drug for Neglected Diseases Initiative. However, amidine compounds including pentamidine, furamidine and their analogues do not fit these criteria due to their lack of oral bioavailability [16]. Further to this, several analogues of furamidine exhibit interesting activity on intravenous dosing regimens but are not effective when given orally. Hence, to encourage oral administration, a prodrug strategy has been implemented for

these compounds (aza analogues) in order to overcome their limited oral bioavailability [16].

Aza analogues and prodrugs initiatives of furamidine

To accomplish this goal, a series of aza analogues of **(15-20)** (Figure 6), exemplified by furamidine **(15),** and its prodrug **(16),** and DB820 **(17)** with its prodrug DB844 **(18)** have been assessed for their activity against CNS stage 2 HAT. Compound **15** has poor oral bioavailability, but its further structural development led to synthesis of its prodrug DB868 **(16)**, which demonstrated favourable potency and oral activity in a mouse model at the CNS stage compared to its parent molecule **15** [22]. Analogues DB1058 **(19)** and DB1284 **(20)**, also exhibited similar CNS activity in a GVR35 mouse model (that imitates the CNS inhabitant stage of HAT), of which can be considered for oral administration with the exception of DB829 **(15)**.

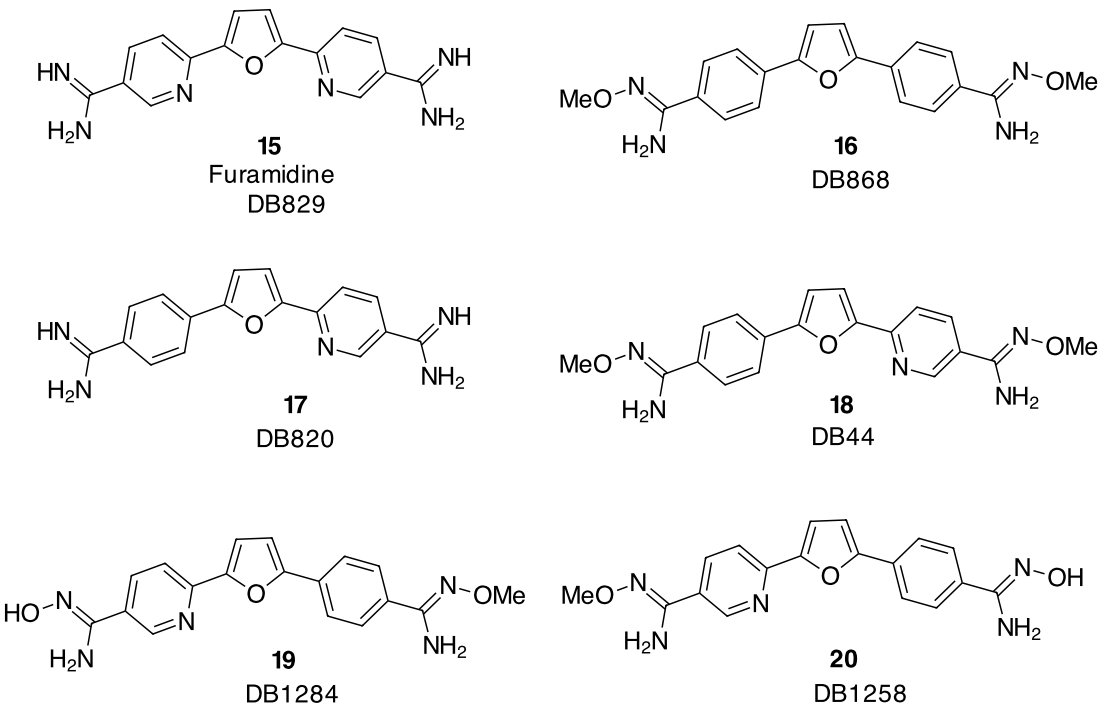

Figure 6. Diamidines compounds, analogues of pentamidine

In respect to both the *in-vitro* and *in-vivo* testing, DB868 **(16)** has been advanced into clinical trials. At present there appears to be a temporary delay in clinical trials due to renal toxicity, a concern that needs to be confirmed [6].

Despite this, furamidine has provided an interesting platform for further evaluation of other related analogues aiming for development of newer anti-trypanosomal analogous. One approach for development of newer analogues to furmaidine, was through replacement of the central furan ring with other isosteric heterocycles such as thiophene [23], isoxazole [24] and tetrazole [25], with some of these resulting motifs were resulted in better activity.

Dicationic isooxazole derivatives

Tidwell group has reported synthesis to a range of cationic diphenylisoxazole analogues of furamidine (Figure 7), where its central ring was substituted with an isoxazole and their activities were evaluated against *T.b. rhodesiense*. As a general trend in SAR, isoxazole compound **21** and **22** exhibited excellent *in-vitro* activity within the nanomolar range but **21** retained higher cytotoxicity to L6 mycoplast compared to **22**, although both had favorable solubility compared to their furamidine counterparts. Compound **21** was also selected for *in-vivo* testing. In the acute mouse model for stage 1 HAT. Compound **21** exhibited excellent curative potential (4/4 mice were cured) amongst the selected compounds using a dose of 1 mg/kg over 60 days of survival period. However, reduction of this dose schedule by half resulted in only one cured mouse under the same conditions [26].

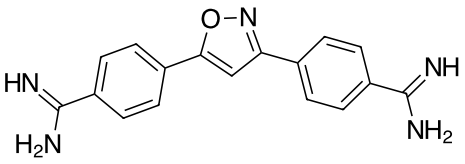

21

T.b. rhodesiense IC_{50}: 0.0051 µM
L6 rat mycoblast IC_{50}: 2.1 µM

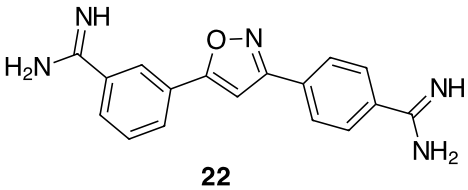

22

T.b. rhodesiense IC_{50}: 0.0035 µM
L6 rat mycoblast IC_{50}: 31.2 µM

Figure 7. dicationic isoxazol-based diamidine compounds

Triazole series of amidine compounds

Tidwell and co-workers [25] screened 60 diamidine analogues, for example compounds **23** and **24** (Figure 8), against *T.b. rhodesiense*, containing a 1,2,3-triazoles fragment as an isosteric replacement of the central furan ring system owing to its geometrical similarity to furamidine. Eight compounds were reported with antitrypanosomal activity, which was comparable to that of pentamidine and melarsoprol. However, compound **24** was the best in the series for both the *in-vitro* (IC_{50} 5 nM) and the *in-vivo* analysis (mice were cured at 1 mg/kg over four days by an i.p. dose regimen) [25].

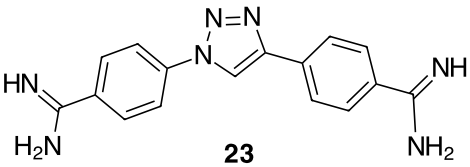

23

T.b. rhodesiense IC_{50}: 0.004 µM
L6 rat mycoblast IC_{50}: 8.10 µM

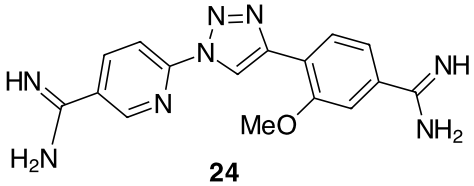

24

T.b. rhodesiense IC_{50}: 0.005 µM
L6 rat mycoblast IC_{50}: 164 µM

Figure 8. Dicationic triazole-based diamidine compounds

New generation of Benzyl phenyl ether amidine

A recent report by the Tidwell group [27] introduces a series of next generation benzyl phenyl ether-based amidine analogues which were evaluated for *T.b. rhodesience in-vitro* activities. Compounds **25** and **26** (Figure 9) were the most potent and selective in the series with an IC_{50} of 0.005 µM and 79 µM respectively. In the acute animal stage model of HAT, compound **26** (25 mg/kg, over four days of oral regimen) was reported to cure 4/4 mice within 60 days of the survival period subsequent to the infection.

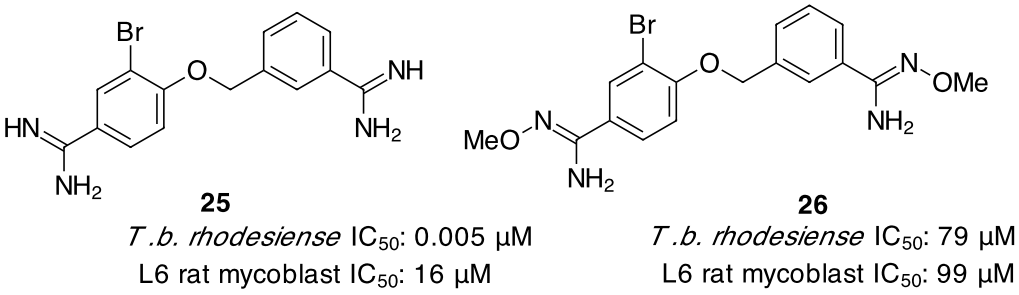

Figure 9. Recent new series of benzyl phenyl ether-based diamidines by the Tidwell group.

The exact mechanism underlying the kinetoplastid and undesirable mammalian toxicity of these amidine-based compounds remains unclear. Moreover, side effects such as hypoglycaemia and nephrotoxicity remain unpredictable and are a source of concern [6]. Nevertheless, a follow-up process and careful monitoring may lead to fruitful access to the next generation of amidine candidates.

1.4.2 Nitroheterocycles for HAT

Nitroheterocycles encompass an important class of well-known anti-infectives and anti-protozoal compounds that contain one or more nitro groups incorporated onto an aromatic ring. Examples of nitro-heterocyclic compounds (Figure 10) include the

trichomonad killing agent metronidazole **(27)**; antitrypanosomal agent megazole **(28)** and anti-Chagas agent benznidazole **(29)**. Although these later compounds have long been in use, they are suspected to be mutagenic due to the presence of a nitroaromatic group [12].

However, through extensive consideration of the mechanism of action of these compounds, some have suggested that mutagenicity should be of less concern than previously thought leading to a renewed interest in this class of compounds [28].

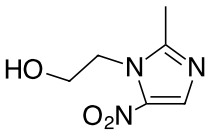

27
metronidazole

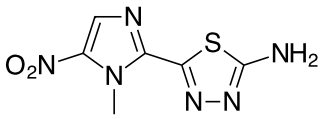

28
megazole

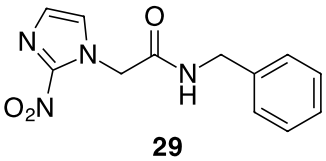

29
benznidazole

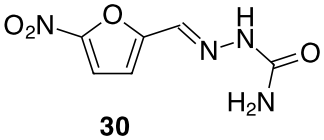

30
Nitrofurazone
T. brucei IC_{50}: 230 ± 80 nM SI: 157

Figure 10. Selection of Nitroheterocycles known as antiprotozoals inhibitros

Revival in the interest of nitro-heterocyclic compounds for the treatment of HAT began mid late-century following the successful findings of nitrofurazone **30**, which demonstrated interesting trypanocidal activity. However, concerns arose following reports of failure to completely eradicate infection and side effects including CNS toxicity, resulting in the suspension of clinical trials [28]. A recent report by Wilkinson *et al.* [29] demonstrated that minor modification to nitrofurazone such as the introduction of a thiosemicarbazone **(31)** or carbazate moieties such as compound **32**

and **33** into the parent structure **30** has led to improvement in the *T. brucei* inhibition activity of IC_{50} 180 nM and 120 nM and 170 nM respectively (Figure 11).

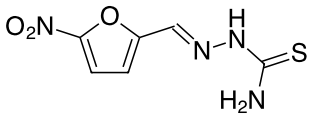

31

T. brucei IC_{50}: 180 ± 10 nM SI: 133
SI: 133

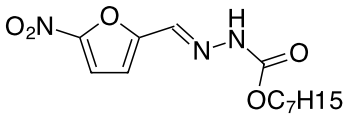

32

T.brucei IC_{50}: 120 ± 20 nM SI: 116
SI: 116

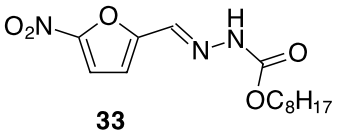

33

T. brucei IC_{50}: 170 ± 11 nM SI: 264
SI: 264

Figure 11. Selection of modified analogues of nitrofurazone resulting in a better trypanocidal activity.

Fexinidazole

Fexinidazole **(34)** as shown in Figure 12, is a 2-substituted 5-nitroimidazole drug, and a member of the 5-nitroimidazole classe known for its anti-infective activity. It has been described as a forgotten antiparasitic drug, abandoned due to inconclusive mutagenic concerns. A wide range of action, lower toxicity and comparatively easy synthesis, are factors that led to its preclinical development in the 1970s and early 1980s as a broad-spectrum antimicrobial agent. In 1983, although its *in-vivo* activity was evaluated its development was not pursued further at the time. The interest in fexinidazole was not renewed until the Drugs for Neglected Diseases Initiative began their campaign for a comprehensive *in-vitro* assessment of a library of 700 new and existing nitroheterocyclic compounds, screened as part of an HTS campaign aiming to select drug candidates suitable for oral administration for the treatment of HAT, including those in the advanced and fatal CNS stage 2 [30].

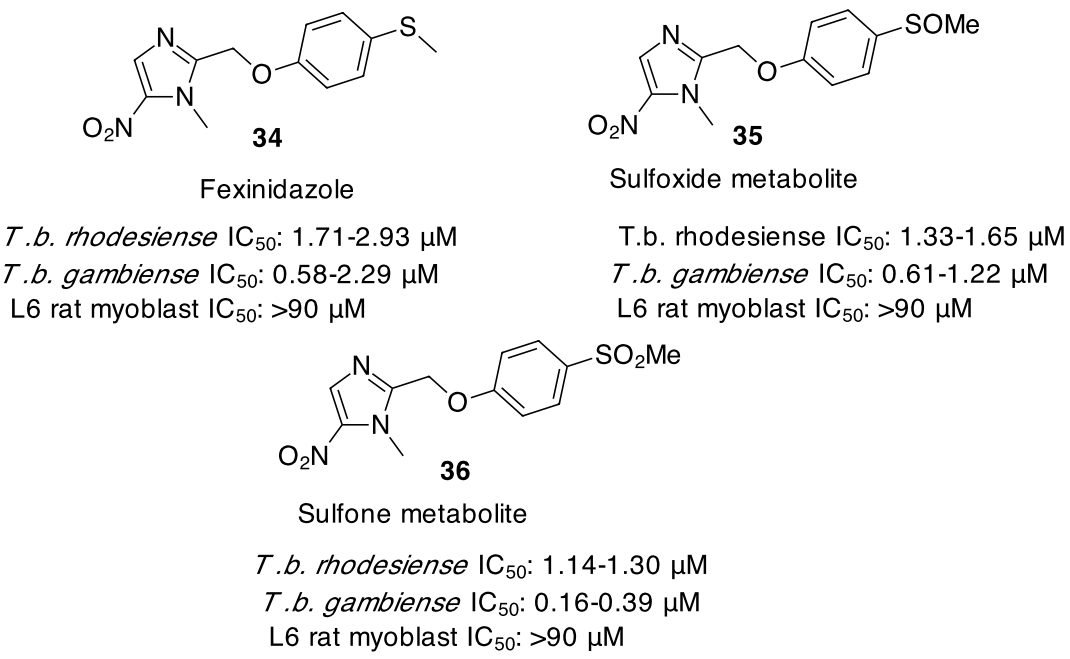

Figure 12. Fexinidazole, a drug in the preclinical and drug development trials for HAT

Fexindazole **(34)** progressed to clinical phase 1 trials in 2009 as a monotherapy initiated by the Drugs for Neglected Diseases Initiative [30]. So far no adverse issues have been identified [6] and it has recently entered phase II/III trials [31]. In 2010, Torreele *et al*, described its trypanocidal efficacy and preclinical profile [30]. They claim that fexinidazole **(34)** could be safe and can be used for oral treatment at a cost that is acceptable in the endemic regions and that it will be effective for both stages 1 and 2 HAT against *T. brucei* including *T.b. gambiense* and *T.b. rhodesiense*. Fexindazole is absorbed rapidly and metabolised into the sulfoxide **(35)** and sulfone **(36)** (Figure 12) derivatives, which have similar *in vitro* activity to the parent drug without causing toxic accumulation of the drug and its metabolites; thus leading to high *in-vivo* activity caused by the triple action of the three active compounds [30].

Mechanism of action of nitroheterocycles

Given that fexinidazole is a prodrug as it is the case with other nitroheteroclic compounds, it is activated by nitroreductases (NTRs), which are also known to reduce nifurtimox **(5)**. The two main classes of NTRs are class I and class II NTRs (Figure 13) [28].

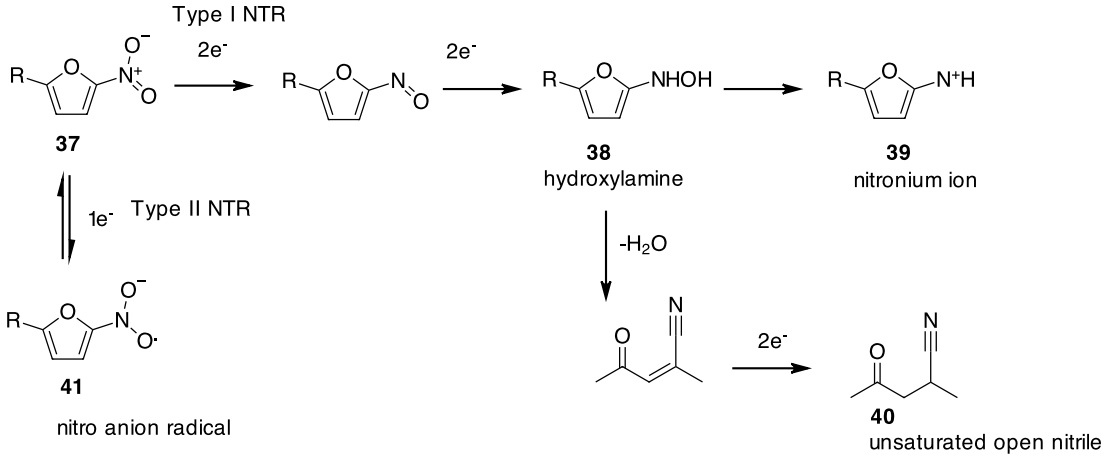

Figure 13. Schematic representation of reduction of nitrofurans X by type 1 and II NTR. Mechanism is adapted from XX.

Class I NTRs (oxygen insensitive) mediate the reduction of the nitro group **(37)** to form a hydroxylamine product **38** *via* a nitroso intermediate, then **38** is converted into nitronium ion **(39)** or into the open form of the unsaturated toxic nitriles **(40)**. The formation of the nitrenium ion **(39)** triggers DNA breakage and DNA-linked adduct while an open-chain nitrile would possess equal cytotoxicity to both trypanosomal and mammalian cells. Although some portion of an open nitrile **(40)** can be transformed rapidly into a safer saturated state, this only occurs at a low rate. In contrast, with type II NTRs the reduction of the nitro group leads to the formation of unstable nitro radicals **(41)**, which subsequently form superoxide in the presence of oxygen, which may result in the regeneration of a nitro-containing prodrug.

For example, compound **(42)** (Figure 14) is reduced sequentially by class I NTRs into a series of imidazole compounds leading to formation of a dihydroxy-dihydro imidazole **(44)** (*via* intermediates including hydroxylamine **43**), which undergoes decomposition into guanidinoacetamide **(45)** and glyoxal **(46)** [28].

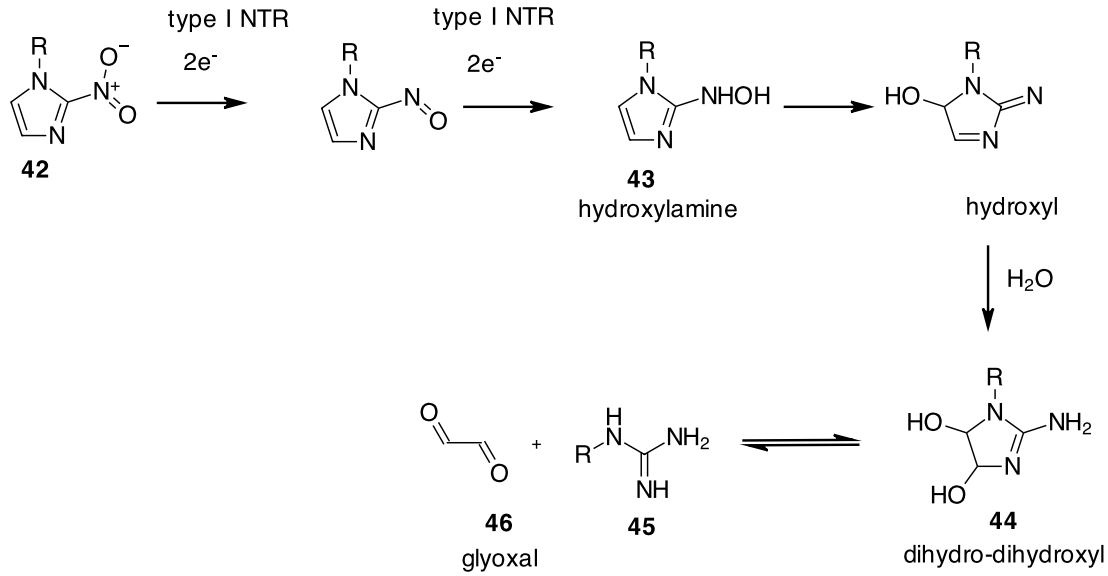

Figure 14. Reduction of 2-nitroimidazoles by type I NTR [28].

Either compound **44** and/or glyoxal **(46)** trigger adduct formation with an array of biological molecules, including DNA. This process is often linked to the concern of mutagenicity and cytotoxicity associated with nitroheterocyles [28]. Fexinidazole's mode of action has not yet been elucidated but it may act as a prodrug as with other 5-nitroimidazoles which are toxic to parasites due to bio-reductive activation by bacterial-like nitroreductase, which also exists in trypanosomes.

Mutageneicity/genotoxicity of fexinidazole

Similarly to other nitro heterocyclic compounds, fexinidazole is potentially mutagenic, which is often linked to the reduction of the nitro group, as evidenced by

its positive outcome in the mutagenicity testing by the standard bacterial mutagenicity Ames test [30].

However, Torreelle et al. [30] has shown that this effect is dependent on the presence of the bacterial nitroreductases. Evidence for this is the reduced or abolished mutagenic activity of fexinidazole and its metabolites with nitroreductase deficient Salmonella strains and the negative mammalian genotoxicity in the *in-vitro* and *in-vivo* assays [30]. Supporting this is the fact that the preclinical development trials suggested that fexinidazole is devoid of any genetic toxicity in mammalian cells and may not pose a genotoxic risk to patients [30]. They explained that this enzyme can activate nitroimidazole drugs into reactive intermediates that in turn cause cellular damage to parasites without causing any harm to mammalian cells, since this compound and its metabolites have low single redox potential [30]. Unlike bacterial nitroreductase which reduce compounds at lower redox potential, mammalian counterpart enzymes only reduce compounds with relatively high redox potential [30].

Resistance to fexindazole be a concern?

Down-regulation of these enzymes has also been linked to resistance to nifurtimox. It has also been suggested that resistance is likely to occur with fexinidazole by the same mechanism that led to resistance to nifertimox [32]. Sokolova et al. [32] have raised the issue of drug resistance, recommending that fexinidazole not to be used as a monotherapy. Rather a combination of fexinidazole with other compounds would be potentially more effective in reducing the risk of drug resistance before the drug is launched on a wide scale [32].

Aryl-4-nitroimidazole

Following the successful entry of fexinidazole to preclinical assessment, a series of nitroimidazoles has been recognised with an optimised activity and a reduced genotoxicity to humans while excluding those that are substrates for the nitroreductases. Optimisation and development in chemistry has led to the finding of a series of aryl-4-nitroimidazole such as compound **47** and **48** (Figure 15), also reported to have curative potential in murine models of acute and late-stage infections of *T.b. rhodesience* and *T.b. brucei* [33].

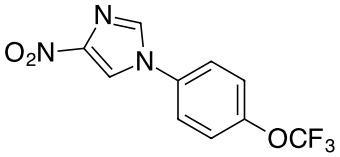

47

T.b. rhodesiense IC_{50}: 0.16 µM
L6 rat myoblast IC_{50}: >90 µM

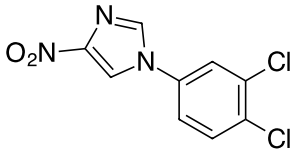

48

T.b. rhodesiense IC_{50}: 0.10 µM
L6 rat myoblast IC_{50}: >90 µM

Figure 15. aryl-substituted 4-nitroimidazoles active against T. b. rhodesience and its selectivity for trypanosomes over mammalian cells.

For the acute mouse model of stage-1 HAT, compounds **47** and **48** cured 100% of infected mice with an oral regimen of 25 mg/kg and 50 mg/kg respectively for four days. In the CNS infection model, compounds **47** and **48** exhibited excellent efficiency by completely curing all infected mice using oral administration of 50 mg/kg and 100 mg/kg respectively for five days. The interest in these compounds resides in the fact that none were found to be substrates for human nitroreductase and were also considered safe to mammalian cells [33].

Halo-nitrobenzamides

Nitrobenzamides (Figure 16) have also been reported with interesting trypanocidal activities. The best initial success of this series is the compound **49**, which had good inhibition to *T.b brucei* but poor selectivity against mammalian cells. Introduction of a methyl and a halogen groups as in compounds **50** and **51** have remarkably improved the selectivity against mammalian cells while maintaining the potency to inhibit *T.b. brucei* [34]. The mechanism of inhibition was not elucidated for these compounds and it is not yet confirmed if they are active as a substrate for NTRs.

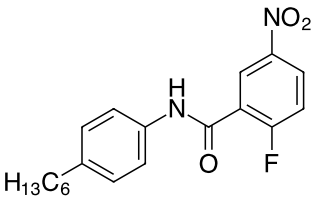

49

T.b. brucei IC_{50}: 1.5 µM
HepG2 IC_{50}: 2.5 µM

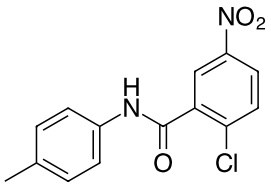

50

T.b. brucei IC_{50}: 7.7 µM
HepG2 IC_{50}: > 50 µM

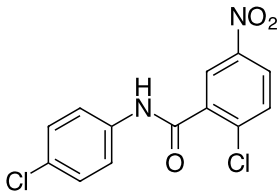

51

T.b. brucei IC_{50}: 1.5 µM
HepG2 IC_{50}: > 50 µM

Figure 16. selection of nitrobenzamides as potential inhibitor of *T.b. brucei*

1.4.3 Benzoxaboroles

Benzoxaboroles are a new class of boron containing compounds which have recently emerged as prospective compounds for the treatment of stage 1 and stage 2 HAT, originally discovered by Anacor Pharmaceuticals as antifungals, antibacterial and anti-inflammatory agents [5]. In 2010, the Sandler Centre of Drug Discovery (UCSF), identified several compounds through an antitrypanosomal screening campaign of 400 compounds, leading to the discovery of AN2920 **(52)** and AN3520 **(53)**, with IC_{50} of 0.02 and 0.04 µg/ml respectively to inhibit *T.b. brucei* [35], as presented in Figure 17.

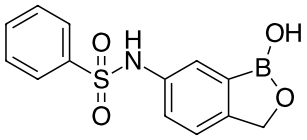

52

T.b. brucei IC_{50}: 0.02 µg/ml
Cytotoxicity L929 IC_{50}: 2.65 µg/ml
Mouse S9 metabolism $t_{1/2}$: 28 min

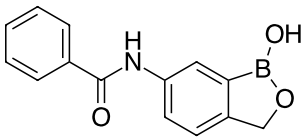

53

T.b. brucei IC_{50}: 0.04 µg/ml
Cytotoxicity L929 IC_{50}: >10 µg/ml
Mouse S9 metabolism $t_{1/2}$: 29 min

Figure 17. Benzoxaboroles as inhibitors of *T.b brucei* infection.

Therefore, these compounds were considered suitable for their potential of optimisation [35], although it was found that **52** was more cytotoxic (IC_{50} to L929 mouse fibroblast > 2.65 µg/ml) compared to **53**, making the former unattractive for further development [36]. In addition concern regarding lack of stability was addressed with both candidates **(52)** and **(53)** based on instability and pharmacokinetic studies using an S9 mouse metabolism model, which demonstrated the apparent rapid disappearance of these compounds from the mice plasma [5,36].

Further development in the SAR, resulted in the discovery of several candidates with a better stability profile when introducing substituents on the terminal phenyl ring, including a methyl, chlorine and triflоromethyl groups (i.e. compound **54**, Figure 18) at different positions, although the observed increase in cytotoxicity of **54** was still disadvantageous [36]. However, introduction of a fluorine atom to the *para*-position of the benzmide moiety afforded a better candidate such as compound **55** in respect to the in-vitro *T.b brucei* inhibition, cytotoxicity and stability to mouse S9 metabolism [36].

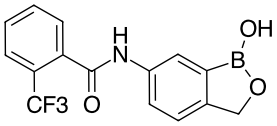

54

SCYX-6759

T.b. brucei IC_{50}: 0.03 µg/ml
T.b. rhodesience IC_{50}: 0.038 µg/ml
T.b. gambiense IC_{50}: 0.012 µg/ml
Cytotoxicity L929 IC_{50}: >3.77 µg/ml
Mouse S9 metabolism $t_{1/2}$: >350 min

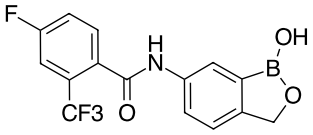

55

SCYX-6759

T.b. brucei IC_{50}: 0.05 µg/ml
T.b. rhodesience IC_{50}: 0.038 µg/ml
T.b. gambiense IC_{50}: 0.009-0.033 µg/ml
Cytotoxicity L929 IC_{50}: >10 µg/ml
Mouse S9 metabolism $t_{1/2}$: >350 min

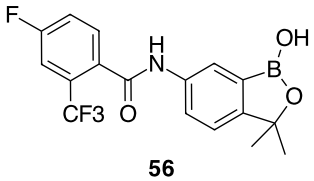

56

SCYX-7158

T.b. brucei IC_{50}: 0.292 µg/ml
T.b. rhodesience IC_{50}: 0.294 µg/ml
T.b. gambiense IC_{50}: 0.07-0.363 µg/ml
Cytotoxicity L929 IC_{50}: >10 µg/ml
Mouse S9 metabolism $t_{1/2}$: >350 min

Figure 18. selected benoxaboroles tested against second-stage HAT.

Both compounds **54** and **55** were also tested for an *in-vivo* acute stage-1 HAT model, demonstrating that compound **54** cured all mice completely at 5 mg/kg with oral dosing twice a day over four days, while candidate **55** was found to be more effective by curing all infected mice even at an oral dose as low as 2.5 mg/kg. Both candidates had the same average of mice survival over 30 days [37].

Compounds **54** and **55** were also successfully progressed for testing against a stage-2 infection model. In this testing, compound **54** was found active at a 50 mg/kg intraperitional dose given twice daily over a week or two weeks, and was curative to 71 or 78 % respectively with a survival average of 52 or 57 days respectively. In

contrast, compound **55** cured infected mice using an intraperitional regimen and oral dosing, at cure rates of 100% and 83 % for 14 days and 7 days (twice daily) respectively. It was also reported that dosing of **55** at 25 mg/kg or lower did not provide substantial protection to infected mice under the CNS model [37].

Following these results the program focus has moved to improving efficacy and/or brain exposure of benzoxaboroles, given the importance of improving dosing strength feasible for a once-daily oral treatments for stage 2 HAT, as outlined by the DNDi. However there was an apparent concern regarding a disconnect between plasma and brain exposure of compounds **54** and **55** [36]. For example, it was reported that permeability testing across the blood brain barrier for a series of 6-carboxamides-benoxaborole, revealed no evidence for efflux liability by p-glycoprotein. However, it was hypothesised that the presence of other transporters could at least be responsible for the apparent efflux of the weakly acidic benzoxaboroles out of the brain [36].

Therefore, development and optimisation of **55** were described to electronically and/or sterically limit access to the acidic B-OH moiety, which led to the reported finding of 3,3-dimethyl analogues exemplified by SCYX-7158 **(56)** (Figure 15) [36,38]. Following stage 1 and 2 HAT's models, SCYX-7158 **(56)** exhibited impressive efficacy, leading to the observed complete treatment of mice infected with TREU667 strain in the stage 2 model following an oral dose regimen of 5 mg/kg once a day for four days of treatment [38]. Based on these reported efforts, **56** preceded to phase 1 clinical trials supported by the European Medicines Association[12].

1.4.6 Biochemical pathways a target for *T. brucei* inhibition

HTS screening of a library of compounds against a specific enzyme or protein, also called a target-based approach, has been described as a promising starting point for the mining of *T. brucei* inhibitors. Targeting enzymes involved in polyamine biosynthesis, energy metabolism or glycolysis pathway, purine and pyrimidine metabolism are all examples of target-based campaigns used in this field.

Polyamine biosynthesis

Polyamines are essential for growth and multiplication *of T. brucei*, and the discovery of drug candidates that inhibit the enzymes (e.g *trypanothione reductase*) involved in the pathway of polyamine biosynthesis represents a promising approach. Mining libraries and screening commercially available compounds against *T. brucei* identified a series of tricyclic piperazines including **57**. Compound (BCTP) **(58),** a derivative of phencyclidine which is an anaesthetic drug, was identified as an inhibitor of *trypanothione reductase* and further optimisation in medicinal chemistry led to a number of marginally improved compounds such as the substituted piperidine analogue **(59)** [12]. (Figure 19).

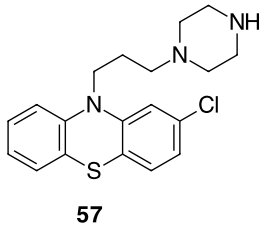

57

TR IC50: 7.5 µM

T. b. rhodesiense IC_{50}: 4.5 µM

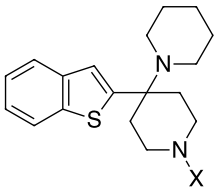

58: X = CH2; TR IC_{50} = 3.3 µM, *T.b rhodesience* = 10 µM

59: X = NCH2Ph; TR IC_{50} = 12 µM, *T. b rhodesience* = 4.3 µM

Figure 19. Polyamine biosynthesis inhibitors by high throughput screening

Sinefungin **(60)** is a natural nucleoside produced by *Streptomyces grizeolus* and *S. incarnates;* that is a structural analogue of *S*-adenosylmethionine **(61)** (SAM), a biomolecule required for biosynthesis of polyamines and used in the transmethylations of biomolecules including proteins and lipids [39].

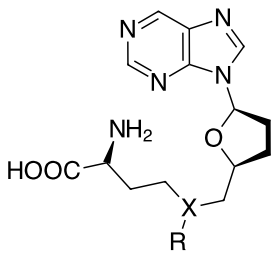

60: X = CH, R = NH2; *T.b. rhodesience* IC_{50} = 4 nM
61: X =S, R = CH3

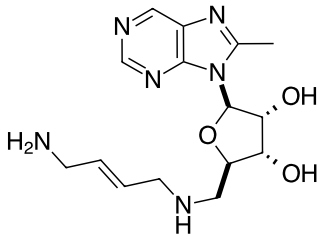

62

T.b rhodesince $IC_{50:}$ 1 nM

Figure 20. Purines containing molecules with potent trypanocidal activities against *T.b. rhodesience*.

Sinefungin **(60)** has been identified as a strong inhibitor for SAM-dependent transmethylation reactions, which exhibited excellent *in*-vitro activity against the growth of *T. b. rhodesiense* with an IC_{50} in nanomolar range (IC_{50} = 4 nM) with a very high selectivity (SI > 10^6). In the *in-vivo* testing it demonstrated a good cure rate in mice infected with *T. b. brucei* when administered intraperitoneally and is well tolerated in mice. Reports of nephrotoxicity with **60** have retarded any further development [39].

However, compound **62**, an analogue of **60**, has been identified with excellent *in-vitro* activity against *T.b rhodesience* with an IC_{50} of 1 nM. Compound **62** was also tested for a murine stage 1 model of HAT, finding that a 50 mg/kg interperental dose given once daily over a week is effective in clearing parasites from the blood. In addition,

62 was also effective at a doses as low as 2 mg/kg using the same dosing schedule (interperental dose once daily over 7 days).

For a stage 2 model of CNS HAT, it was found that **62** only exhibited partial activity using 100 mg/kg given intraperitoneatally over two weeks [40].

DNA topoisomerase inhibitors

DNA topoisomerases comprise a family of enzymes that play an important role in the modification and catalysis of the topological isomer of DNA, including its role to mediate mechanistic interactions such as knotting, un-knotting or catenation and decatenation supercoiling and relaxation of DNA double helices. Topoisomerases can be divided into types 1 and 2. Type 1 catalyses single strand breakage of DNA and are further subclassed into 1A and 1B, while the latter has been recognised as a target for the camptothecin class of anticancer agents. Type 2 topoisomerases construct double stranded breaks on DNA. Trypanosomatids contain the subclass 1B topoisomerase. *T. brucei* Trypanosomatide differs from its mammalian host counterpart, which is a single polypeptide, by its hetero-multimeric nature comprising double separated encoded proteins. The interest in DNA topoisomerase as a target to inhibit *trypanosome* has been recognised [7]. Classical topoisomerase inhibitors and approved anticancer drugs were screened against bloodstream *T. brucei* and HL-60 cell-lines. All of the tested compounds exhibited antitrypanosomal activity ranging from 3 to 30 nM. For example, Camptothecin **(63)**, mitoxantrone **(64)** and doxorubicin **(65)** (Figure 21) exhibited good antitrypanosomal activity with an ED_{50} of 0.43 μM, 0.0026 μM and 0.027 μM respectively. However, these compounds were also not selective and very cytotoxic to mammalian HL-60 cell-lines [41].

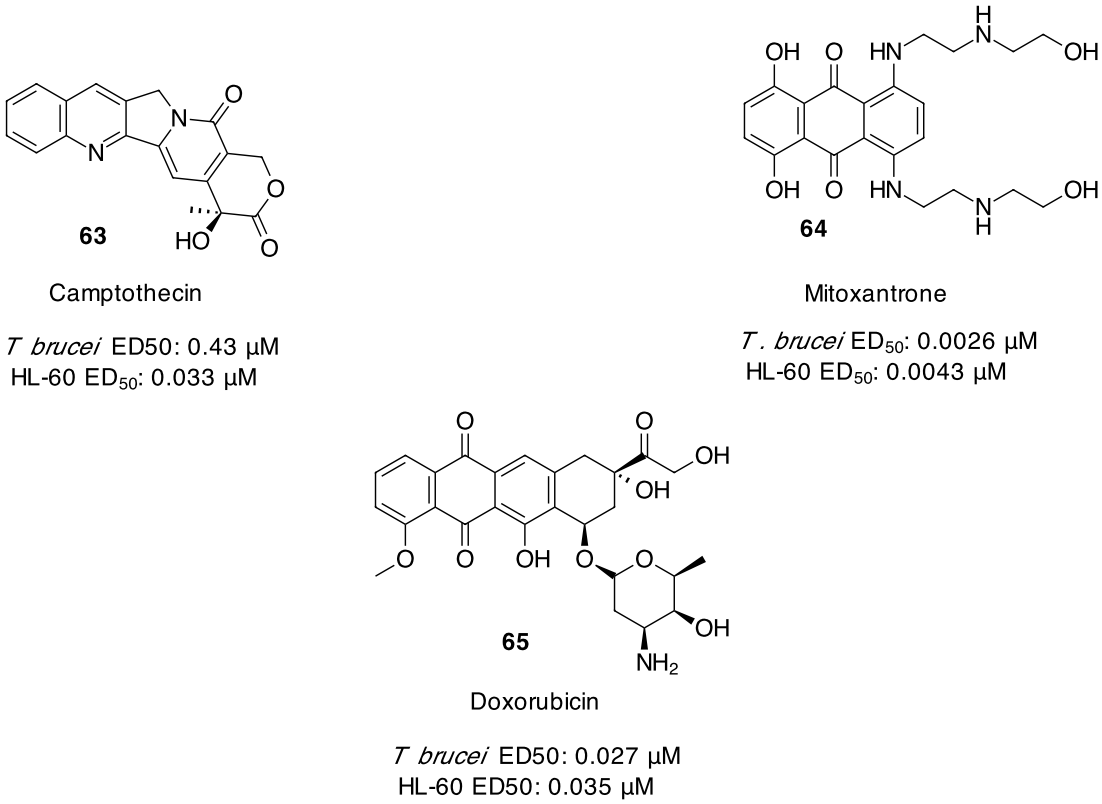

Figure 21. A selection of classical DNA topoisomerase inhibitors with *T.brucei* activity.

Glycolysis

Another example of biological pathway-based drugs for HAT is the targeting of glycolysis or the energy metabolism pathway. Several aspects make the glycolysis pathway (Figure 22) an ideal target for intervention, since the bloodstream stage of trypanosomatidae utilise it as the only source of ATP, and it has no functional mitochondrial respiratory chain coupled to ATP synthesis. This accounted for the rapid death of parasites due to the inhibition of this pathway. Moreover, evolutionary distance exists between trypanosomatidae and their mammalian hosts, where the glycolytic enzymes of these parasites have distinct properties that differentiate them from their mammalian counterparts. Unlike other organisms where glycolytic enzymes are cytosolic, *T. brucei* is characterised by an unusual compartmentation

system where the enzymes are confined within peroxisome-like organelles called glycosomes. Thus, this compartmentation has resulted in different kinetic properties and regulatory mechanisms that correspond to a high glycolytic efflux which is the highest ever reported for an organism [42,43]. For the above reasons, this approach has been attractive and was reported to provide new compounds with antitrypanosomal activity.

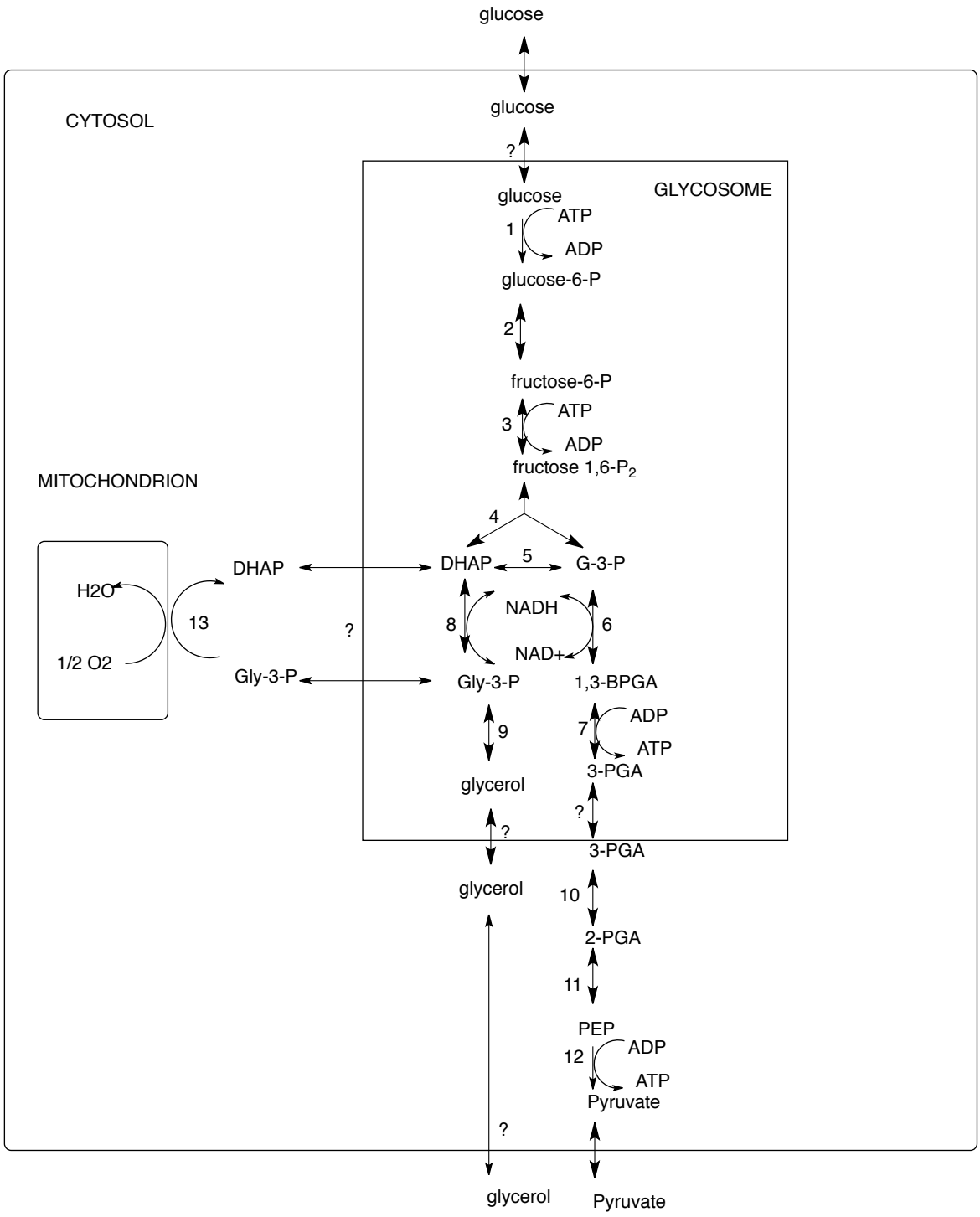

Figure 22. General scheme of glycolysis in bloodstream-form *T. brucei* [42].

1) Hexokinase, 2) glucose-6-phosphate isomerase; 3) phosphofructokinase; aldolase; 5) triosphosphate isomerase; 6) glyceraldehyde-3-phosphate dehydrogenase; 7) Phosphoglycerate kinase; 8) glycerol-3-phosphatedehydrogenase; 9) glycerol kinase; 10) phosphoglycerate mutase; 11) enolase; 12) pyruvate kinase; 13) glycerol-3-phosphate oxidase. Abbreviations: 1,3-PGA, 1,3-bisphosphoglycerate; DHAP, dihydroxyacetonphosphate; G-3-P, glyceraldehyde-3-phosphate; Gly-3-P, glycerol-3-phosphate; PEP, phosphoenolpyruvate; 2-PGA, 2-phosphoglycerate; 3-PGA, 3-phosphoglycerate, ? are enzymes that are not yet identified.

Pentalenolactone **(66)** isolated from *Streptomyces areae* and koningic acid **(67)** (Figure 23) from the fungous *Trichoderma koningii*) are natural antibiotics known as potent inhibitors of glycolytic enzyme glyceraldehyde-3-phosphate dehydrogenase (GADPH) where they bind irreversibly to this enzyme. GAPDH is a key enzyme in glycolysis, catalysing the oxidative phosphorylation of the triose glyceraldehyde 3-phosphate to form 1,3-diphosphoglycerate in the presence of NAD^+ and inorganic phosphate.

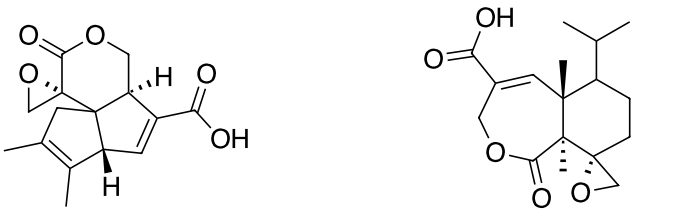

66 Pentalenolactone **67** Koningic acid

Figure 23. Natural inhibiters of glycolytic enzymes

These two compounds have a highly hydrophobic character and contain an epoxide and α-enone which represent the reactive functionality in both pentalenolactone and koningic acid. However, toxicity of the two compounds is a limitation, besides the difficulty and cost factors associated with their synthesis [43].

The design and synthesis of trypanocides that can act to block the glucose metabolism of *T. brucei* has been reported. Analogues of glyceraldegyde-3-phosphate (Figure 24), containing these reactive groups, epoxide or α-enone have been described to exhibit anti-glycolytic activities that can be used to develop antiparasitic compounds [43,44]. Lauth *et al* [44] presented kinetic inhibition studies of the glycolytic enzyme GAPDH and found substrate analogues bearing reactive groups epoxide or α-enone

with substituents on the phosphorus atom play a crucial role in the efficiency of these inhibitors. This is due to their affinity for the hydrophobic part of the protein, in close proximity to the residue responsible for the covalent binding. Wilson *et al* [43] studied the activity of similar compounds carrying these reactive functional groups and on the basis of their simplicity and small size. These substrates **68**, **69** and **70** presented in Figure 24 were claimed to inhibit the enzymes irreversibly due to nucleophilic attack of a thiol group of the cysteine residue of the enzyme, to the C1 of the epoxide and the enone compounds and the subsequent formation of the covalent bond between the cysteine sulfur and the electrophilic carbon of these compounds [43].

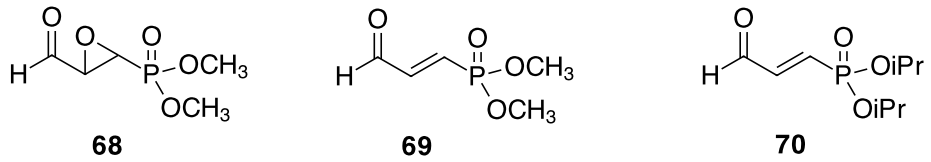

Figure 24. Glycolytic enzymes inhibitors

Interestingly, measurement of the effect of these compounds on the multiplication of trypanosome *in-vitro* cultures shows that the α-enone derivatives **69** and **70** were found to be far more active than compounds with epoxides **68**. Furthermore, they claim that inhibitor **70** exhibited an inhibitory activity at a concentration significantly lower than that routinely used in trypanocides, namely pentamidine and (difluoromethyl)ornithine [43].

Another independent study on 6PGDH as a glycolysis target was reported by Dardonville *et al* [45]. They proposed compounds that mimic the transition state and high energy, leading to the finding of **71** (Figure 25). Although it is potent against the enzyme, it was inactive against *T.b. brucei* due to poor membrane permeability [45].

As a result, compound **71** was further optimised into a prodrug candidate **72** and **73** with IC_{50} against parasites of 1.7 µM and 0.008 µM with $t_{1/2}$ of 2.1 and 8.0 hours respectively [46,47]. Higher $t_{1/2}$ for compound **73** might be due to its high stability compared to its counterpart **(72)** incorporating the less stable thio ester. Therefore this modification led to an adequate membrane passage of compound **73** into the parasite where it is metabolised back into its parent molecule, which is cell impermeable. Consequently, the advantage is that **73** accumulate in the parasites, leading to better *in-vitro* activity [47]. However, further work on these types of compounds may be necessary to confirm the success or not of this class.

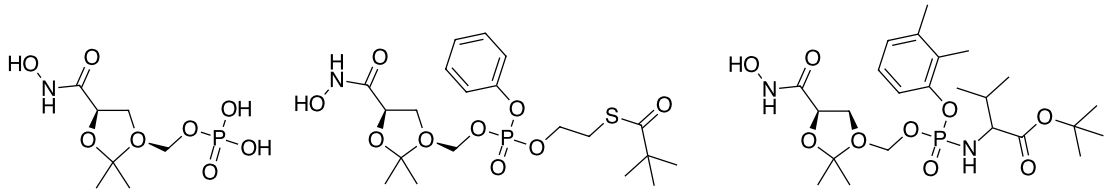

Figure 25. Selection of phosphoros-based compounds with trypanocidal activity against *T.b. brucei*

In addition, these glycosomal enzymes carry relatively high positive charges at physiological pH. Three dimensional modelling indicated that positive charges were concentrated in two distinct areas on the surface of the *Trypanosoma* protein separated by a distance of 4 nm [48]. Suramin is one of the highly effective trypanocides found to reduce glycolytic capacity [42]. Wilson *et al* [49] synthesised a series of symmetrical long-chain molecules (i.e **74**) as depicted in Figure 26 where a distance of 4-nm was claimed as optimal distance for separating the two symmetrical

buds of the molecules without losing effect. The molecule **74** also contained two negative charges or strong dipoles at each end at physiological pH.

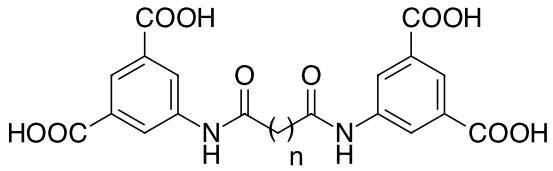

74

Figure 26. Symmetrical long-chain molecules as glycolytic inhibitors of *T. brucei.*

Several compounds based on the general structure in Figure 26 were claimed to inhibit the glycosomal enzymes and *T. brucei* more strongly than suramin [49].

A sugar-like drug has also been reported to target the glycolysis pathway in the trypanosome. For example, Nowicki *et al* [50] reported the screening and evaluation of a of substituted anhydro-1-deoxy-D-mannitol such as compounds **75** and **76** were the most active inhibitors against trypanosomatide phosphofructokinase (TbPFK) with an IC_{50} of 23 µM and 80 µM respectively, and also inhibited *T.b brucei* with IC_{50} of 30 µM and 35 µM respectively [50].

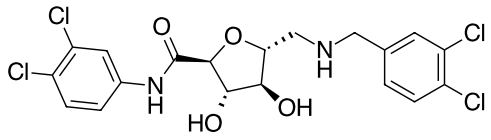

75

TbPFK IC_{50}: 23 µM

T. brucei S427 IC_{50}: 30 µM

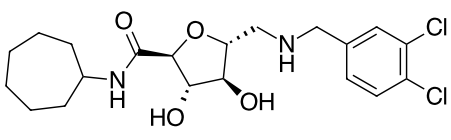

76

TbPFK IC_{50}: 23 µM

T. brucei IC_{50} S427: 35 µM

Figure 27. Manitol analogues as inhibitors of *T. brucei*

Inhibitors of purine and pyrimidine biosynthesis

Inhibitors of purine and pyrimidine biosynthesis have been described as having anti-trypanocidal activity. These organisms do not synthesise purines *de novo* by themself and are dependent on salvage mechanisms *via* use of transporters and enzymes from the host. Therefore, the inhibition of these salvage mechanisms has been used for the development of trypanocides. For example, cordycepin **(77)** (Figure 28) and a similar analogue **78** (substrates for *T. brucei* adenosine kinase) were found to terminate RNA synthesis and parasite growth [51].

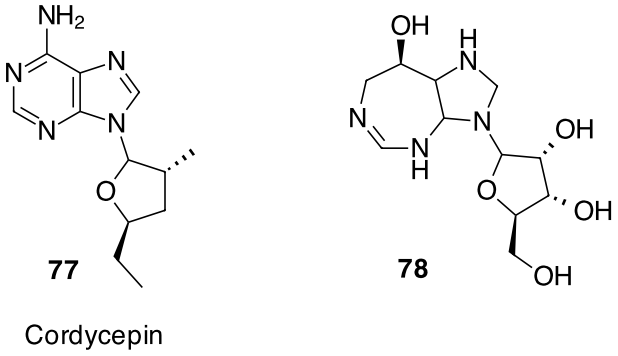

Figure 28. Cordycepin, an example of purine and pyrimidine biosynthesis inhibitor

Kinases inhibitors

Protein kinases play an important role in the life cycle of parasites, thus making it an attractive target. A number of kinases have been deemed essential for the survival of *T. brucei* and their activity has been validated. However, only a few compounds have been discovered with chemical probes.

Glycogen synthase kinase 3 (GSK-3) is one of the kinases which has been explored as a target for inhibition of *trypanosoma brucei*. Compounds **79** and **80** (Figure 29) were identified as potent inhibitors for GSK-3 with an IC_{50} of 4 nM and 12 nM which

blocked the survival of *T.b. brucei* at IC_{50} with an of 50 nM and 20 nM, respectively [52].

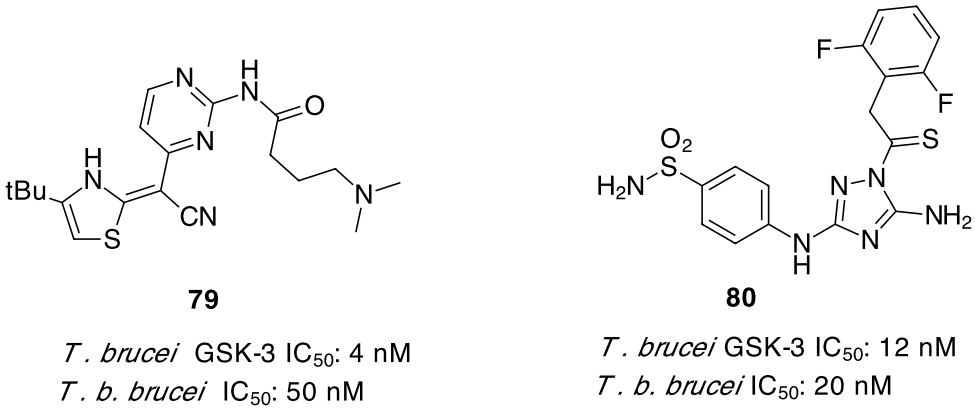

Figure 29. Selection of kinases inhibitors with potent anti *T. brucei* activities.

Lapatinib **(81)** is an EGFR tyrosine kinase inhibitor, identified as an antitrypanosomal agent (*T.b brucei* EC_{50} = 1.54 µM) from HTS library screening of the EGFR tyrosin kinase [53]. Thus, lapatinib was selected as a starting point for the development of new antitrypanosomal derivatives and was further optimised into **82** following a SAR study conducted by Pollastri's group (Figure 30). Compound **(82)** exhibited higher anti-trypanosomal activity and selectivity over mammalian cells. Compound **(82)** was also identified as suitable for oral administration and exhibited moderate efficacy in an acute mouse model at 20 mg/kg [53].

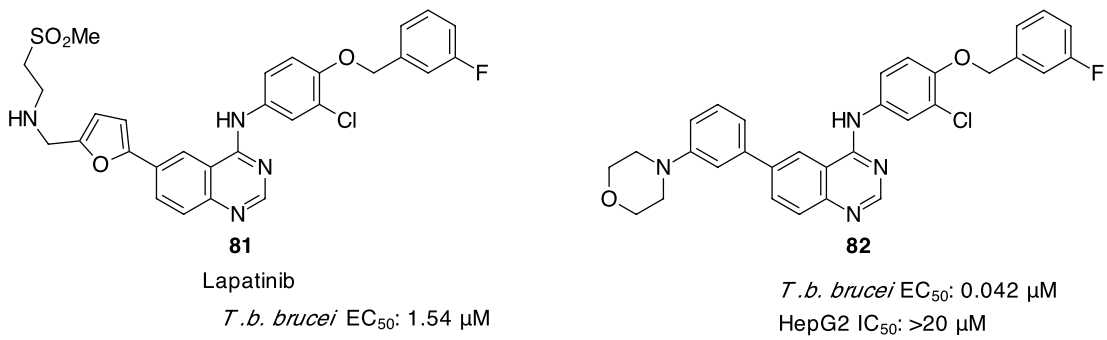

Figure 30. EGFR tyrosin kinase inhibitors as antitrypanosomal agents

1.5 Background for the scope of this thesis

1.5.1 Background to the lead compound selected for medicinal chemistry optimisation

Collaborators at the Avery group at the Eskitis Institute and the Baell group from Monash Institute of Pharmaceutical Science (MIPS), conducted whole-organism high throughput screening of a library of 88,000 compounds against HAT.

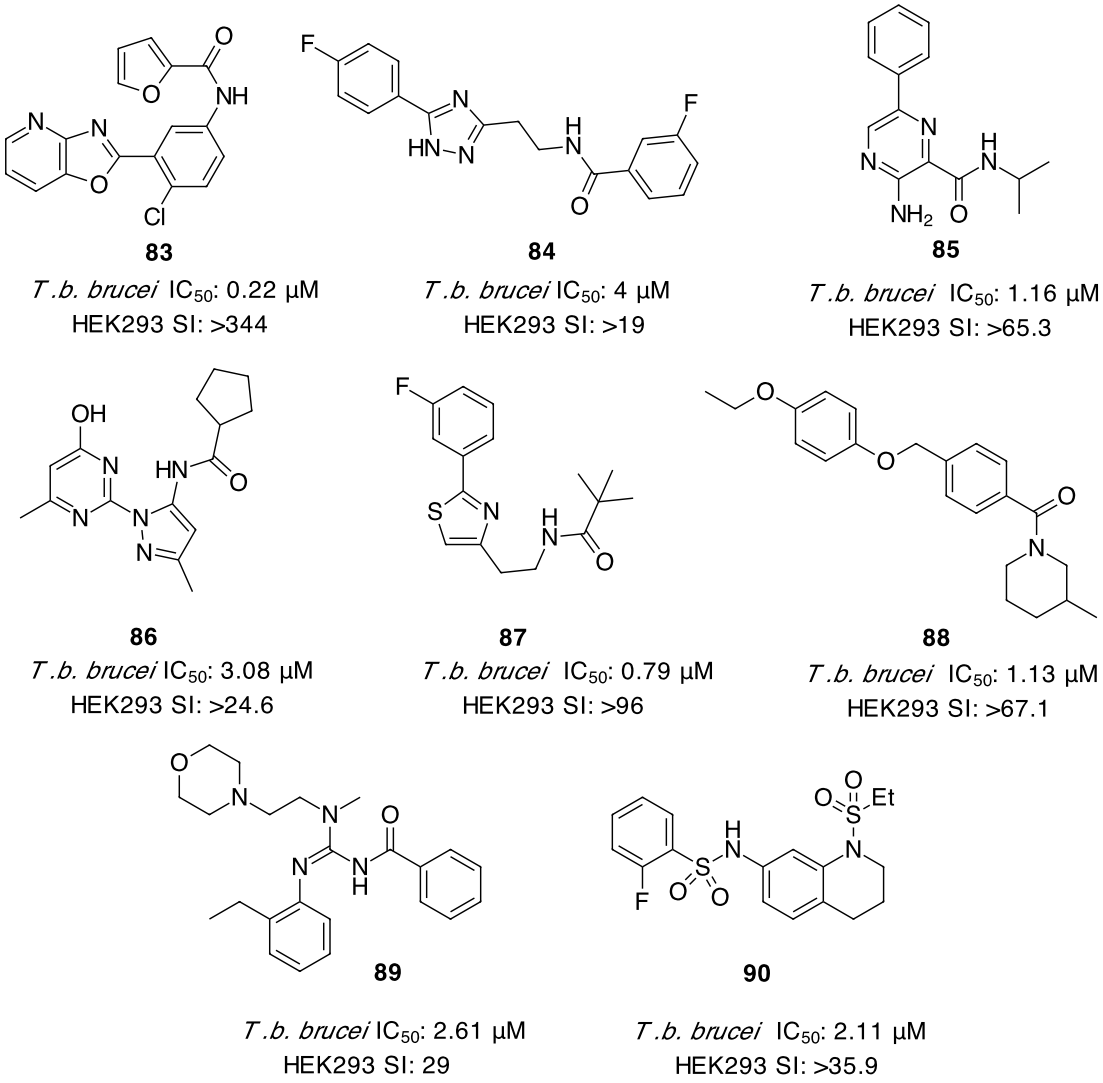

Figure 31. Lead compounds identified from high throughput screening in the Eskitis institute whole-organism against *T.b. brucei*.

This screening campaign resulted in the identification of 8 potential drug candidates with a range of activity from sub- to low micromolar and selectivity from 344 to 19 (Figure 31) [54] [6] . These candidates were all considered suitable for medicinal chemistry optimisation with the exception of candidate **86** due to the presence of a pyrazolyl-pyridinyl junction which would be sensitive to nucleophilic attack [6]. Amongst these compounds,the oxazolopyridine **83** exhibited the best trypanocidal activity against *T.b brucei* and *T.b. rhodesience* with an IC_{50} of 0.22 µM and 0.59 µM and selectivity of >345 and 39. In addition, candidate **83** was also potent against *T. cruzi* and mildly active against *p. faciparum* with an IC_{50} of 0.23 and 7.8, respectively (Table 2).

Table 2. Antiproliferative activty of lead candidate oxazolopyrdine against parasites.

Parasite	IC_{50}	SI
T.b. brucei	0.22	>345[b]
T.b. rhodesience	0.59	39[c]
T. Cruzi	0.23	99[c]
P. falciparum	7.8	_

[a] Values are the mean of 3 experiment, < ±50%
[b] Selectivty relative to HEK293 cells.
[c] Selectivty relative to L6 (rat skeletal myoblast) cells.

Furthermore, compound **83** also showed favourable physicochemical properties suitable for early oral druglikeness including a moderately low molecular weight (339.73 g/mol), acceptable polar surface area of 81 $Å^2$ and an excellent cLogP of 2.6, and calculated aqueous solubility is extraordinary low (25 nM). It has 6 hydrogen bond acceptors and one hydrogen bond donor. These characteristics correspond to the well-known Lipinski's Rule of Five [4] for the assessment of druglikeness, namely: not

to exceed five hydrogen donors; no more than ten hydrogen bond acceptors; a molecular mass of less than 500 Daltons and an octanol-water partition coefficient log *P* not greater than 5.

Herein, in connection with the baell group compound ***83*** *was selected for optimisation and design of similar analogues to fulfil the need for a SAR as required to pursue improvement in the trypanocidal activity against parasites, which will be the discussion of the following chapters.*

1.5.2 Oxazolopyridine and the importance of SIRT1 in trypanosomes

The lead compound **83** belongs to a compound class that activates the NAD^+ dependant deacetylase sirtuin or silent information regulator 2 (SIR2) enzymes. Activation of SIRT1 by oxazolopyridine derivatives and related compounds has been reported as a novel approach for drug discovery (e.g. type-2 diabetes and other metabolic disorders) [55]. These enzymes are unique because they are dependent on NAD^+ to catalyse acetyl-lysine deacetylation processes (Figure 32) rather than Zn^{2+}, unlike other related histon deacetylase enzymes.

They are considered a conservative family of enzymes found in all living beings , ranging from bacteria to humans. Interestingly, a recent finding reports sirtuins in many human parasites including plasmodium (malaria) [56] and trypanosomes [57]. Silent regulator 2 or SIR2-like proteins have been implicated in a wide range of cellular events in humans such as gene silencing, chromosome segregation, DNA repair, DNA replication and plasmid segregation [57], and was found in *T. brucei.* Three Sirtuin proteins were identified in *T brucei*: TbSIR2rp1, which is found primarily in the nucleus and is responsible for histone modification, while TbSIR2rp2

and TbSIR2rp3 are located in mitochondria. Garcia-Salcedo *et al* [57] found that SIR2 homologue TbSIR2rp1, is involved in response to DNA damage. For example, treatment of trypanosomal nuclei with a DNA alkylating agent such as methyl methanosulfonate (MMS), which generates DNA legions, corresponds with the TbSIR2RP1 expression.

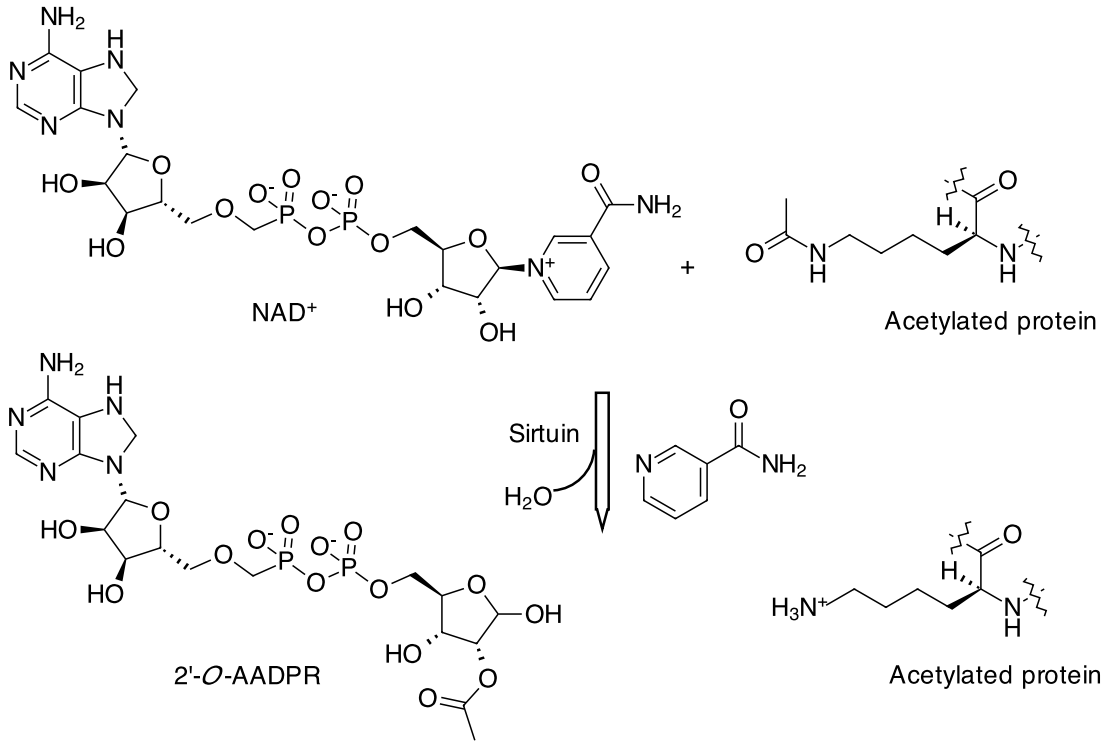

Figure 32. A schematic representation of the sertuin-catalysed deacetylation reaction.

NAD+, β-nicotinamide adenine dinucleotide; 2'-O-AADPR, 2'-acetyl-ADP-ribose.

SIR2rp1 overexpression is thought to be toxic in *T. brucei* due to unsuitable de-acetylation of cytosolic substrates or hypo-acetylation of nuclear substrates. Garcia-salcedo *et al* found that SIR2rp1 overexpression did not exhibit toxicity in the insect-stage of *T. brucei* life-cycle [57]. They found that a reduction in the level of TbSIR2RP1 led to increased sensitivity to the DNA alkylating agent MMS, while

overexpression led to an increase in resistance to the agent [57]. This has confirmed the role of SIR2rp1 in DNA repair at the cellular insect-stage and might play a similar role in bloodstream form of mammalians infected with *T. brucei* [57]. However, the mechanism behind the SIR2 in trypanosomes is not fully understood and information discussed here in this thesis is the only available to date. Moreover, SIR2rp1 substrates have not yet been defined. A review by Zheng, W [56] suggests that sirtuin might emerge as a new target for antiparasitic drugs, including trypanosomes. However, there are no further reports regarding any sirtuin inhibitors with antitrypanosomal activity to date.

1.5.3 Other biological activity for oxazolopyridine

The oxazole ring system is a rigid and stable moiety that is often found in natural products and incorporated widely with other heterocycle in medicinal chemistry such as pyridine. Analgesics, antipyretic and antinflammatory [58], antimicrobial [59,60], antifungal [61], and anticancer activities [62] of pyridooxazole derivatives and/ or related compounds have been reported.

This is not surprising, particularly with oxazolopyridine core as it has an additional advantage from a medicinal chemistry point of view, since the pyridine portion may provide better water solubility with its additional site for protonation and salt formation or it could improve intermolecular interactions with a target protein by formation of an additional hydrogen bond [63]. In one instance, antifungal activity was reported by Sener *et al.* [61] including SAR for some benzoxazole and oxazolo[4,5-*b*]pyridine against *C. Albicans*.

Imidazopyrdine derivatives are an important class of heterocyclic compounds that is part of vitamin B_{12} structure. In addition to that, parasitic infection is one of the health-related arenas that has benefited greatly from the use of this class of heterocycles. In particular, benzimidazoles are well known as a class of broad spectrum anthelmintic (i.e kill parasites) such as the marketed compounds oxfendazole, fenbendazole and flubendazole, which are effective against GIT and parasites and are mainly used for the protection of livestock [64]. In another instance, Keurulainen *et al.* [65] found that a number of 2-arylbenzimidazoles (analogue of our lead compound **(83)** were active against *Chlamydia pneumonia*, which is an intracellular bacterium known to respond poorly to antibiotic treatment, leading to chronic infection, and also linked to asthma, atherosclerosis and Alzheimer's disease [65]. Most of these studies were extensively carried out on benzoxazoles and benzimidazoles analogues while the oxazolopyridine moiety is by far less common in the literature.

1.6 This Study

In addition to the above-mentioned review of the literature, this thesis describes the design, synthesis and characterisation of 20 novel compounds, which were prepared in our lap and combined with compounds prepared by the Baell group at Monash Institute of Pharmaceutical Sciences, Monash University and these compounds were tested against *T. brucei* at the *Eskitis* Institute for Cell and Molecular Therapies, Griffith University. The synthesised compounds along with their intermediates containing the amine were also to be tested (by A/prof Nuri Geuven, at the school of medicine at University of Tasmania to survey the DNA damaging potential of these compounds.

Initial Plan:

To the best of our knowledge, at the time this study was initiated there was no report on oxazolopyridine compounds, represented by our lead compound **83**, with anti-trypanocidal activities against the *T. brucei* parasite.

The general aim here was to obtain structural information of importance for *T. brucei* inhibition and to elaborate the plan based on activity data collected during this study. It was hoped that an increase in activity will be achieved relative to the lead

compound **83**. The proposed structural modifications are summarised in Figure 33 which involves changes to the central phenyl ring, heterocycle core and investigation of substituents effect.

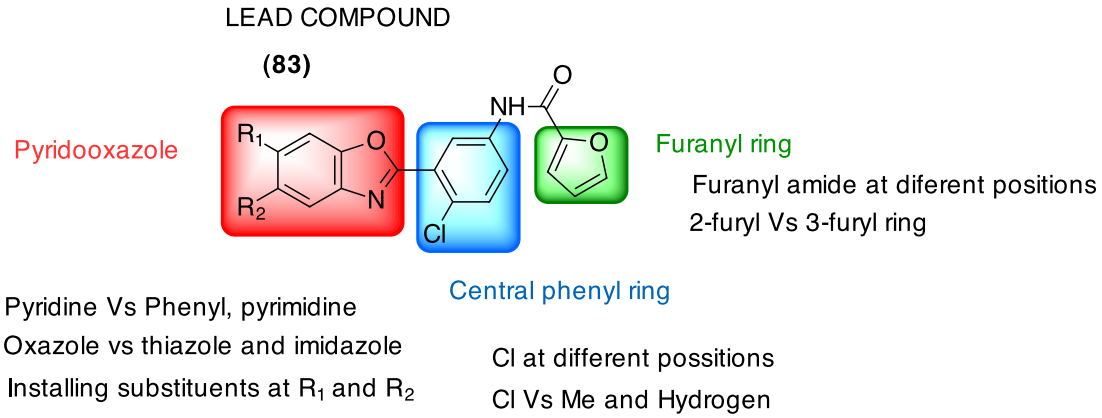

Figure 33. Synthetic plan for similar analogues of **(83)** [a]

In order to gain SAR data for further development of *T.b. brucei* inhibitors, the following were to be explored by targeting

a) The central phenyl ring:

- The substitution of chlorine for a hydrogen or a methyl group
- Placement of chlorine into different positions
- Variation of the furancarboxamide positions from the *meta*, *ortho* and *para* positions

b) The furyl ring with a 3-furoic isomer was the only explored compound in this series, since this area was targeted more extensively by the J. Baell group

c) The oxazolopyrdine core

- The substitution of the oxygen in the oxazole by an NH or sulphur group to provide an imidazopyridine or thiazolopyridine analogue.

- Investigation of introducing substitutes (R_1 and R_2) on to the fused pyridyl ring of the oxazolopyridine system.
- The introduction of electron withdrawing (e.g. NO_2), electron-donating (e.g. MeO) and electronegative groups (e.g. Cl) will be also be investigated.

Oxazolopyridine analogues with substitution at R1 and/or R2 were planned, using bromine-substituted derivatives at these positions. These derivatives will also allow the synthesis of many compounds using palladium catalysed cross-coupling *via* a Suzuki coupling reaction and commercially available boronic acids such as furanylboronic acid.

The chemistry and synthesis of these compounds is discussed in Chapter 2 and the biological results for the antitrypanosomal activity and the DNA damaging activity are discussed in Chapter 3 and Chapter 4 of this thesis.

CHAPTER 2 Chemistry and synthesis of Oxazolopyridine and related compounds

2.1 Synthesis and Chemistry of oxazolopyridine and related analogues

To develop a synthetic scheme for the synthesis of analogues of compound **83**, a retrosynthetic analysis is presented (scheme 1) which indicates that the lead compound can be formed by two simple steps: (A) amide coupling reaction between aminophenyl oxazolopyridine **(91)** and 2-furoic acid **(92),** and (B) cyclic condensation/dehydration between 2-amino-3-hydroxypyridine **(94)** and a carboxylic acid **95,** through intermediate **93,** to produce the oxazolopyridine ring.

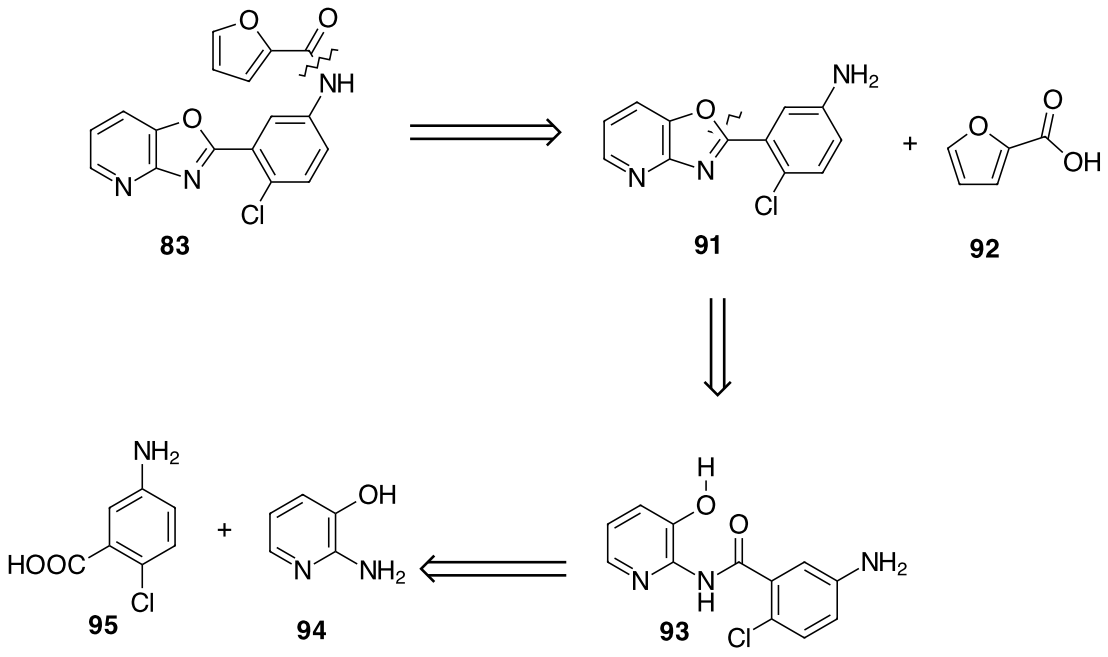

Scheme 1: Retrosynthesis analysis of the lead compound 83

Based on this, not only could the furanyl amide be targeted, but also the same method could be exploited to generate a series of analogues based on modification to a) the

position of the carboxylic acid on the furyl ring, b) the position of the amine on the central phenyl ring and c) changes to the pyridyloxazole core. These tasks constitute the initial plan for optimisation of the lead compound **83**. The modification around the central phenyl ring could be exploited using a variety of substituted benzoic acid derivatives. Therefore different benzoic acids, such as 6-chloro-2-nitrobenzoic acid, 3-chloro-2-nitrobenzoic acid and 2-chloro-3-nitro benzoic acid will be used.

Based on scheme 1, the rate-limiting step for the cyclisation between 2-amino-3-hydroxypyridine **94** and benzoic acid **95** to form oxazolopyridine **91** is the formation of an amide intermediate **93** (formed after the attack of the nucleophile NH_2 from 2-amino-3-hydroxypyridine **94** with the electrophilic carbonyl carbon of benzoic acid. Cyclisation and condensation are then facilitated in the presence of acidic media such as polyphosphoric acid, which is a classical reagent for oxazolopyridine formation, but high reactions temperature up to 160 - 220 ^{O}C are required [66].

In acidic media, the protonation of the carbonyl carbon occurs followed by the attack of the nucleophile to give a tetrahedral intermediate followed by elimination of water. The nucleophilic amine is anticipated to be also protonated but a small concentration is assumed to be present due to dissociation at higher temperature. As the amide is formed, the second step is simply acid promoted cyclisation. This method also applies to the synthesis of related analogues such as pyridothiazoles, and pyridoimidazoles if the appropriate 2,3-diaminopyridine or 2-amino-3-mercapto substrate is available.

2.2 Exploring alternative methods to form oxazolopyrdine

Traditionally oxazolopyridines have been synthesised by acid catalysed condensation of *2*-amino-3-hydroxypyridine with carboxylic acids and polyphosphoric acid [67] but trimethylsilylpolyphosphate [68] has also been used as the dehydrating agent at high temperatures. Polyphosphoric acid has been used extensively in synthesis including alkylation, acylation on aromatic and olfeinic reactions, Fischer-indole synthesis, dehydration, cyclisation, Beckmann and Schmidt rearrangements [69]. However, its high viscosity is a disadvantage that hinders it from being easily poured or stirred and gets very thick when cooled. In addition to that, the work up procedure is tedious [69] as it needs to be neutralised to isolate the product amines.

For the above reasons, we were initially interested to explore alternative methods to form the oxazolopyridine core. Therefore, we initially explored the use of a mixture of 1:10 solution of phosphorous pentoxide in methanesulfonic acid, which has been reported as a substituent reagent to polyphosphoric acid [69]. Unfortunately decomposition occurred when applied to 2-amino-3-hydroxypyridine and 2-chloro-5-nitrobenzoic acid.

An attempt to synthesise the pyridyloxazole core by a 2-step synthesis was also carried out through formation of an amide intermediate prior to the cyclisation. The amide intermediate (scheme 2) can be formed using an acid chloride or with a peptide-coupling agent, followed by a dehydration step promoting cyclisation. For this purpose, we initially tried to prepare the amide intermediates **98** and **99** using 1-ethyl-3-(3-dimethylaminopropyl) carbodiimide (EDCI) promoting amide coupling but

no reaction occurred with the starting material remaining unreacted, presumably due to poor solubility of the reactants.

Therefore, the acid chloride route was used instead. Acid chloride **96** and **97** was formed from the benzoic acid by oxalyl chloride in DMF. The acid chloride was then reacted with 2-amino-3-hydroxypyridine resulting in the formation of the amide intermediates **98** and **99** in 57 and 46 % yield.

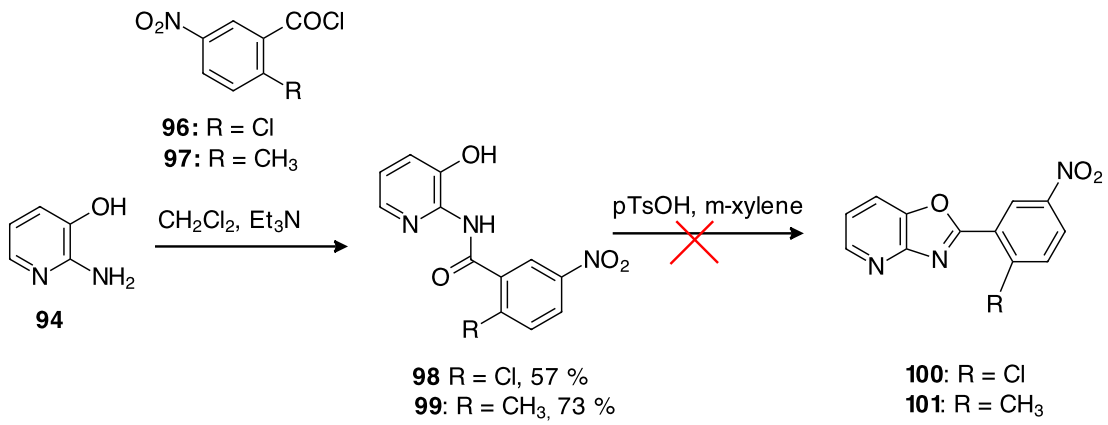

Scheme 2. Formation of pyridyloxazole *via* 2-steps synthesis

The ^{1}H NMR spectrum is comprised of the aromatic protons of the 3-phenyl methines and the 3-pyridyl methines, which resonates at 6.90 - 9.5 ppm. The amide derivatives **98** and **99** were characterised by a broad singlet for –NH proton at 9.5 ppm and 9.0 ppm in the ^{1}H NMR respectively. The three-methyl protons for compound **99** were observed as a singlet at 3.60 ppm. Compounds **98** and **99** both display two absorption bands at ~ ~3280 cm^{-1} and ~1655 cm^{-1} for the NH-stretch and the carbonyl of the amide group respectively. Similar compounds are reported in the literature with the same reaction condition as part of drug discovery of Sirtuin modulators [70] and antimicrobial agents [71].

With the pyridyl amide in hand, we attempted to explore the reported reaction for synthesis of benzoxazoles analogues using a method reported by Utter et al [72]. Therefore, the resulting pyridyl amides were treated under Dean-Stark conditions with m-xylene and *p*-toluene sulphonic acid monohydrate. However, the reaction was deemed unsuccessful with the starting material being isolated even after prolonged heating for 5 hours. Rather than attempt to optimise the procedure an alternative method was sought.

A one-pot microwave-assisted direct condensation of pyridyloxazole compounds in the absence of solvent and catalyst has also been reported [73]. Microwave assisted synthesis is often a convenient method that shortens the time of the reaction [73] and the absence of polyphosphoric acid simplifies the work up. Initially, we were interested to explore the microwave-assisted method published by Myllymaki [73], in which a benzoic acid and 2-amino-3-hydroxypyridine were reacted neat (without solvent) and heating at high temperature. To investigate this method, 2-amino-3-hydroxypyridine **(93)** with either 2-chloro-5-nitro-benzoic acid **84** or the *m*-aminobenzoic acid **101** was irradiated for (300 W) at 200 ^{0}C for 15 mins neat (with no solvent) in a CEM Discover microwave reactor (scheme 3). However, tar-like materials and decomposition occurred with no desired product being observed. This is similar to the results reported by Myllamiki *et al* [73] in which some compounds with electron donating groups have undergo decarboxylation rather than condensation (i.e 2- and 4-hydroxy and 4-dimethylaminebenzoic acids) while in many cases tar-like materials or the recovery of starting materials (i.e 2-chloro-, 4-acetyl- and *o*, *m* and *para* nitrobenzoic acids was observed. Therefore the microwave method is not suitable for amino or nitrobenzoic acids.

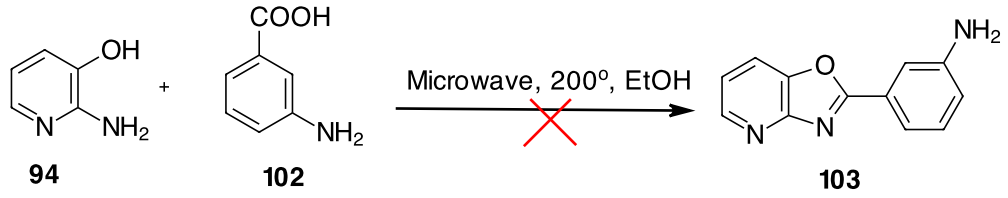

Scheme 3: Microwave assisted condensation reaction

The reaction was then repeated using ethanol as a solvent to help the dissolution of the starting materials with high melting point as a way of promoting the amide formation. However, after heating in a sealed tube in the microwave at 200 ^{o}C, the NMR data shows that another compound was formed instead of compound **103**. Reaction between the ethanol and the benzoic acid occurred exclusively giving ethyl 3-aminobenzoate. The ester could still be an acyl donor under microwave conditions but continued heating did not result in any further reaction. The modified method did not prove successful and therefore the common method of heating in polyphosphoric acid was used in the reminder of the process.

2.3 Modification to the central phenyl ring

The intermediate pyridinoxazole 3-(oxazolo[4,5-*b*]pyridin-2-yl)aniline **(103)**, was synthesised following the conventional method [70], as per the general reaction sequence in Table 3 using polyphosphoric acid as the catalyst and the solvent at 180 ^{0}C. After addition to ice and neutralising with solid sodium carbonate, the precipitate was filtered giving **103** a yield of 91%, which was used without further purification.

Table 3. Aminooxazolopyrdine intermediates

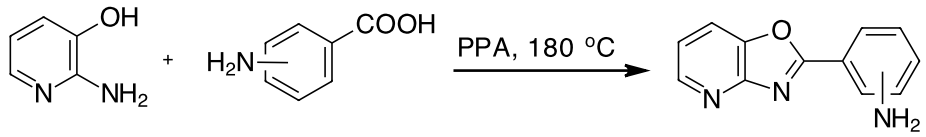

Product ID	Benzoic acid	Product	Yield	Ref
103	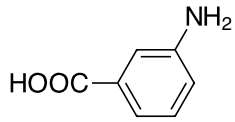	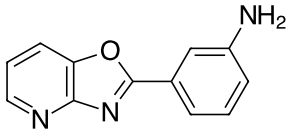	91 %	[67] [70]
104	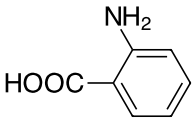	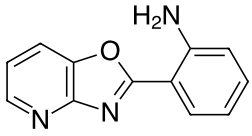	12 %	[67]
105	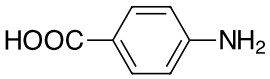	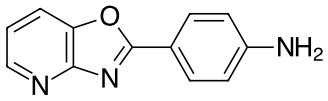	20 %	[67]

Two protons from the three-pyridyl methines of the aniline **103** were observed downfield at 8.20 ppm and 7.61 ppm as doublet of doublets in the ^{1}H NMR, while the remaining CHs: one pyridyl methine at four phenyl CHs were observed as one doublet of doublet of doublet at 6.63 ppm and 2 multiplets at 7.03 and 7.31 ppm. The amine was observed as a broad singlet at 3.32 ppm in the ^{1}H NMR and the IR supported the presence of the two NH-stretches for the amine group at 3453 cm^{-1} and 3328 cm^{-1}. Compound **103** has been reported previously in a patent for the synthesis of sirtuin modulators [70] but only MS data was given. The *ortho*- and the *para*-amino 2-phenyloxazolopyrdines **104** and **105** were obtained in 12 % and 20 % yield using the same reaction sequence (Table 3) and their structures were assigned by ^{1}H NMR, ^{13}C NMR and IR.

The amine protons were observed as a broad singlet in 6.30 ppm and 4.50 ppm by NMR for compounds **104** and **105** respectively and both were also characterised by 2-NH stretch at ~ 3400 and 3300. Compounds **103 – 105** were first reported in 1985 as precursors for the synthesis of dyes and pigments [66] but no structural data was available apart from their melting point which are in agreement with our results.

Similar compounds were synthesised using the appropriate nitro-benzoic acid derivatives giving compounds **106**, **107** and **101** in 60 %, 70 % and 82 % yield following the same sequence in Table 3. Briefly, cyclisation of nitrophenyl-pyridyloxazole derivatives were made from 2-amino-3-hydroxypyridine **93** and the appropriate nitrobenzoic acid derivatives as the corresponding amines derivatives were not commercially available but nitro derivatives were available. The reduction of the nitro group was achieved by a mild procedure using iron powder in a solution of hydrochloric acid in refluxing ethanol, reported for the reduction of nitro-substituents on the central phenyl of pyridyloxazole [72]. The reduction of the nitro group gave the amine derivatives **110**, **111** and **112** in 66 %, 61 and 54 % yield after flash chromatography (Table 4).

^{1}H NMR and IR supported the accomplishment of the nitro reduction. The two-amine protons were observed at 4.50 ppm and 4.25 ppm as a broad singlet for derivatives **110** and **111** while they observed at 7.57 ppm for derivative **112** as a defined singlet in the ^{1}H NMR. The IR showed the typical characteristic of the two NH-stretches for the amino group at ~ 3200 and 3360 cm^{-1} for compounds **110, 111** and **112**. Mass spectrometry indicated two molecular ions observed at 245 and 243 with the 1:3 ratio supporting the presence of chlorine for compound **110** and **111** respectively.

Table 4. Nitrooxazolopyridine precursors and their reduced amine product

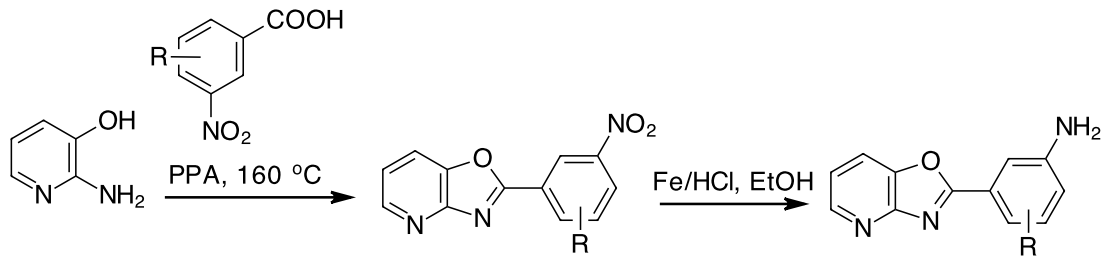

ID	Product	Yield	ID	Product	Yield
106	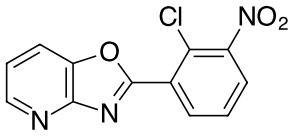	60 %	**110**	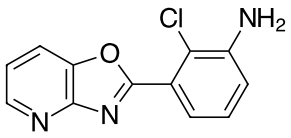	66 %
107	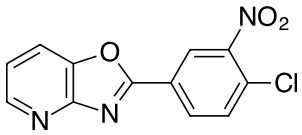	70 %	**111**	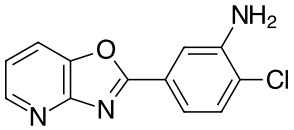	61 %
101	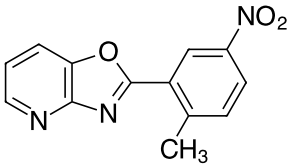	82 %	**112**	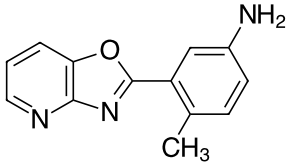	54 %
108	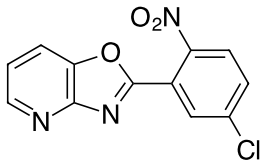	0			
109	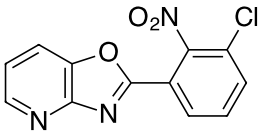	0			

The polyphosphoric acid method was also applied to the synthesis of pyridoxazole derivatives **108** and **109** (Table 4) from *ortho*-nitro benzoic acid derivatives and 2-amino-3-hydroxypyridine. However, the reaction was not successful, presumably due to stereo-hindrance of the nitro group adjacent to the carboxylic acid. Nunes *et al* [70]

reported the synthesis of similar compounds to derivatives **108** and **109** with the *ortho*-nitro substituents but *via* two steps: starting with a) the formation of the pyridyl-amide intermediate (from the coupling reaction of 2-amino-3-hydroxy pyridine with benzoyl chloride) and b) treating the resulting pyridyl-amide with polyphosphoric acid to furnish its cyclisation into oxazolopyridine. Therefore, we anticipate that the formation of the pyridyl-amide (the limiting step) does not occur under the acid catalysed conditions with polyphosphoric acid when the *ortho*-nitro benzoic acids are used.

With the pyridoxazole cores in hand, the initial target compounds could be achieved by forming an amide from the amino group. The amide derivatives **113** and **114** were formed *via* coupling 3-(oxazolo[4,5-*b*]pyridin-2-yl)aniline **(103)** with the 2-furoic and 3-furoic acid using the peptide-coupling agent EDCI (Method A). Progress of the reaction was monitored by TLC and showed disappearance of the aniline **103** after 20 hours and formation of a less polar products in each case. Final products were purified by flash chromatography yielding the amides **113** and **114** in good yields of 83 % and 76 % respectively. Compound **113** and **114** were characterised by ^{1}H NMR, ^{13}C NMR, IR and MS. For the amide **113** (Figure 34), the two respective furyl methines H_e and H_f that are not adjacent to the furyl-oxygen resonated upfield as a doublet of doublets at 6.24 ppm (H_e) and a doublet at 7.28 ppm (H_f). The furyl methine H_d that is adjacent to the furyl-oxygen resonated as a doublet at 8.20 ppm. The three-pyridyl methines resonated at 7.58 ppm (H_b, dd, J = 8.1, 0.9), 7.71 ppm (H_a and H_c, dd, 2H). The four phenyl CHs resonated at 6.99 (m, 2 H), a triplet at 7.17 ppm and a singlet at 8.38 ppm. The NH for the amide **113** and **114** were observed

downfield at 9.55 and 8.28 ppm in the ^{1}H NMR as compared to those of the amine intermediates, respectively.

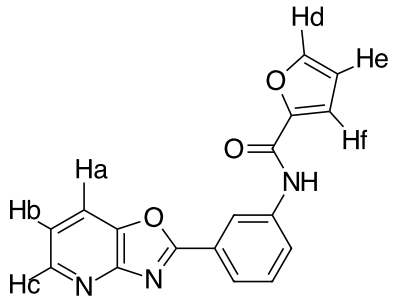

113

Figure 34. Protons numbering for assigning the ^{1}H NMR for compound **113**.

IR was particularly useful as the disappearance of the NH-stretch of the intermediate amine at ~ 3300 and ~ 3400 cm^{-1} and the appearance of the NH-stretch of the amide and the carbonyl (C=O) peak indicated the reaction had proceeded as desired. Both **113** and **114** show characteristic of the amide NH-stretch at 3287 cm^{-1} and 3321 cm^{-1} respectively and the amide carbonyl stretch at 1650 cm^{-1} and 1676 cm^{-1} respectively. Mass spectrometry analysis revealed the presence of the correct molecular ions, and the expected fragmentation patterns (eg. cleavage of the furylamide) for each molecule.

The amides **115** and **116** of the pyridoxazole ortho-amine derivatives were initially formed by the amide-coupling reaction using EDCI but the attempt was not successful with the starting material being recovered. Alternatively, these compounds were synthesised from their *ortho*-amine derivatives with the corresponding acid chloride (method B) giving a yield of 59 % and 13 % respectively.

The *para*-derivative **(117)** was made from the coupling of oxazolopyrdine amine intermediate with 2-furoic acid chloride yielding the product in 59 % yield after flash chromatography.

Mass spectrometry analysis revealed the presence of the correct molecular ions, and the expected fragmentation patterns (eg. cleavage of the furylamide) for each molecule.

Table 5. List of compounds formed from amide coupling reaction

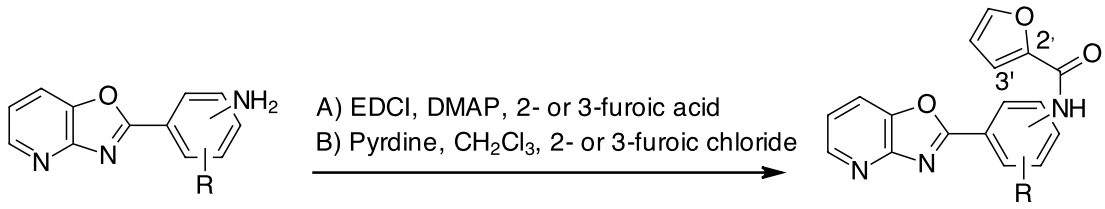

ID	Intermediate	Furoic acid	Method	ID	Product	Yield
103	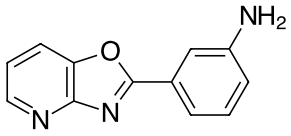	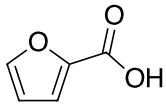	A	**113**	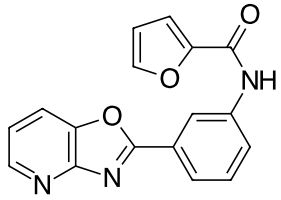	83 %
103	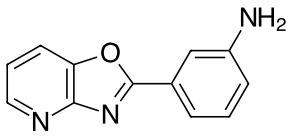	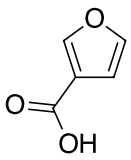	A	**114**	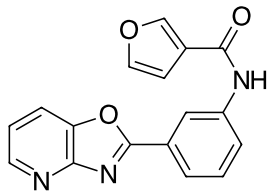	76 %
104	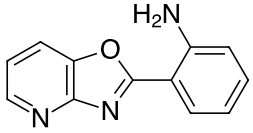	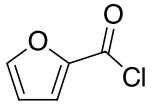	B	**115**	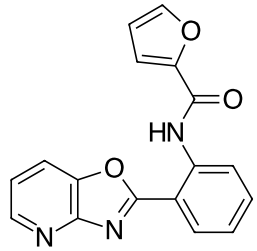	59 %

104	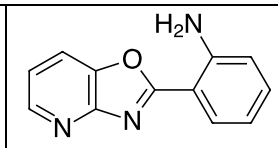	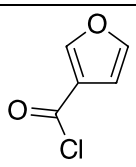	B	**116**	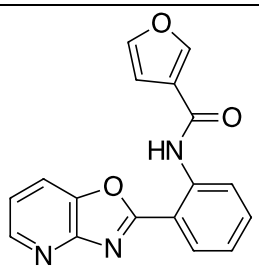	13 %
105	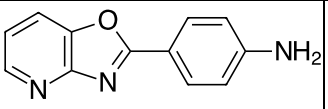	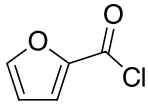	B	**117**	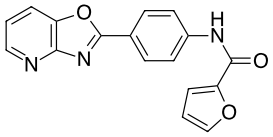	59 %
110	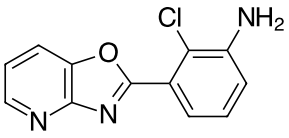	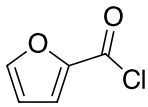	B	**118**	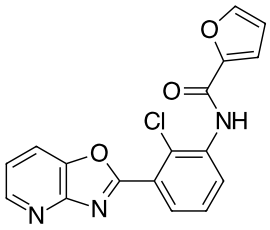	54 %
111	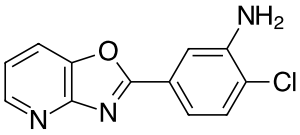	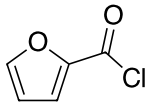	B	**119**	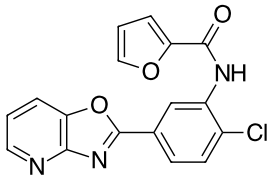	47 %
112	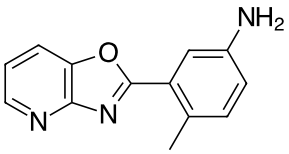	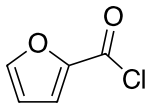	B	**120**	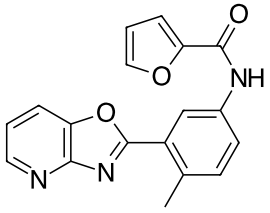	42 %

The EDCI-mediated amide coupling between halogenated pyridoxazole **110**, **111** and **112** and furyl benzoic acids were not successful, presumably due to steric effect of the adjacent halide (except for **112**). Therefore, the corresponding acid chloride was used instead resulting in the derived products **118**, **119** and **120** (Table 5), although a number of undesired side products were also observed. The crude samples were

purified by flash chromatography yielding the desired products in 54%, 47%, and 42 % yield. The products were characterized by 1H NMR, ^{13}C NMR and MS. Mass spectrometry analysis revealed the presence of the correct molecular ions, and the expected fragmentation patterns (eg. cleavage of the furylamide) for each molecule. It has also indicated two molecular ions observed at 304 (M^+, Cl^{35}) and 302 (M^+, Cl^{37}) with the 1:3 ratio supporting the presence of the chlorine for derivatives **118** and **119**.

2.4 Modification of the fused system of oxazolopyridine ring

To further establish SAR of the lead compound **83,** it was was required to make modification of the oxazolopyridine ring. Therefore, an imidazopyridine was synthesised and the the 2- and 3-furylamides were targeted.

The intermediate 3-(1H-imidazo[4,5-*b*]pyridine-yl)aniline **122** (Scheme 4) was formed from heating 2,3-diaminopyridine **(121)** and 3-aminobenzoic acid **(102)** with polyphosphoric acid at 220 ^{o}C for 6 hours, giving the crude product in 70 % yield. It should be noted here that neutralisation with NaOH is preferable to using solid sodium carbonate for the neutralisation as workup is achieved much quicker as there is no gas evolution. The three-pyridyl methines and the four phenyl CHs for 3-(1H-imidazo[4,5-*b*]pyridine-yl)aniline **(122)** were observed as a doublet at 6.71 (d, J =7.6 Hz, 1H), a multiplet of overlapping signals at 7.19 (m, 3H) and a doublet at 7.33 ppm (d, J = 7.1,1H), and a singlet observed downfield at 7.46 (s, 1H) and a broad singlets at 8.29 (bs, 1H). The imidazole –NH resonated at 7.95 ppm as a broad singlet. The two protons for the amine were observed at 5.05 ppm as a broad singlet in the ^{1}H NMR. In the IR the NH stretch for the amine protons were observed at 3303 and 3465 cm^{-1} and the imidazole –NH was observed at 3184 cm^{-1}.

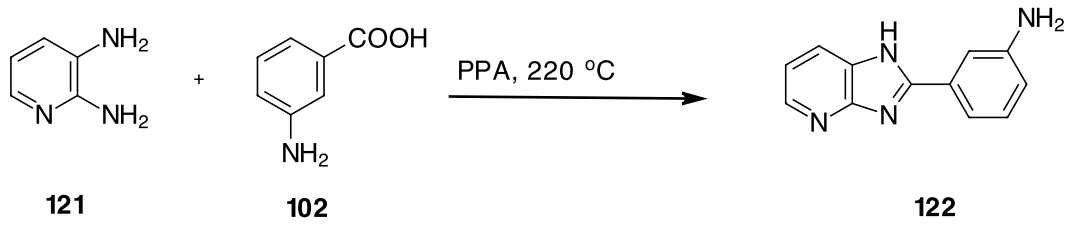

121 102 122

Scheme 4. Formation of Imidazopyrdine intermediate

The pyridoimidazole **122** was reported in 1988 as a precursor for the production of dyes and pigments [74] and by Bemis et al for the design of Sirtuin modulators [55] but no structural data was given. Imidazopyrdines derivatives **(123)** and **(124)** were prepared using pyridoimidazole **(122)** and furoyl chloride (Table 6) using method C in Table 6.

Table 6. Imidazopyridine derivatives

Intermediate	Furoic acid	Method	ID	Product	Yield
122	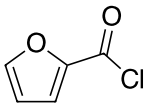	Pyridine CH2Cl2	**123**	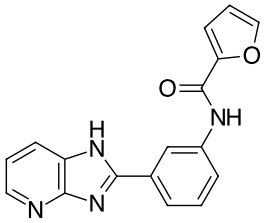	0
122	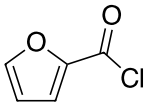	Triethylamine THF	**123**	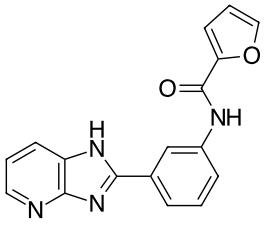	48%

122	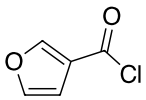	Triethylamine THF	**124**	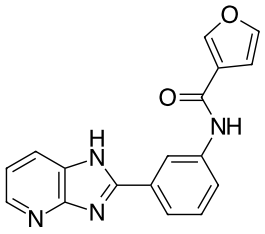	44%

Earlier attempts to make **123** using the acid chloride (method B, Table 5) were unsatisfactory as numerous compounds were formed. It was proposed that acylation may have occurred on the nitrogen of the imidazole resulting in a complex acylation mixture and difficult separation to isolate the product. Therefore, the conditions were modified using triethylamine (1.5 eq) instead of pyridine and 1.2 equivalent of acid chloride in THF (Table 6), which gave the derived compounds **123** and **124** in 48% and 44% yield, respectively. Compounds **123** and **124** structures were supported by ^{1}H NMR, ^{13}C NMR and IR. The ^{1}H NMR showed the imidazole and the amide –NH protons resonating at 8.10 ppm and 9.33 ppm as a singlet for compound **123**. Compound **124** is characterised by the amide –NH proton at 10.15 as a singlet while the imidazole –NH proton was observed but in an overlap with another proton signal. The IR showed the presence of the amide carbonyl stretch NH at 1655 and 1650 cm^{-1} respectively.

We were also interested to prepare thiazolopyridine derivatives but the required starting materials were not commercially available and therefore were not investigated due to time constraints.

2.5 Substitution of the pyridine ring on the oxazolopyrdine core

Given the initial results of the biological assays for our first set of pyridoxazole derivatives with the investigation centred around the central phenyl ring (discussed in Chapter 3), we became interested to explore the effect of substituents at C6 and C5 positions (R_1 or/and R_2) of the fused pyridoxazole core on activity. The initial goal was to synthesise bromine-substituted compounds, at C5 and C6 of the fused pyridyl ring, accordingly to our developed plan (scheme 5) and to carry out substitution of the halogen with other functional groups.

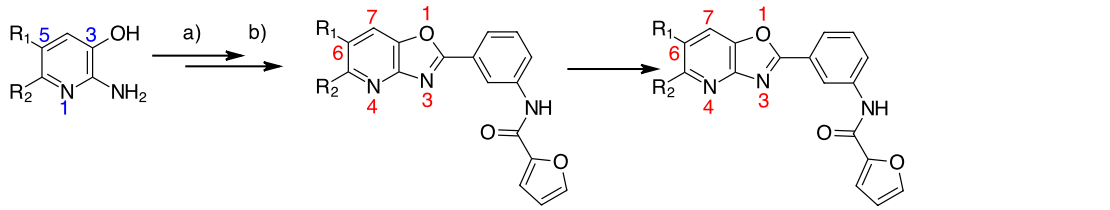

Scheme 5: substitution of oxazolopyridine at R_1 or R_2 position and possible derivatives that can be obtained from replacement of bromine; a) oxazolopyridine synthesis, b) amide coupling

These potential functional group transformations may include introduction of amino [75], methyl [76], cyano [76-78], phenoxy [76], and methoxy [77] groups which are often exploited as part of SAR studies [76]. To explore the effect of the presence of aryl groups on activity, Suzuki–Miyaura reaction [79] with available aryl-boronic acids building blocks can also be exploited.

To our knowledge there is only 2 reports the of pyridoxazole with substituents (i.e bromine, aryl) installed on C5 or C6 in the literature, (Figure 35): a) by Viaud *et al.* [79] in 1995 on 6-bromo-2-phenyloxazolo[4,5-*b*]pyridine **(125)** and b) by O'Donnell et

al. [76] in 2010 4-(6-bromooxazolo[4,5-*b*]pyridin-2-yl)-1,4-diazabicyclo[3.2.2]-nonane **(126)** as part of a drug discovery project for the design of modulator of the nicotinic acetylcholine receptor agonist for the treatment of cognitive disorders in schizophrenia. The synthesis of bromo-pyridoxazoles **125** and **126** were also targeted by the two previous reports for the synthesis of other derivatives (i.e aryl formation) using known coupling methods such as Suzuki-Miyaura reaction. Therefore this has prompted us to investigate the introduction of bromine onto C5 and C6 position of our pyridoxazoles **113** and **114**.

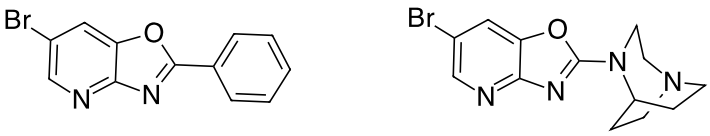

125 **126**

Figure 35. Previously reported pyridoxazoles with halogen substituents

Synthesis of the substituted pyridoxazoles from halogenated 2-amino-3-hydroxypyridine is required as the starting material. However, 2-amino-3-hydroxypyridine with a halogen on the 6- and 5-position is not commercially available. 2-Bromo-5-hydroxy-6-aminopyridine can be formed in two steps using a reported procedure for the synthesis of 6-bromo-2-nitro-3-pyridinol **(128)** [80]: Briefly 2-nitro-3-pyridinol (**127**) can be treated with a solution of NaOMe in MeOH to deprotonate the pyridinol followed by electrophilic bromination by adding bromine. Then the resulting 6-bromo-2-nitro-3-pyridinol **(128)** then can be reduced using standard methods such as Fe/HCl mediated reduction of the nitro group or catalytic hydrogenation using Pd/C. Subsequently, **128** can be used to target new derivatives of oxazolopyridine with the bromine installed at the 5-position of the fused pyridoxazole system. Bromine can be then exploited for metal-mediated coupling reaction with

boronic acid building blocks. Further to this, bromine can further investigated for other functional group transformation as proposed in our initial reaction sequence (scheme 5). However, due to time constraints, the proposed 5-substituted pyridoxazoles were not investigated and only the 6-substituted pyridoxazoles were investigated in this thesis.

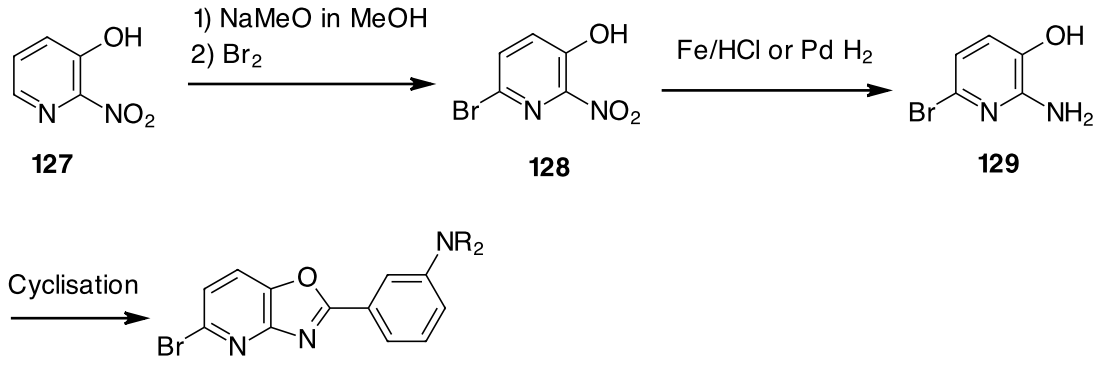

Scheme 6. Proposed scheme for the formation of pyridoxazole substituted on C5 of the fused system

Therefore our initial plan was to prepare 5-bromo-2-amino-3-hydroxypyridine (**132**) and 6-bromo-[4,5-*b*]oxazolopyridine-2-yl)-phenylamine **135** on a large scale as the latter is our key intermediate.

Therefore, 5-bromo-2-amino-3-hydroxypyridine (**132,** scheme 7**)** was prepared according to the literature [81] [79] in three steps: a) starting with carbamate **130**, a masked form of 2-amino-3-hydroxypyridine **(93)**, formed by the reaction with carbonyldiimidazole (CDI); b) bromination of the carbamate **130** to form 6-bromooxazolo[4,5-*b*]pyridine-2(3H)-one **(131);** c) an alkaline hydrolysis of **131** to give 5-bromo-2-amino-3-hydroxypyridine **(132)** in 65 % total yield (Scheme 7).

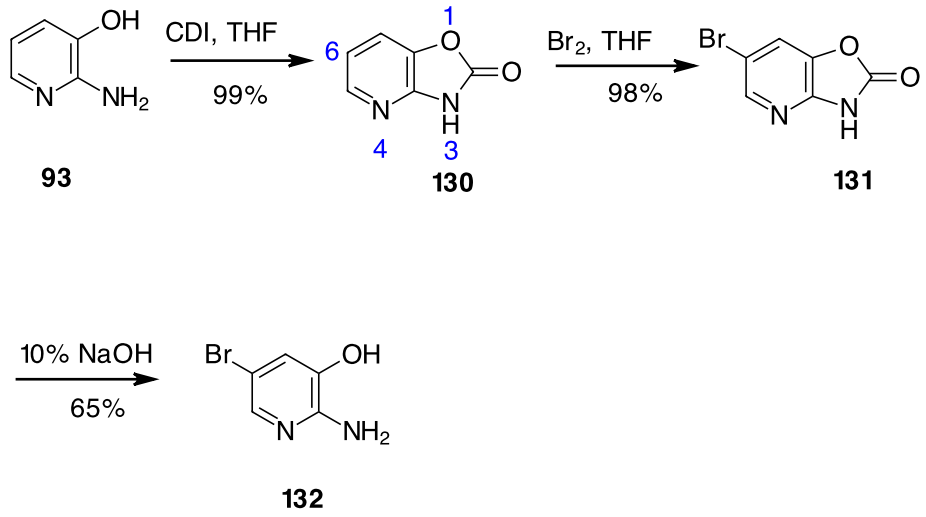

Scheme 7: Bromination at C5 of 2-amino-3-hydroxypyridine

Direct bromination on 2-amino-3-pyridinol is not selective due to the potential for random bromination [82]. Therefore the indirect bromination on the carbamate **130** is a better method for selective bromination at the 5-position [79]. Based on the method by Flouzat *et al.*, [81] the first step was made by treating 2-amino-3-hydroxypyridine with carbonyldiimidazole (CDI) **(133)** and refluxed at 70 ^{o}C for 6 hours giving **130** in one-step at 99% yield. CDI is used as a source of carbonyl that is attacked by the nucleophilic NH_2 from 2-amino-3-hydroxypyridine to give an intermediate urea **134**. Then cyclisation of urea **134** occurs due to the attack of the hydroxyl group lone pair to the carbonyl group and the subsequent elimination of imidazole (Scheme 8).

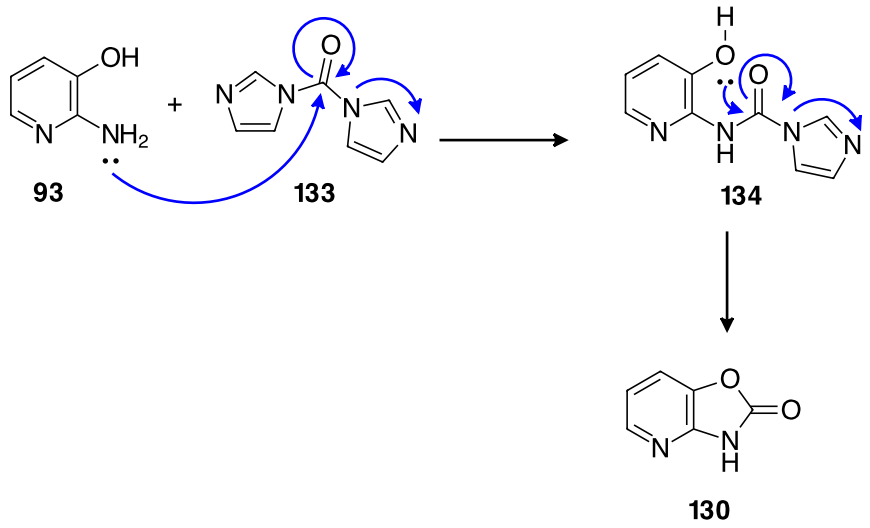

Scheme 8. Using carbonyldiimidazole as a carbonyl donor

The ^{1}H NMR for **130** showed the three-pyridyl methines resonating at 7.04 as a doublet of doublet and two doublets at 7.52 ppm and 7.94 ppm respectively. The IR was a useful technique in characterising **130** as the disappearance of the 2 –NH stretchs of the starting material amine and the appearance of the amide NH stretch and the carbonyl signal at 2972-3090 (broad) cm^{-1} and 1793 cm^{-1} respectively were very diagnostic and in agreement with literature [81]. The ^{13}C NMR showed the presence of 3 quaternary and 3 non-quaternary carbons as supporting the formation of the cyclised amide.

The desired mono-brominated carbamate **131** was supported by ^{1}H NMR, ^{13}C NMR and IR. The ^{1}H NMR for **131** showed the characteristics of two doublets at 7.98 ppm and 8.15 ppm with a coupling constant of 2.1 Hz indicating a meta coupling between the two methines at C5 and C7 of the fused pyrido-carbamate and in support that they are from the desired product **130.** Thereby this supports that the bromination occurred exclusively at the 5-position. The ^{13}C NMR showed the presence of two quaternary and four non-quaternary carbons. The IR and the melting points are in agreement

with literature [81]. Then alkaline hydrolysis was carried out on **131** to give 5-bromo-2-amino-3-hydroxypyrdine **(132)** in 65 %. In the IR the amine –NH stretch for **132** was observed at 3340 $cm^{-1}$and 3438 cm^{-1}. The two –NH for the amine were observed as singlets at 5.70 ppm, and the two-pyridyl methines resonated at 6.93 ppm and 7.44 ppm as singlets in the ^1H NMR for **132**. The melting point for **132** was also in agreement with the literature [79].

6-Bromopyridooxazole **135** (Scheme 9) was synthesised using polyphosphoric acid by heating s at 160 ^oC. However, the reaction required longer reaction time of 20 hours for complete consumption of the starting material giving **135** in 35% yield, which was used without further purification. The ^1H NMR of compound **135** showed the two pyridyl methines resonating at 8.59 ppm and 7.89 ppm as doublets with a coupling constant of 2.1 Hz. The four phenyl CHs for **135** were observed as a multiplet, a triplet and a doublet of doublets at 7.6 ppm, 7.29 ppm and 6.89 ppm respectively in the ^1H NMR spectrum. The amine protons were observed at 5.23 ppm as a broad singlet in the ^1H NMR spectrum. Mass spectrometry indicated two molecular ions observed at 289 m/z (Br^{79}) and 287 m/z (Br^{81}) with the 1:1 ratio supporting the presence of bromine. The two –NH stretches for the amine group was observed at 3342 cm^{-1} and 3440 cm^{-1} respectively supporting the presence of the amine.

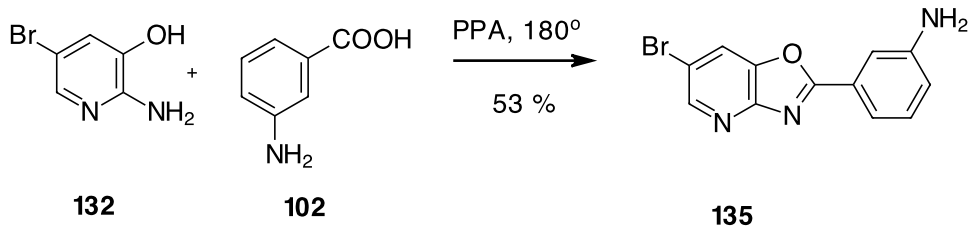

132 **102** **135**

Scheme 9. Synthesis of brominated oxazolopyrdine at C6

The amides **136** and **137** were formed from reaction of 6-bromo-pyridoxazole amine **(135)** with 2-furoic acid and 3-furoic acid in EDCI giving the desired products in 60% and 50 % yield after flash chromatography.

Table 7. The amide formation

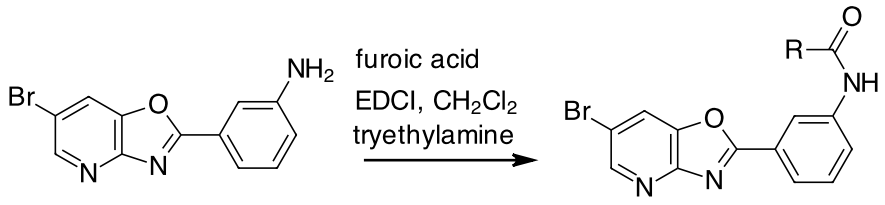

ID	R	Product	Yield
136	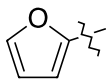	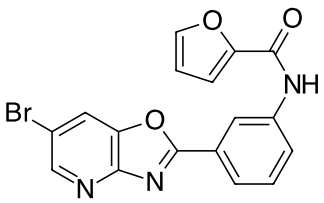	60%
137		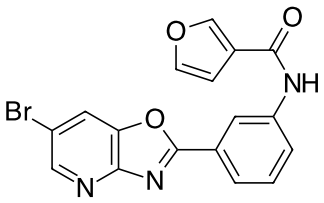	50%

The compounds were assigned the structure of **136** and **137** by analysis of the ^{1}H NMR and ^{13}C NMR, IR and MS spectra of both compounds. Compound **136** showed a resonance consistent with the two respective pyridyl methines H_a and H_b at 8.64 ppm and 8.50 ppm as doublets with coupling constants of 2.1 Hz indicating a meta coupling between the respective pyridyl methines. The amide –NH was observed as a singlet at 8.30 ppm. Two of the methine protons for the furyl were observed upfield as a doublet of doublets and a doublets at 6.60 ppm (H_d) and 7.30 ppm (H_e) respectively,

while the third methine (H_c) adjacent to the furyl-oxygen resonates at 8.03 ppm (is overlapped with the protons of the phenyl group).

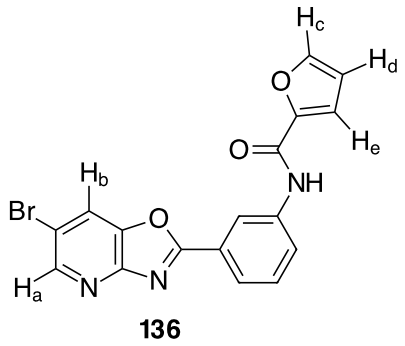

136

Figure 36. Proton numbering for assigning ^{1}H NMR for compound 136

The IR indicated the presence of the two diagnostic IR bands of the –NH and the carbonyl stretch for the amide compounds **136** and **137** at ~ 3300 cm^{-1} and ~ 1650 cm^{-1}. Mass spectrometry indicated two molecular ions observed at 384 m/z (Br^{79}) and 386 m/z (Br^{81}) with the 1:1 ratio supporting the presence of bromine.

Using the Suzuki-Miyaura reaction, compounds **136** and **137** were reacted with different aryl boronic acids, such as *p*-methoxyphenyl boronic acid, in the presence of Pd (0) catalyst to give the 6-arylpyridoxazoles as shown in Table 8. The Suzuki-Miyaura reaction proceeded well for compounds **138-141** to give the desired products in 90 to 33 % yield after flash chromatography, but was not successful when applied to the furan boronic acid. Structural assignment for compounds **138-141** were supported by ^{1}H NMR, ^{13}C NMR, IR and HRMS. Molecular mass and formula for these compounds were supported by HRMS.

Table 8. List of compounds made by suzuki reaction

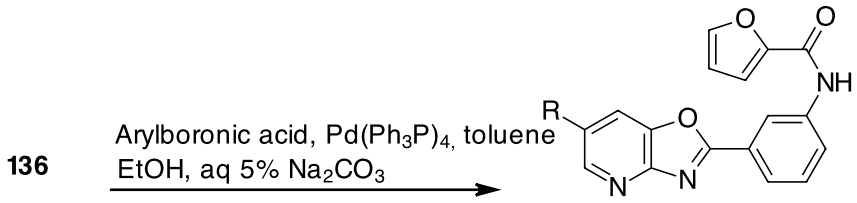

ID	Boronic acid	Product	Yield
138	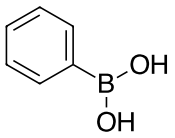	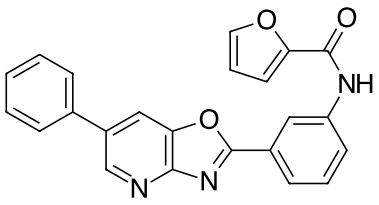	90 %
139	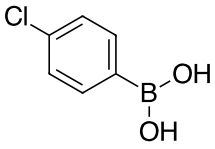	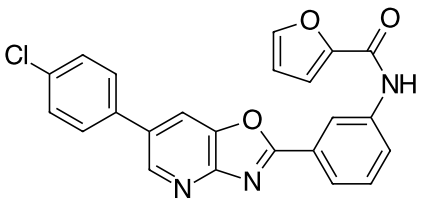	69 %
140	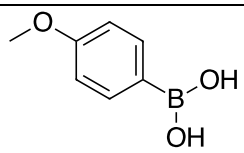	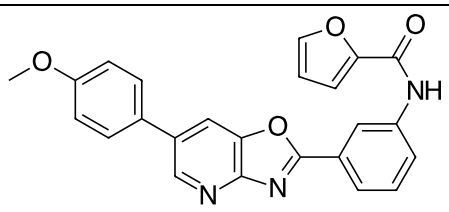	33 %
141	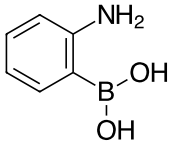	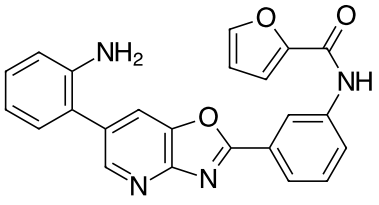	53 %
142	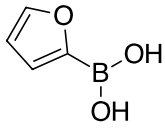	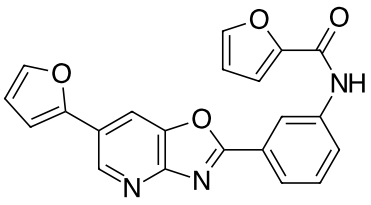	0

For example, the ^{1}H NMR of compound **140** (Figure 37) showed the incorporation of the aryl group as the aromatic methines H_a and H_b were observed at 7.05 ppm and 7.65 ppm as a doublet and a multiplet with the latter in overlap with a three CHs from the central phenyl ring. The methine between the two substituents on the central phenyl ring was observed as a singlet at 8.52 ppm. The two-pyridyl methines H_c and H_d were observed at 8.78 ppm and 7.98 ppm as a doublet with a coupling constant of 2.00 Hz in the ^{1}H NMR spectrum. The three-furyl methines resonated as a multiplet at 8.12 ppm (H_e) and two doublet of doublet at 6.60 ppm (H_f) and 7.30 ppm (H_g). The three protons for the p-methoxy group were observed at 3.89 ppm. The –NH of the amide was observed at 8.28 ppm as a broad singlet in the ^{1}H NMR.

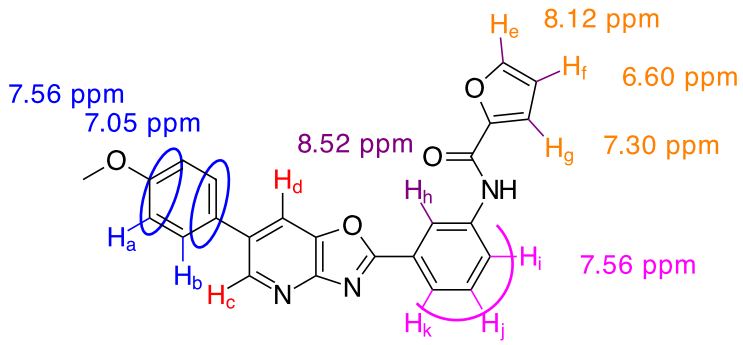

140

Figure 37. HNMR for compound **140**

Also 3-furoyl amide derivatives of the 6-aryl substituent was prepared following the same conditions as in table 8 but using brominated pyridoxazole **(137)** giving compounds **(143-145)** in 48 %, 60 % and 47 % yield respectively (Table 9).

Table 9. List II of compounds made by suzuki reaction

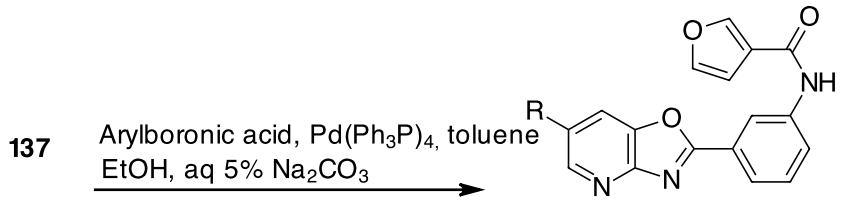

ID	Boronic acid	Product	Yield
143	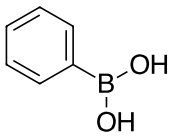	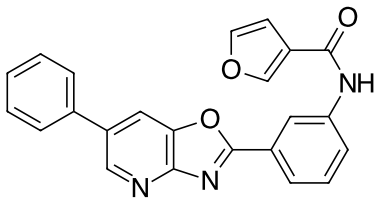	48 %
144	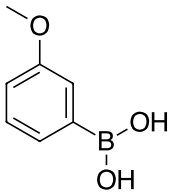	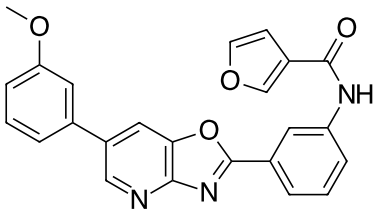	60 %
145	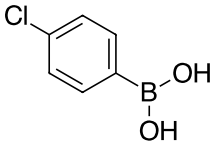	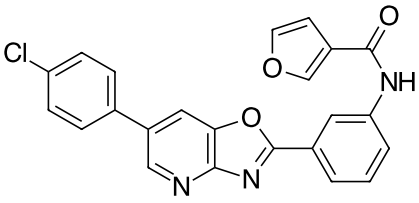	47 %

Synthesis of the methoxy derivative **(146)** was also attempted from the 6-bromopyridoxazole amine **136** using methanol, copperiodide and 1,10 phenanthroline as a catalyst in the microwave reactor (scheme 10).

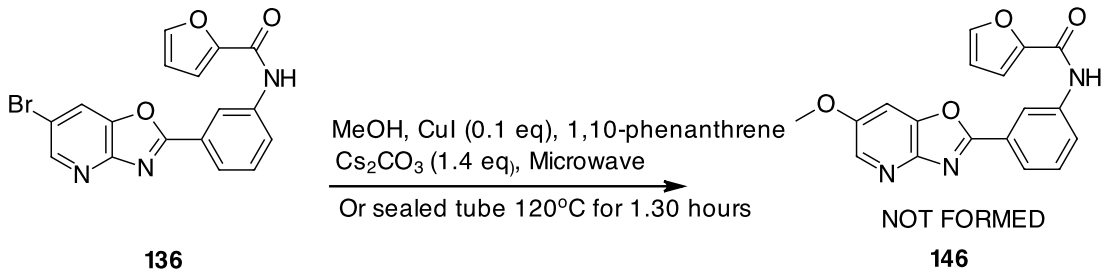

136 **146**

Scheme 10: synthesis of 6-methoxy derivative from pyridoxazole 136

However, based on the NMR and TLC analysis decomposition occurred under these conditions. The reaction was again repeated but this time sealed in a tube and heated at 120° for 3 hours as was reported for a similar reactants [76]. However, the reaction was deemed unsuccessful and no further investigation to make **146** was attempted.

2.6 unsubstituted central phenyl ring with amide on the pyridine ring of the oxazolopyrdine core

A pyridoxazole with un unsubstituted central phenyl ring of **149** has been reported previously as a precursor for biologically active compounds [79,83-85]. Viaud *et al.* [79] reported the utility of **125** for a number of palladium catalysed cross coupling including Suzuki-Miyaura, Stille and Heck reactions. To our knowledge, synthesis of an aryl amide on the pyridyl rather than the oxazole. For example, compound **125** and similar analogues) with the amide (replacing the bromine) installed on C6 of the pyridoxazole have not been reported before. As such we wanted to examine the effect of 6-(2-furylamide) functionality (and its 3-isomer), as relative to the fused pyridoxazole, on the biological activity.

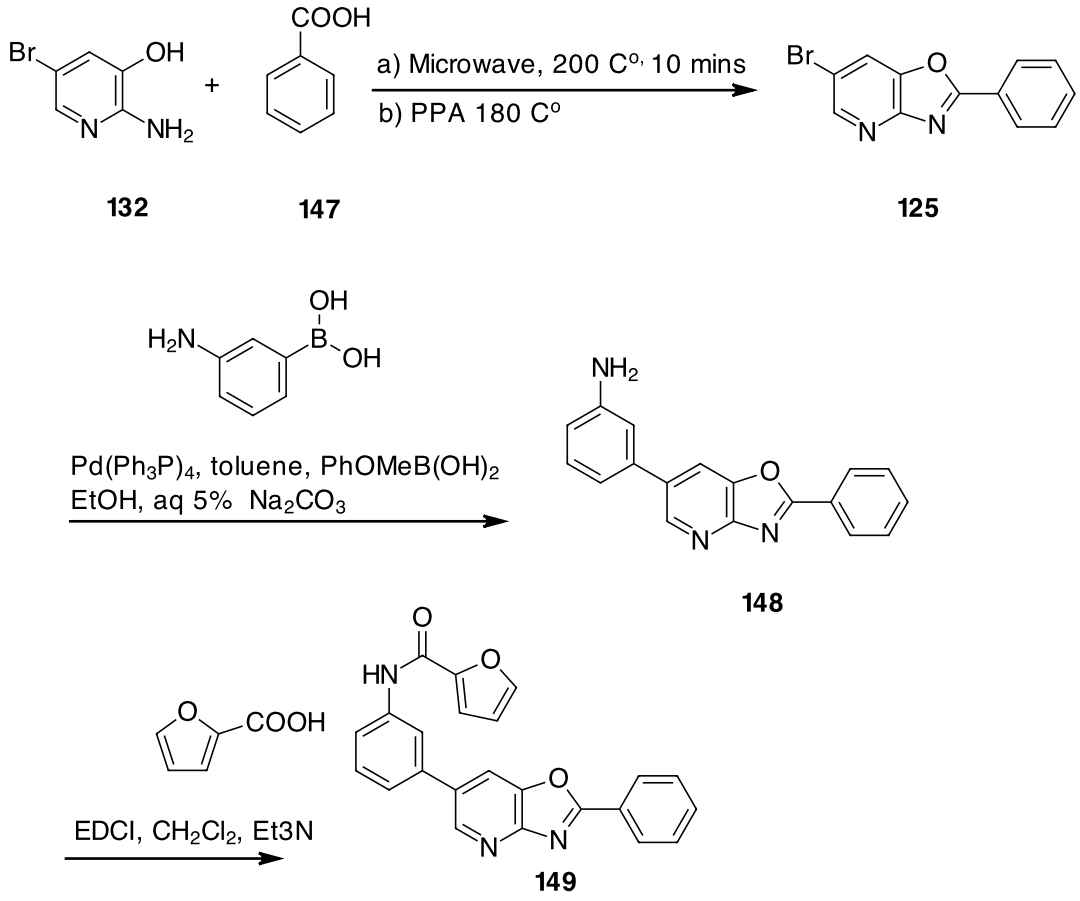

Scheme 11: Synthesis of unsubstituted central phenyl ring with amide moiety placed on pyridine ring

Our initial plan was to prepare key intermediates such as compound **148** *via* **a** Suzuki-Miyaura reaction from 6-bromopyridoxazole **125** with (aminophenyl)boronic acid followed by the formation of the furyl-amide **149** (Scheme 11). The synthesis of compound **125** was first reported by Viaud *et al.* [79] by treating compounds **132** and **147** with a solution of phosphorus pentoxide and hexamethyldisiloxane (1 : 1.6 mmol) as an alternative method to polyphosphoric acid [79]. Initially we decided to examine whether **125** could be achieved using microwave-assisted synthesis as reported by myllymaki [73] for the synthesis of a similar analogue of compound **125** with the absence of the bromine. Briefly, 2-amino-3-hydroxypyridine **(132)** and benzoic acid **(147)** were subjected to microwave irradiation (200 C°, 300 W) for 15 mins under

solvent-free conditions. ^{1}H NMR revealed that the product **125** was obtained in good yield and that no starting materials were present. Further support of the formation of compound **125** came from the comparison with the ^{1}H NMR spectra data reported by Viaud *et al.* [79] (Figure 38).

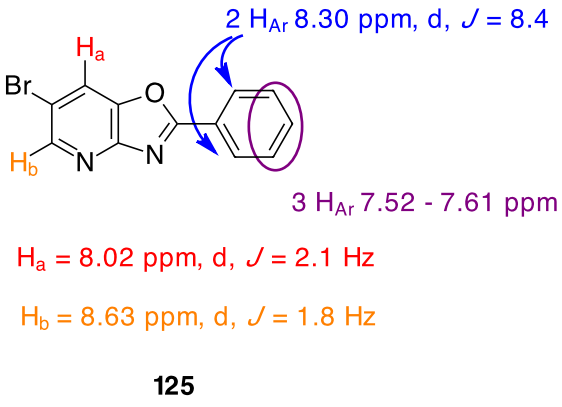

125

Figure 38. Assignation of ^{1}H NMR for compound **125**

Unfortunately, we did not take the reaction further in the synthesis sequence due to time constraints.

2.7 Summary of the synthesis and future targets

Our initial target for the synthesis of analogues of the lead structure **83** was centred around the central phenyl ring which was prepared in a 2 steps by the formation of the pyridoxazole amines from 2-amino-3-hydroxypyridine and the appropriate arylbenzoic acids followed by the formation of the target amides (Figure 39) . Using different building blocks of the arylbenzoic acids allowed access to different substituents installed around the central phenyl ring (i.e chlorine in the lead compound **83** vs CH_3 and H).

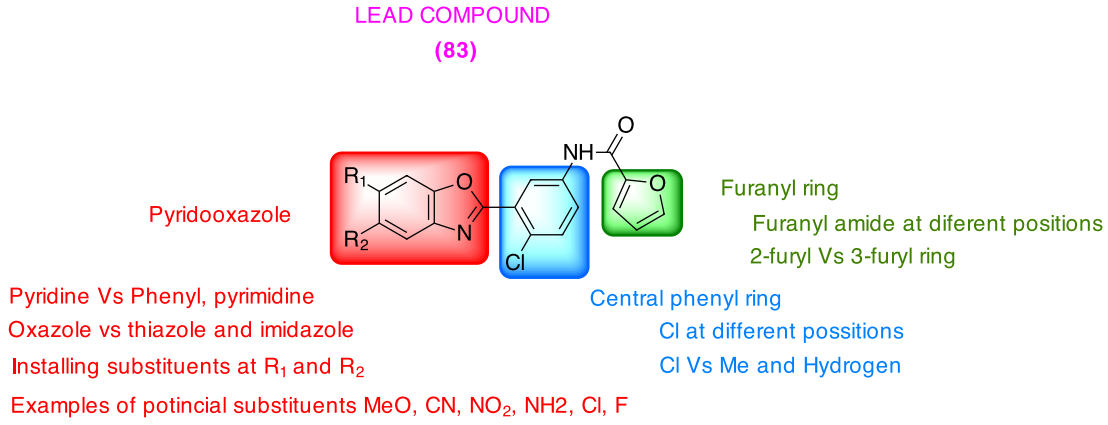

Figure 39. Summary of the current target synthesis and the open target for the future

Our initial aim was also to enlarge the repertoire of compounds *via* a preliminary investigation around the pyridoxazole core including the imidazopyridine derivatives and installing substituents on the C6 of the fused pyridoxazole ring. Both required the same sequence as for the synthesis of pyridoxazoles, but using 2,3-diaminopyridine and 2-amino-5-bromo-3-hydroxypyridine for the synthesis of the respective imidazopyridines and 6-bromopyridoxazoles.

Apart from this, the initial results for the biological assays of imidazopyridine (discussed in Chapter 3), revealed tolerance in the activity and as such it was deemed important to prepare alkylated pyridoimidazoles (i.e NH of imidazole vs *N*-CH_3) derivatives as analogues to **123** and **124**. This has spurred our interest to investigate alkylated derivatives of **123**, for instance *via* the *N*-methylation of the imidazole –NH group in the fused ring. To do this, aniline **122** can be directly alkylated using standard alkylation conditions for which there is literature precedence [65] [70].

The 6-bromopyridoxazole amides **136** and **137** proved useful for Suzuki-Miyaura coupling reactions as was explored by installing 6-aryl substituents.

Other functional groups transformations (i.e the cyano, ester, alkyl group) [76] [78], which are also possible and require further investigation in the future to enlarge the compound library.

In fact the cyano group would be quite useful for other chemical transformation such as a hydrolysis into carboxylic acid derivatives, or reduction into amines or into aldehydes (i.e DIBAL-H) [86] and these could be undertaken in the future.

3. SAR towards inhibition of *T. brucei*

3.1 Selection of the lead compound

Baell and Avery *et al.,* [54] reported screening of 87,000 compounds against *T.b. brucei* using an Alamar Blue® based 384-well viability assay. *T.b. Brucei* is different sub-species that it is not pathogenic to humans. Therefore, viability assay for *T.b brucei* are conveniently used for early HAT drug discovery as a surrogate for *T.b. rhodesience* and *T.b. gampiense*. As discussed in Chapter 1 (section 5.1), the Avery group identified eight compounds by screening against *T.b. brucei* (Figure 31). Compound **83** was of particular interest as in regard to both of the physiochemical and the biological properties (Figure 40). Compound 83 had an IC_{50} of 0.22 µM, it also has a moderately low molecular weight of 339.5 g/mol, a reasonably low polar surface area of 81 $Å^2$ that could have potential for CNS penetration to treat stage two HAT, and an attractively low clogP of 2.6.

Compound **83** was also tested against a wide panel of parasites and was found potent not only to *T.b rhodesience* (IC_{50} 0.59 µM) but also against *Trypanosoma Cruzi* (IC_{50} 0.23 µM). In both cases **83** was highly selective for these kinetoplastids when compared to L6 mammalian cell line with respective selectivity index of 39 and 99. The selectivity parameter is used to see whether the drug preferentially exerts its effect on the parasites as compared to healthy mammalian cells and a higher number indicates that the drug is highly selective for parasites. Compound **83** had also showed weaker activity to the *plasmodium falciparum* (IC_{50} 7.8 µM) a major causative agent of malaria.

MW 339.5
PSA (A^2) 81
clogP 2.6

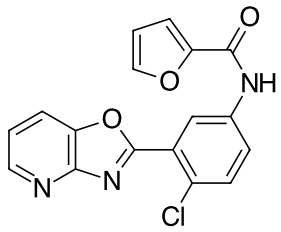

(a) Lead compound **(83)**

R = 2-furyl or 3-furyl isomer

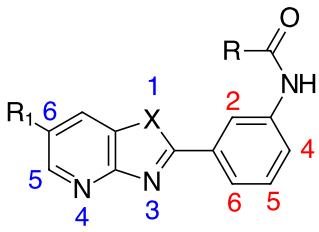

(b) **114-121**, **124-125**, **131**, **133-135**

Parasite	IC_{50}	SI
T.b. brucei	0.22	>345
T.b. rhodesience	0.59	39
T. Cruzi	0.23	99
P. falciparum	7.8	_

Figure 40. a) Structure, physicochemical properties and biological actvities of an intial screening hit; b) numbering used herein for around the central phenyl ring (red) and pyridine (blue).

3.2 SAR study of oxazolopyrdine and related analogues.

Based on the respective physiochemical and biological analysis, compound **83** was regarded as a starting point for drug development and hence it was selected as our lead compound resulting in this SAR focused study. Therefore the focus of this work was on three parts of the oxazolopyridine structure: the furyl amide ring, the central-phenyl ring and the oxazolopyridine ring core.

Therefore, synthesis for similar analogues to compound **83** as in respect to those suggested core changes was performed (as discussed in Chapter 2). The synthesised compounds reported in Chapter 2 were to be combined into a larger library of compounds for evaluation against *T.b. brucei* at Monash Institute of Pharmaceutical

Sciences at Monash University and Eskitis Institute for Cell and Molecular Therapies at Griffith university. Therefore, compounds from Chapter 2 were evaluated against *T.b. brucei* using an Alamar blue® viability assay as part of the anti-trypanosidal screening program. The relative selectivity of these compounds over mammalian cells was also examined using HEK293 cytotoxicity assay but only those compounds that had potent anti-trypanocidal activity were evaluated.

3.1 Generation 1: modification around the central phenyl ring

Initially we focused our investigation around the position of the furyl amide around the central phenyl ring and the effects of substituents on the activity resulting in the target compounds listed in Table 10. Substitution of the chlorine in the lead compound **83** (IC_{50} = 0.22 μM) for a hydrogen **(113)** is well tolerated with an IC_{50} of 0.34 μM and only slightly less selective (**113**, SI = 89) in respect to **83** (SI = >354), while substitution of the 2-furyl amide for the 3-furyl isomer **114** resulted in slight loss of the activity and the selectivity (IC_{50} = 0.60 μM, SI = 89).

As listed in Table 10, replacement of the furyl group into different positions, the *ortho*-position **(115)** and **(116)** retained activity with an IC_{50} of 0.78 μM and 1.1 μM while the *para*-position **(117)** led to a loss in the activity.

Table 10. Furyl at different possitions[a] of analogues of the oxazolopyridine core

ID	Product	IC50 (μM)	SI
83	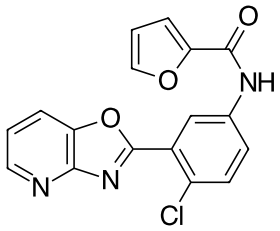	0.22	>345
113	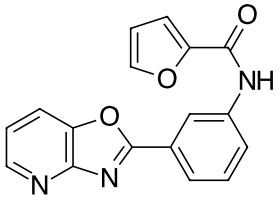	0.34	>245
114	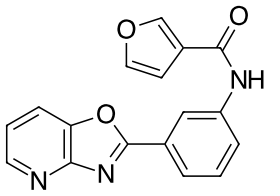	0.60	89
115	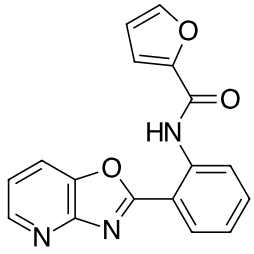	1.80	–
116	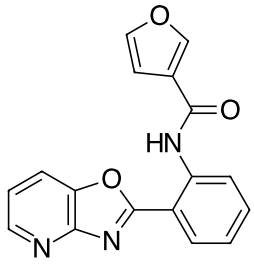	1.00	–
117	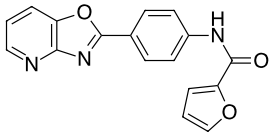	>10	–

118	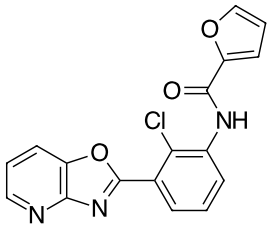	>10	–
119	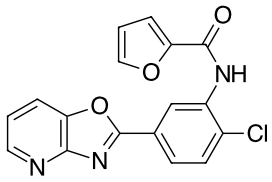	>10	–
120	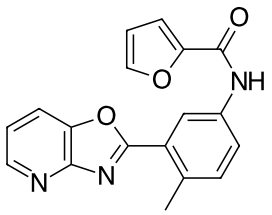	0.94	>88

[a] Values are the mean experiments < ±50%

[b] Selectivty relative to HEK293 cells for selected potent compounds

Substitutions around the central phenyl ring were investigated (Table 10). The chlorine at C2 and C4 of the central phenyl ring with compounds **118** and **119** respectively, appears to be unfavourable since they led to a loss in activity. Thus the central group appears to be intolerant to substitution at the *2*- and the 4-positions. Replacement of the C6-chloro in the lead compound with a methyl group **(120)** is somewhat tolerated (IC_{50} = 0.94 μM, SI = >88). On the other hand, as in the earlier example with the replacement of the 6-chloro group with hydrogen **(113)** was seen as more preferable since it led to nearly equal activity while lowering the molecular weight, the hydrophobicity and the simplification of synthesis. In most cases it appears unlikely that permeability would differ greatly amongst this set of compounds and so we attribute this SAR – at least at the 2- and 4- positions to steric interactions with the intracellular target [1].

3.2 Generation 2 - modification of the heterocyclic core

While the focus of this work is on the right central phenyl ring, some initial exploration was undertaken around the left hand side fused heterocycle resulting in interesting results as presented in Table 11. Replacement of the oxazole into an imidazole **(123)** and **(124)** showed that activity is slightly diminished but the observed slight loss in the activity is possibly due to poor membrane permeability since at physiological pH possibly at least a portion of the imidazole may be protonated. This prompted us to further investigate this, for instance *via* substitution of the –NH group of the imidazole ring but due to time constraint this has not been investigated.

The effect of the substitution at C6 of the pyridoxazole-fused ring has been investigated (Table 11). The more complex compounds **138-140** containing the extra phenyl ring on C6 of the pyridoxazole-fused ring such as the phenyl **(138)** and the substituted phenyl derivatives **139** and **140** were synthesized using palladium mediated cross coupling using brominated oxazolopyridine **136** and thus allowing synthesis of numerous derivatives from a common bromopyridoxazole intermediates.

Compound **(136)** with the bromine led to a complete loss in the activity, while with the C6 phenyl ring **(138)** gave a significant increase in the potency with an IC_{50} of 0.12 μM compared to the lead compound (83, IC_{50} 0.22 μM), while the incorporation of substituents on the phenyl ring, as in compounds **139** and **140** resulted in a slight decrease in the activity with IC_{50} of 0.55 μM and 0.63 μM respectively.

Table 11. *T.b. brucei* inhibition activty[a]

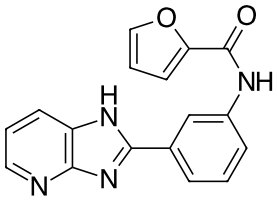

123

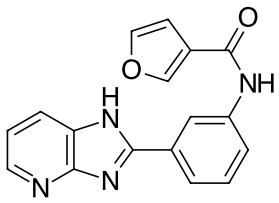

124

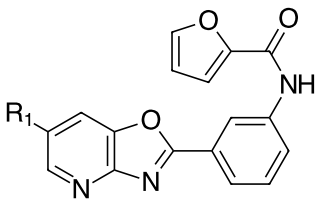

136, 138-140

ID	R_1	IC_{50} (µM)	SI
123	_	0.78	54
124	_	1.00	39
136	Br	>10	-
138	Ph	0.12	84
139	4-Cl-Ph	0.63	130
140	4-OMe-Ph	0.55	150

[a] Values are the mean experiments < ±50%

[b] Selectivty relative to HEK293 cells for selected potent compounds

We also have prepared other compounds by Suzuki reaction using 2-furyl amide **136** and its 3-furyl isomer **137** (discussed in Chapter 2). However, these results presented herein are the only results available to date while biological results for compound **141** and **143-145** are not currently available.

3.3 Recent report of oxazolopyrdine compounds

This work was a part of a larger effort with the Baell group at Monash University and this works resulted in interesting antitrypanosomal activity of the compounds library as summarised below (Figure 41).

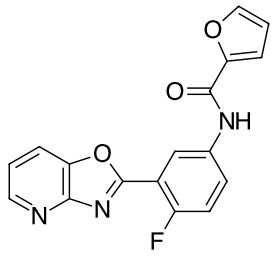

150

IC_{50} = 0.12 µM, SI = 680

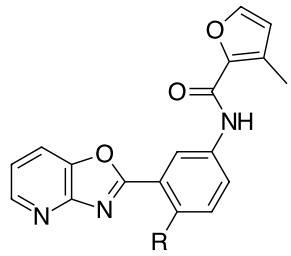

151: R = H, IC_{50} = 0.17 µM, SI = 115
152: R = F, IC_{50} = 0.10 µM, SI = 840

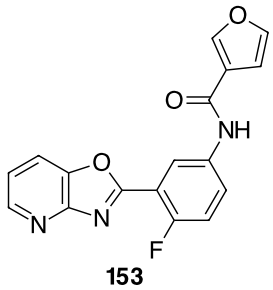

153

IC_{50} = 0.12 µM, SI = 680

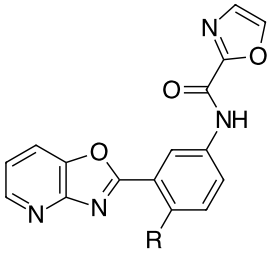

154: R = H, IC_{50} = 2.9 µM, SI = 29
155: R = F, IC_{50} = 2.0 µM, SI = 43

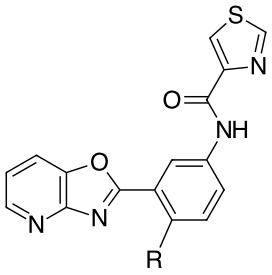

156: R = H, IC_{50} = 1.3 µM, SI = 63
157: R = F, IC_{50} = 0.76 µM, SI = 110

Figure 41. A selected compounds made by our colaborator Baell group

Although the lead compound and a number of its analogues show a reasonable activity against *T. Brucei*, stability testing reveals that they have a short half-life and high clearance rate due to susceptibility to cytochrome p450-mediate metabolism [1]. In fact the furyl ring is known to be potentially metabolically liable [87] and therefore the furyl ring might be the driving force for this observed instability based on the *in vitro* metabolic stability of this current study [1].

In contrast, compounds **155** and **157,** which have the furan been replaced by an oxazole and thiazole, were less active compared to the unsubstituted furyl isomers, yet they have resulted in better metabolic stability as represented by their higher half-lives of 124 min and 36 min and low clearance rates of 14 and 48 [1].

Just After our results published [1], independent work by the Gelb group [88] (January, 2014), reporting the SAR centred around the pyridooxazole **83** and its imidazopyrdines analogue. Selected compounds from Gelb and his co-workers study are presented in Figure 42.

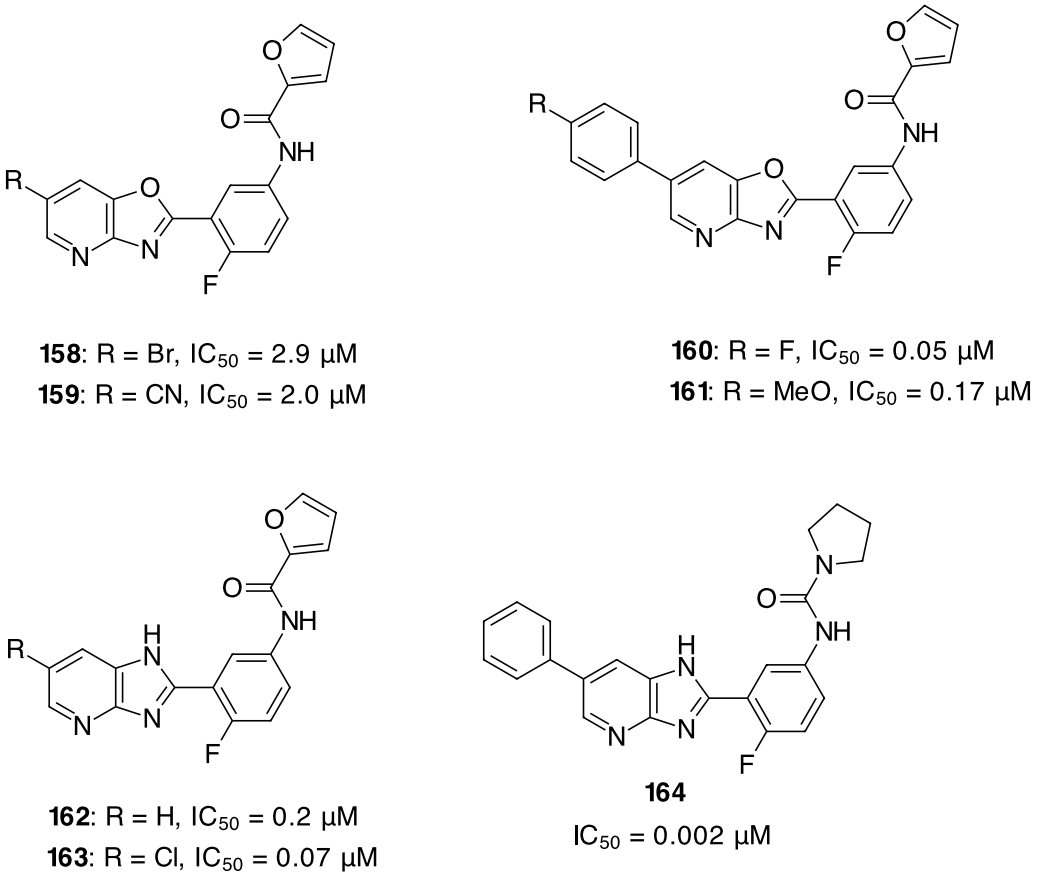

Figure 42. Selected compounds from Gelb and co-workers work on *T.b. brucei* strain BF427

Compound **164** was the best in the series with an IC_{50} of 0.002 μM which differ from our series of compounds by the presence of the ureas replacing the furyl amide group. Compound **164** was claimed as the best in their SAR study in respect to both the antitrypanosomal activity and the metabolic stability. Their study of the metabolism stability in the mouse and human liver microsomes revealed a half-lives of 10 and 31 mins respectively which is lower compared to the Baell's group derivatives **155** and **157** [1]. Pleasingly their work supports our initial findings that the pyridoxazoles and imidazopyridines give comparable trypanocidal activity.

3.4 Conclusion

This thesis described the synthesis and SAR around a pyridyloxazole lead compound resulting in a number of novel compounds with promising antitrypanosomal activity. The modification of the lead structure was made on the central phenyl ring and the pyridoxazole core. Figure 43 summarises the SAR for the work from this thesis.

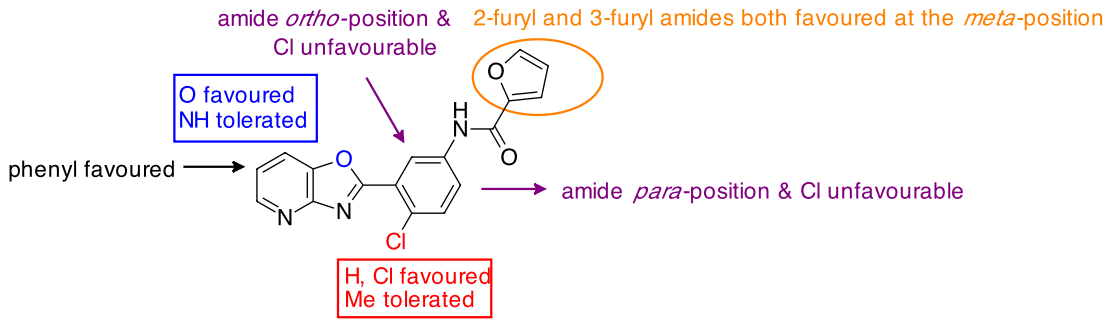

Figure 43. A representative summary of the SAR of pyridooxazol

From inspection of the SAR, we found that the central phenyl ring is of less impact on activity, while the most potent compounds in the series remained as 1) the original lead compound with chlorine at C6 of the central phenyl ring (**83**, IC_{50} *T.b. brucei* = 0.22); 2) its analogue **113** that has the chlorine been replaced with a hydrogen (**113**, IC50 *T.b. brucei* = 0.34); and 3) the 3-furyl analogue **114** (IC_{50} *T.b. brucei* = 0.60). Replacement of the chlorine into the 2- and 4-positions in respect to furyl moity was found unfavourable for activity while replacing the furyl group to the *ortho*-position of both 2-furyl and 3-furyl moieties were tolerated. We also found that substitution around the oxazolopyridine core is better tolerated, given that the compound with the 6-phenyl group (**138**, IC_{50} *T.b. brucei* = 0.12) was the most potent in the series. So the pyridoxazole core has better potential to modulate the activity favourably, where these current SAR results can be interrogated during future refinement of next set of compounds generation.

3.5 Future work

Those compounds that were deemed active from this study suffered from metabolic instability as discussed in section 3.3. Therefore, it is necessary to design compounds that overcome this issue without affecting the activity. Some of the widely used tactics to circumvent instability is to install steric-shielded substituents like ortho-methyl substituents around the amide bond at the 2-and 4-positions on the central phenyl of our lead compound or a bulky alkyl group on the amide nitrogen [21]. The latter, alkylation of the amide, was made by the Baell group but it diminishes the activity [1]. Steric shielding in general might not be a good option due to the likelihood to diminish the activity.

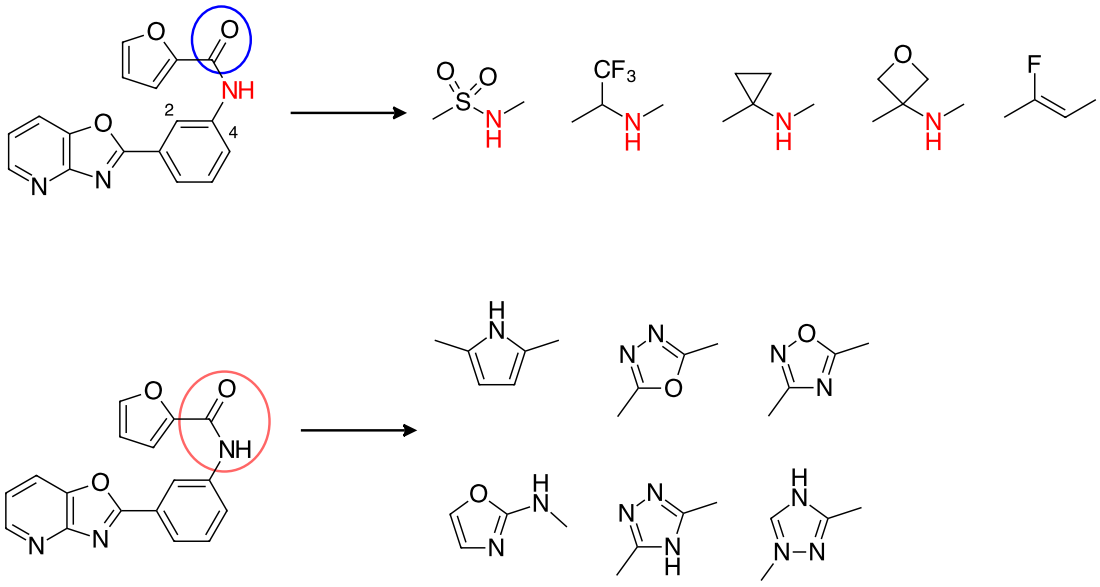

Figure 44. Sypnosis of some of the known amide isosteres [21]

Isostere replacements are widely used to enhance the chemical and metabolic stability for drugs [21]. Figure 44 represents some of the known isosteric tactics to enhance the chemical and metabolic activity of the amide bond. There are many examples in the

literature where isosteric replacement improved the metabolic stability which is reviewed by Meanwell [21] . For example replacement of a carbonyl group for a fluorine atom (C-F bond), (i.e gem-difloro, trifloro moiety, or trifloroethylamine) are known isosteres for amide bonds (i.e peptide-based enzyme inhibitors) [21]. They are known to possess functional mimicry as they reduce the basicity of the amide without compromising its H-bonding formation [21].

Cyclic isosteres are also very promising substituents to replace the amide due to their rigidity and stability. Replacement of the amide of sultopride (Barnetil), an antipsychotic benzamide drug for the treatment of schizophrenia, by a pyrrole ring is a known example which improved its pharmacokinetic properties [89].

This study represented the first application, to our knowledge, of a metal- mediated reaction as from our initial investigation exploiting Suzuki-Miyaura reactions on the pyridoxazole structures **136** and **137** with the 6-bromine. In the current study, we sought to build on this initial work in the future and to enlarge the repertoire of metal-mediated reactions applied in our developed reaction sequence. Examples of the possible application of pyridoxazole-like structures **(136)** and **(137)** are presented in Table 12 and Figure 45. Cyclopropanes are commonly found in pharmaceutically active compounds and is often part of SAR studies due to their structural and electronic properties [90]. Therefore, investigation to form the cyclopropane **165** can be conveniently made using metal mediated transformation along with other alkyl substitutions.

Investigation of the effect of an aliphatic chain like the benzyl group **166**, butyl group **(167)**, vinyl group **(168)**, which can be obtained *via* Stille's reaction using alkyltin or

cuprous reagents and palladium catalyst. Other possible functionality that can be useful are an acrylate group **169** and compound **170** or similar analogues [79]. In both cases **169** and **170** can be useful for the potential chemical transformation.

Table 12. Potential reactions that can be investigated for future refinment based on litratures

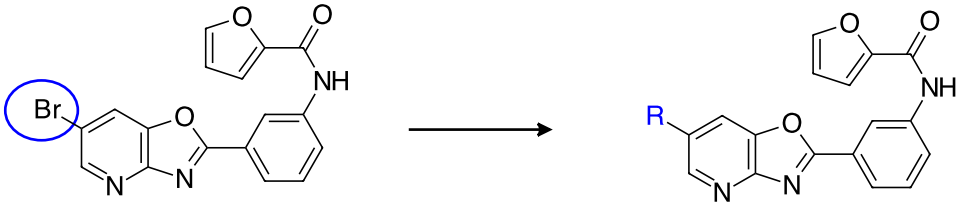

131

ID	R	Starting material	Ref
165		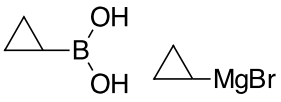	[91]
166	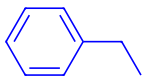	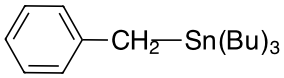	[79]
167		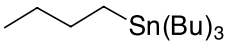	[79]
168		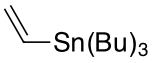	[79]
169	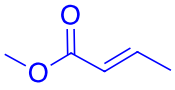	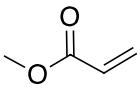	[79]
170		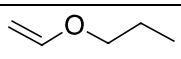	[79]

Apart from bromoamide **136** and **137** which can be used for the synthesis of numerous compounds *via* Suzuki-Miyaura reaction, they can also be further exploited

to generate another set of compounds *via* other palladium catalyzed reactions such as C-N bond (amines), C-O bond (ether), C-S bond (sulfide) [92] (Figure 45). The aryl amine functionality can be formed *via* buckwald/hartwig method [93] [76].

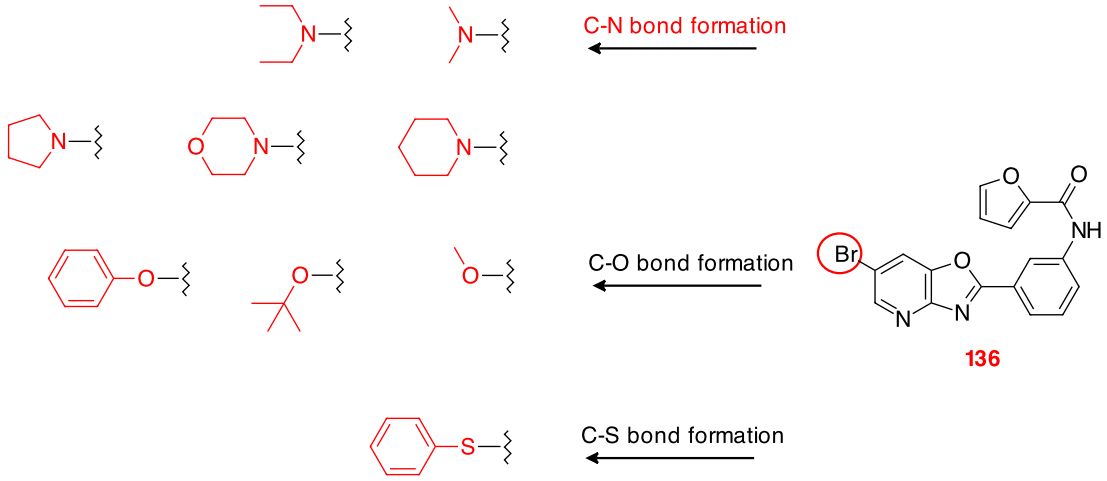

Figure 45. Potential palladium catalyzed reactions for C-N, C-O, C-S bond formation

Nitration of oxazolopyridine **(130)** can be also used to develop 6-amino pyridoxazoles derivatives (i.e **173**) after reduction of the nitro. These amine derivatives would be not only interesting for testing, since amine might help the solubility of these compounds, but also can be further used as an intermediate to produce another amide derivatives. Further to this, the amine might be also transformed into the fluoro analogue through using known method, for example, Sandmeyer reaction of the diazonium derivative using HPF_6 as the fluorine source (Figure 46) [94].

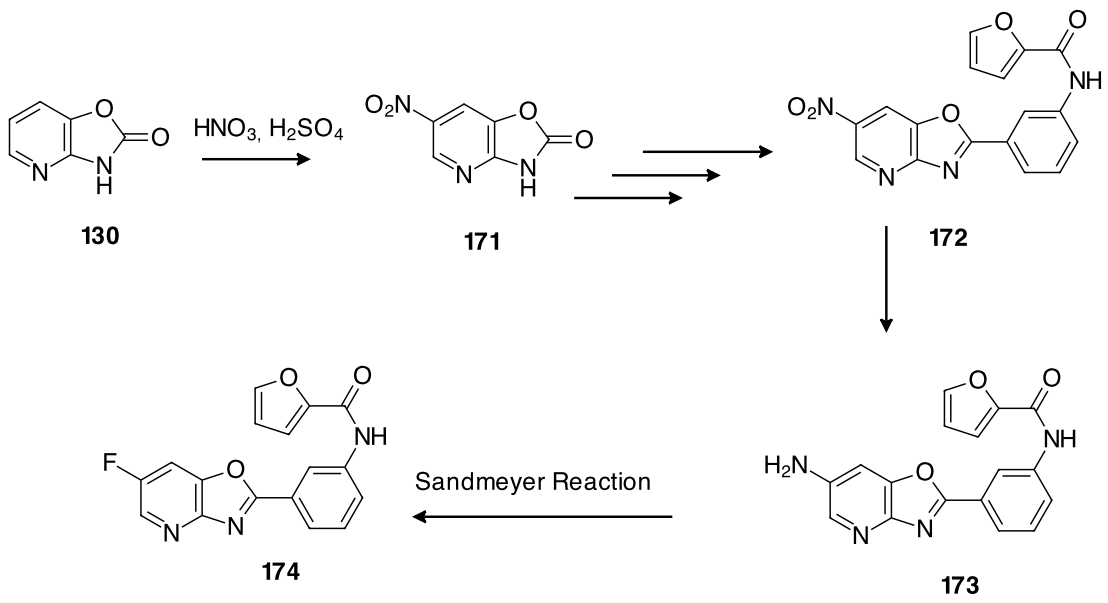

Figure 46. Synthesis of 6-fluoro pyridoxazole

Most importantly, related compounds particularly bromo-substituted derivatives of the imidazopyridine derivative (with the replacement of oxygen in the oxazolopyridine into NH) can be made using the commercially available 5-bromo-2,3-diaminopyridine, which might have the potential to save time and effort that might allow the synthesis of more compounds using the known methods for the substitution of bromine into other functional groups and known palladium catalysed reactions as mentioned above. The rational behind making such an effort for the plan of next set of generation of compounds is by large supported by the biological activity results, which revealed that oxazolopyridine core could be further explored.

CHAPTER 4: Mutagenicity potential of oxazolopyridines

4.1 Introduction

Our food and dietary intake are prone to contamination with nitrosoamines, during food preservation, while polycyclic aromatic hydrocarbons and heterocyclic amines that are formed during the cooking processes, may have carcinogenic activity [95]. Those heterocyclic amines contain an pyridoimidazole ring with an exocyclic amino group and are found in protein-rich foods such as meat and fish [96]. They are also found in alcoholic beverages and cigarette smoke [96]. Examples of these heterocyclic amines reported as mutagens are presented in Figure 47.

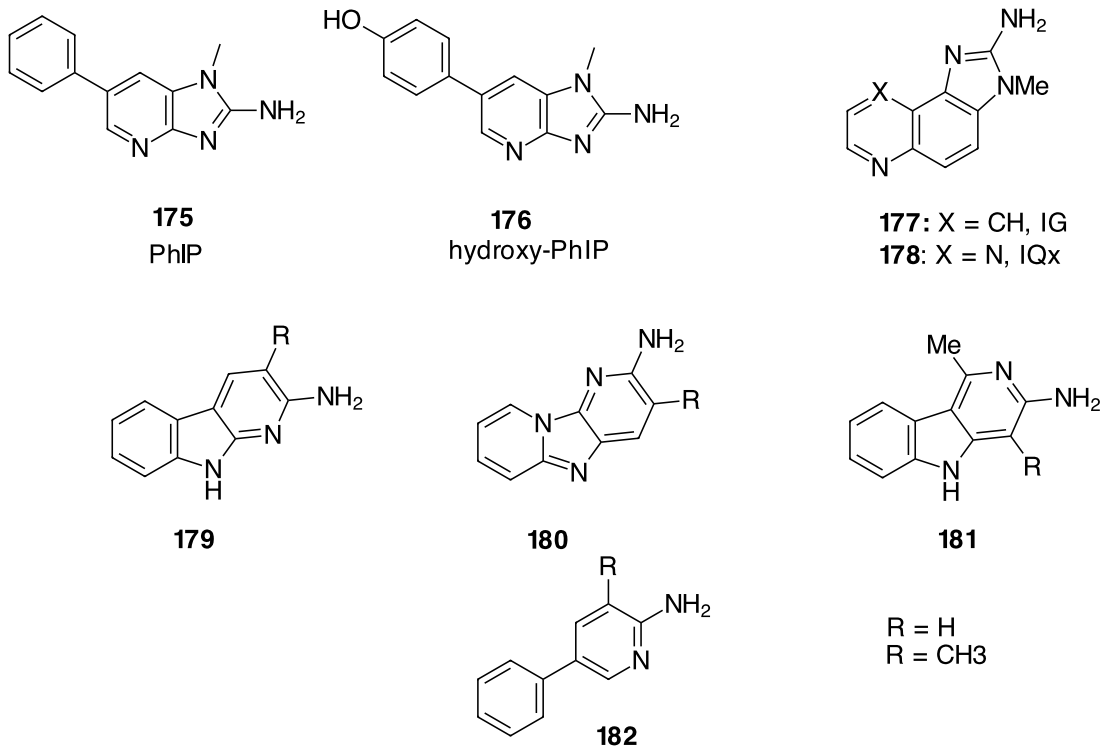

Figure 47. Examples of carcinogenic hetrocyclic amines [97], [98]

These heterocyclic amines presented are classified into 2 classes: the IQ (common abbreviation) HCAs series, also named aminoimidazoazaarenes, including imidazopyrdines **177** and **178**, imidazoquinoline **179** and imidazoquinoxalines **180**, and non IQ HCAs series of 2-aminopyridine-containing compounds such compounds **181-184** [98]. This classification is based on the observation regarding mutagenicity, which is maintained even with the conversion of the amine into a hydroxylamine group, as it is the case with IQ HCAs only [98]. These IQ HCAs compounds are believed to result from condensation reactions between amino acids, glucose and creatine or creatinine (in muscles) serving as a precursor for the formation of the imidazo moiety, through the Maillard reaction during cooking processes [96]. Generally, concentrations of IQ's are at much higher concentration in cooked or smoked food than non-IQ's series but generally they are all regarded as highly mutagenic in *salmonella typhimurium* testing. They are also reported as mutagenic in *in vitro* and *in vivo* testing to mammalian cell-line [98].

Heterocyclic amines are only carcinogenic after metabolic bio-activation, which is largely carried out by cytochrome p450 (CYP) enzymes. Oxidation of the aromatic and heterocyclic aromatic ring of these heterocyclic amines leads to their detoxification and excretion to the urine [99]. For example, PhIP undergoes hydroxylation by human CYP 1A2 at C4 of the terminal phenyl ring followed by O-sulphonation and O-glucuronidation (Figure 48) and formation of water-soluble metabolites which are excreted through urine [99].

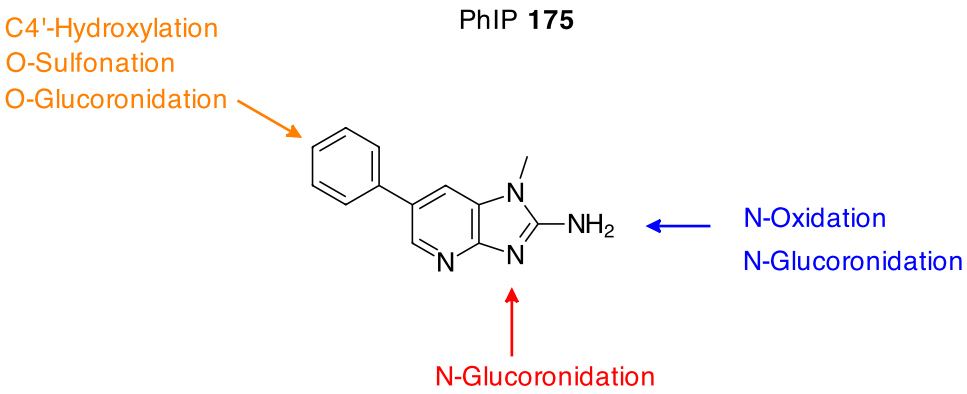

Figure 48. Metabolism of PhIP

However, the oxidation (*N*-hydroxylation) of the exocyclic amine group result in the formation of a hydroxylamine intermediate, which undergo esterification by acetyltransferase and sulfotransferase enzymes to give the corresponding highly reactive metabolite forms of acyl hydroxyl amine and sulfonyl derivatives (Scheme 12) [97] [100].

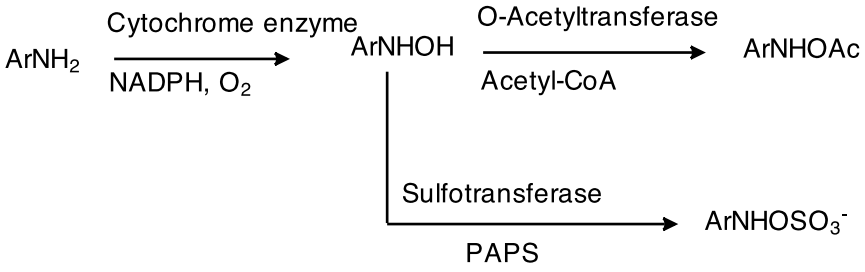

Scheme 12. Metabolic activation of hetrocyclic amin into carcinogenic metabolitese

These forms are spontaneously transformed into arylnitrenium ions ($R\text{-}HN^{+}$), which eventually react with DNA leading to the formation of DNA adducts (Figure 49) through the formation of C-N bond at the 8-position of guanine bases as illustrated for PHIP [98,101]. The formation of highly reactive nitrenium ions is believed to be the ultimate reactive intermediate involved in DNA adduct [87].

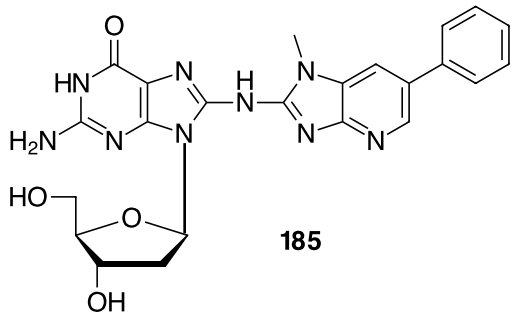

185

Figure 49. Formation of DNA adduct arised from PhIP consumbtion

In particular, 2-amino-1-methyl-6-phenylimidazo[4,5-*b*]pyridine (PhIP) is recognised as the most abundant amongst other HCAs in food compared to other reported heterocyclic compounds. PhIP play a role in forming covalent DNA adducts leading to genetic mutations and was reported to cause cancer in animals and human models [98]. Prostate, breast and colon cancer in humans have been reported with consumption of PhIP [102]. A recent study has also showed the presence of PhIP in human breast milk that might lead to health problems to developing a foetus [102].

The pyridoimidazoles and pyridoxazoles discussed in Chapter 2 are structurally similar to these heterocyclic amines as they share a similar heterocyclic core but differ as they have an amine group on the aryl ring rather than attached to the imidazole ring. Therefore it is possible that these compounds may also form hydroxylamines on oxidation. The furylamide derivatives may also undergo cleavage to release the parent amine and as such we decided to investigate their ability to cause DNA damage.

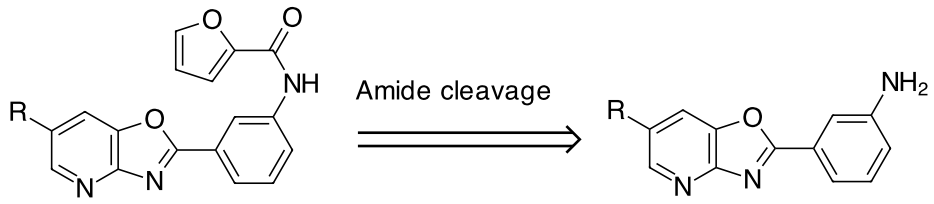

Figure 50. Expected cleavage of pyridoxazole to their intermediate anilines.

4.2 Testing of DNA damage

4.2.1 Background

The DNA of eukaryotic cells is structured and packed in the form of DNA-protein complexes called chromatin, consisting of histones [103]. Histones consist of arginine- and lysine- rich basic proteins with a positively charged *N*-terminus providing high binding affinity for the negatively charged DNA to form nucleosomes, *via* ionic interaction with the anionic phosphate group of the DNA[103]. Therefore, histones assemble chromatin into nucleosome structure resulting in the packaging of DNA [104]. The nucleosome core contains DNA coiled around the histones core consisting of eight histones two pairs from each of the core histones H2A, H2B, H3 and H4 [105]. H2AX belongs to several genes that code for histone H2A and have a role in the formation of the nucleosome, and to the DNA structure [104]. Several factors can lead to double-strand breaks, which is one of the dangerous forms of DNA damage caused by either external factors such as drugs or organic compounds [105] and ionizing radiation or reactive oxygen species [104].

The initiation of DNA double strand breaks, triggers phosphorylation of H2AX on serine 139, and called γ -H2AX. H2AX is observed as discrete nuclear foci indicating

the region of DNA repair [105]. Several kinases of the phosphatidylinositol-4,5-bisphosphate 3-kinase, also called phosphatidylinositide 3-kinases; appreviated as PI 3-kinases, are involved in the phosphorylation event of H2AX. P1 3-kinase are well-known for their cellular functions such as cell growth, proliferation, differentiation, motility, survival and intracellular trafficking [106]. Ataxia-telangiectasia-mutated (ATM), DNA-dependent protein kinase (DNA-PK) and Rad- 3-related (ATR) kinases belong to the family of the PI3 kinases which are responsible for phosphorylation of H2AX, but ATM is accountable for the major response, within seconds, of the DNA damage being initiated [104].

The level of γ -H2AX induced by chemical substances and radiation is in close correlation to the level of cell death [105]. The formation of γ -H2AX foci gives an indication of the occurrence of DNA damage indicating that the measurement of γ -H2AX is frequently used as a sensitive bio-marker for the induction of double strand breaks in cells [104]. The comprehensive role of γ -H2AX in DNA repair has not been yet elucidated but it is generally accepted that as the phosphorylation event occurs, the DNA becomes less condensed allowing access to the necessary DNA repair proteins [107]. Normally within a period of eight hours, nuclear γ-H2AX foci is lost and DNA strands break are consequently repaired in healthy cells [107].

4.2.2 Results and Discussion

A selection of imidazopyridines and pyridoxazoles from Chapter 2 has been sent to A/Prof Nuri Gueven at the School of Medicine (Pharmacy) at UTAS for the testing. Imidazopyrdines, pyridoxazoles with the furyl amide and the amine precursors were tested for their ability to damage DNA by observation of nuclear gamma-H2AX,

which is a biomarker of DNA double strand breaks. Visualisation of γ -H2AX was performed using a Nikon Epi-Fluorescent microscope (ECLIPS 55i) and images were acquired using NIS-element software. Negative control (cells and media) and positive control (cells and H_2O_2 at a concentration of 200 uM) were also used (Figure 51).

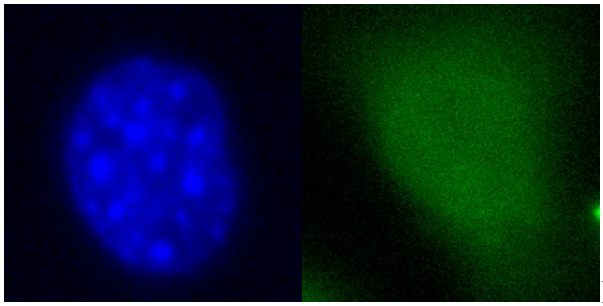

Negative control

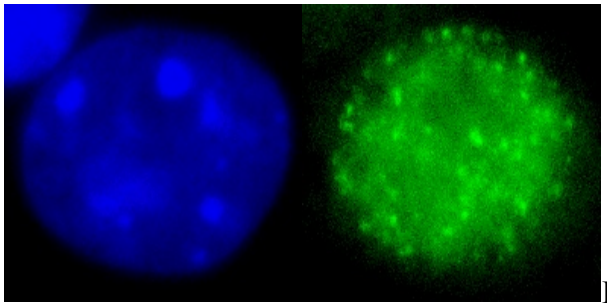

Positive control

Figure 51 Fisualisation of biomarker of DNA damage by observation γ-H2AX

Top is the negative control, the cells with the absence of a DNA damaging inducer; bottom is the positive control in the presence of 200 uM H_2O_2-induced γ-H2AX foci; the left is strain to visualise the cells (blue); the right is stain to visualise the DNA damage (green).

A random testing was performed on 15 compounds tested at different concentrations (2 – 0.0032 uM). The results have shown that the majority of the pyridoxazoles and their aniline precursors exhibit strong nuclear γ-H2AX staining which is indicative of the occurrence of DNA damage, and resembles the positive control containing cells and 200 uM of H_2O_2-induced γ-H2AX (Figure 52). This was the case with all of the tested compounds as having similar activity even at the lowest concentration of

0.0032 uM. The tested compounds showed an elevation of γ -H2AX in the range of 10-20 foci above the background level of 0-3 foci/cell. Therefore this study indicates these tested compounds are extremely potent in inducing DNA double strand breaks and thus caution is to be considered upon handling these compounds.

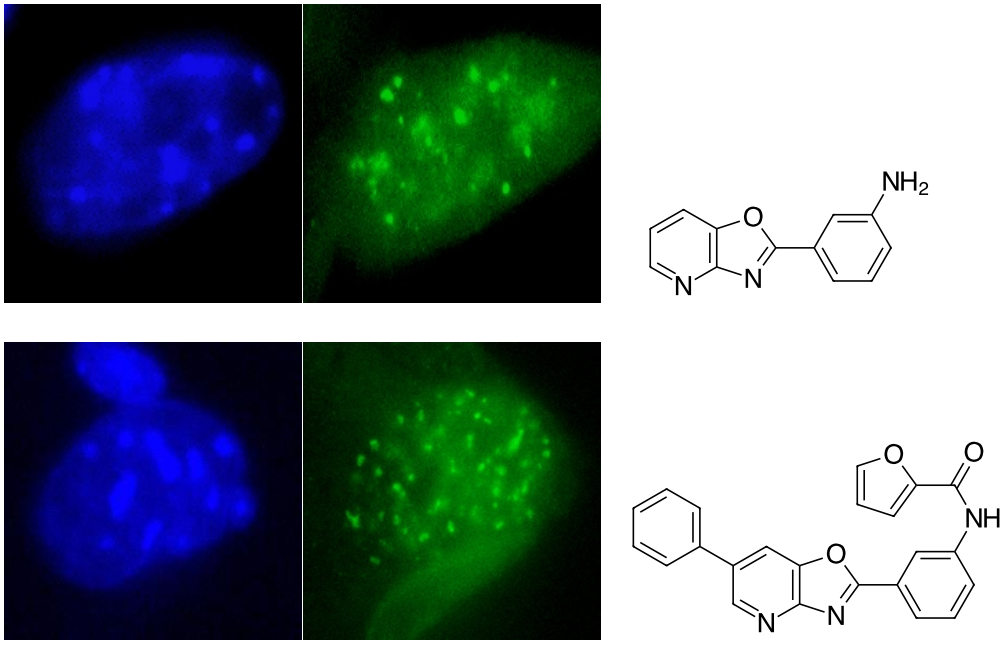

Figure 52. Visualisation of γ -H2AX-induced by pyridoxazole compounds

It also has the obvious consequence that they may not be suitable as therapeutics due to this DNA damaging behaviour. However, the furyl amides do not appear to be relatively toxic from the *T. brucei* study (discussed in Chapter 3). Therefore, the concern is that if these compounds cause DNA damage but have low toxicity then they are potential mutagens.

4.3 Conclusion and Future

This preliminary study demonstrated the ability of these compounds to cause double-strand breaks as supported by their strong γ -H2AX staining. More work is needed to answer questions such as the rate by which those compounds induce DNA damage using a time kinetic assays. Assessment of the mode of action for DNA damage activity is also required to examine whether there is a direct interaction by which the DNA damage occurs or by an indirect interaction *via* reactive oxygen species or by interference with the process of the DNA repair. Another aspect that would be important is whether these compounds have the potential to exert their action by blocking the enzymes needed for the phosphorylation such as PI3 kinase family and DNA-PK kinases since they are involved with the phosphorylation event and indeed they are used as targets for design of anticancer drugs [108]. The results from this current study might led itself into the potential for investigation of anti-cancer agents.

CHAPTER 5: EXPERIMENTAL

5.1 General experimental

Nuclear Magnetic resonance

Proton (^{1}H) and carbon (^{13}C) nuclear magnetic resonance spectra were recorded in deuterated chloroform ($CDCl_3$) unless otherwise stated, on a Varian Mercury 2000 spectrometer at 300 MHz and 75 MHz respectively. Chemical shift were recorded as δ values in parts per million (ppm) and referred to the solvent used. Proton resonances are annotated using the following abbreviations for assigning ^{1}H spectra (s = singlet; d = doublet; triplet; q = quartet; m = multiplet; bs = broad singlet; dd = doublet of doublet; dt = doublet of triplets; ddd = doublet of doublets of doublets, J = coupling constant (Hz) and number of protons.

Infrared spectroscopy

Infrared spectra were recorded on Shimadzu FTIR 8400s spectrometer as a thin film on NaCl plates or as a solid on a Perkin Elmer Spectrum 100 FT-IR spectrometer fitted with a diamond universal ATR sampling accessory.

Mass spectroscopy

Low resolution mass spectrometry was performed on a kratos concept ISQ mass instrument. Positive electron ionisation mass spectrometry measurements were made on a Kratos Concept ISQ magnetic sector mass spectrometer using a heatable direct insertion probe. Sub-microgram quantities were loaded onto the probe and heat was applied to the probe as necessary to vaporise the sample. For nominal mass data a mass resolution of 1000 was used, and the range from *m/z* 35 to 800 was scanned at 2

seconds per decade, and a 5.3KV accelerating voltage. Data were acquired and processed using Kratos Mach3 software.

For accurate mass data the instrument was run in 'peak matching' mode at a resolution of ~8000, and perfluorkerosene was used for the reference masses. A window of 1500ppm around the expected mass was acquired and the peak observed measured against the reference peaks immediately below and above it.

For direct infusion electrospray MS, samples were dissolved in an appropriate solvent, usually either methanol or a chloroform/methanol mixture, and were analyzed using a Waters Xevo triple quadrupole mass spectrometer infusing at ~ 5ul/min. The mass spectrometer was operated in positive ion electrospray mode with capillary voltage of 2.7 kV, and cone voltage of ~15V (adjusted as necessary for different mass ranges). The ion source temperature was 150°C, the desolvation gas was nitrogen at 300 L/hr, the cone gas flow was 0L/hr and the desolvation temperature was 150°C. Scan ranges were adjusted as appropriate for each sample.

Flash chromatography

Merck flash grade Silica Gel (32-63) was used and performed according to Still et al [109]

Thin layer chromatography

Merck Silica Gel 60 F254 aluminium backed sheets were used for analytical thin layer chromatography. TLC plates were visualized under 254 nm UV lamp and or by treatment with phosphoric acid/ ceric sulfate stain, followed by heating. Stain recipes (phosphomolybdic acid (37.5 g), ceric sulfate (7.5g), sulphoric acid (37.5 ml), water (750 mL).

Microwave assisted reactions

Microwave assisted reactions were performed in a sealed tube and heated in a CEM Discover Microwave reactor for 300 W at 200 ^{0}C.

5.2 Synthetic compounds

Reagents were used as received from their suppliers, unless otherwise stated. Dichloromethane, ethyl acetate and hexane were distilled prior to use. Pyridine and triethylamine were dried using molecular sieves for a minimum of 24 h before use.

5.3 General procedures

General Procedure A1: synthesis of the pyridoxazole core

2-Amino-3-hydroxypyridine (1.0 eq) and the relevant benzoic acid (1.0 eq), was added to polyphosphoric acid (30g, 14.5 mL) and the mixture was heated to 180 ^{0}C for 5 h, and poured carefully into a slurry of ice and water while hot, neutralised with solid bicarbonate and the precipitant filtered and washed with water to give the pyridoxazoles.

General procedure A2: synthesis of the pyridoxazole core

2-Amino-3-hydroxypyridine (1.0 eq) and the relevant benzoic acid (1.0 eq), was added to polyphosphoric acid (30g, 14.5 mL) and the mixture was heated to 220 ^{0}C for 5 h, and poured carefully into a slurry of ice and water while hot, neutralised with 5 M sodium hydroxide and the precipitant filtered and washed with water to give the pyridoxazoles.

General procedure A3: amide coupling 1

To a solution of the pyrdioxazole core (1eq) in dichloromethane (10 mL) was added the furoic acid (1.2 eq), EDCI (3 eq), triethylamine (1.3 eq) and DMAP (0.2 eq). The solution was stirred under nitrogen atmosphere overnight. The reaction mixture was diluted with dichloromethane (30 mL) before being washed with 0.5 M of potassium hydrogen sulfate (2 X 10 mL) and saturated sodium carbonate (2 X 5 mL). The combined organic layer was dried over sodium sulfate and evaporated to give the crude amide derivatives.

General procedure A4: amide coupling 2

To a solution of the aniline (1 eq) in dichloromethane (9 ml) was added the acid chloride (2 eq), pyridine (1 ml) and DMAP (0.2 eq). The solution was stirred under a nitrogen atmosphere overnight. The reaction mixture was diluted with dichloromethane (30 ml) before being washed with 2N HCL (2 X 10 mL) followed by brine (2 X 5 mL). The organic extract was dried over sodium sulfate

and solvent evaporated to give the crude amide derivatives.

General procedure A5: amide coupling 3

To a solution of the amine in tetrahydrofuran (7 ml) was added triethylamine (1.5 eq) and DMAP (0.2 eq) and the solution was stirred overnight. The reaction mixture was diluted with ethyl acetate (30 mL) and washed with aqueous bicarbonate (2 X 15 mL) followed by saturated NH_4Cl (10 ml X 1). The organic extract was dried over sodium sulfate, and the solvent was evaporated to give the crude amide.

General procedure A6: Suzuki-Miyaura reaction

A solution of *N*-(3-(6-bromooxazolo[4,5-*b*]pyridine-2-yl)phenyl)fura*n*-2-carboxamide **131** (1.0 eq) or *N*-(3-(6-bromooxazolo[4,5-*b*]pyridine-2-yl)phenyl)furan-3-carboxamide **132** (1.0 eq), boronic acid (3.3 eq) and Pd(PPh3)4 (0.1 eq) in toluene:ethanol: 2 M aqueous sodium carbonate (10:1:1 15 mL) was refluxed for 10 h under an atmosphere of nitrogen. Ethyoursl acetate (20 mL) was added and the organic phase washed with saturated sodium bicarbonate (2 X 10 mL). The organic extract was dried with sodium sulfate, filtered and evaporated to give the crude product which was purified by flash chromatography.

5.3.1 Synthesis of 3-(Oxazolo[4,5-*b*]pyridin-2-yl)aniline (103)

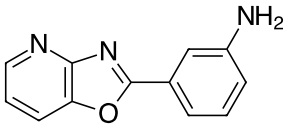

Title compound was prepared according to general procedure A1 from 2-amino-3-hydroxypyridine (1.00 g , 9.1 mmol) and *m*-aminobenzoic acid (1.25 g , 9.1mmol) to give 3-(oxazolo[4,5-*b*]pyridin-2-yl)aniline as a pale-yellow solid (1.75 g, 91 %).

mp > 230 ^{o}C (lit. mp = 232–334) [67]), IR $_{vmax}$ (cm^{-1}, solid): 782, 1260, 1275, 1405, 3328, 3453, ^{1}H NMR δ ($CDCl_3$/drops of DMSO-d_6): 5.02 (bs, 2H), 6.63 (ddd, *J* = 8.1, 2.4, 1.2, 1H), 7.03 (m, 2H), 7.31 (m, 2H), 7.61 (dd, *J* = 8.1, 1.2, 1H), 8.24 (dd, J = 4.8, 1.2 Hz, 1H). ^{13}C NMR ($CDCl_3$): 113.1, 116.7, 117.6, 118.4, 119.4, 126.3, 129.2, 142.3, 145.7, 147.0, 155.5, 165.3; LRMS $[M+H]^+$, 212.2 m/z.

5.3.2 Synthesis of 2-Oxazolo[4,5-*b*]pyridin-2-yl)aniline (104)

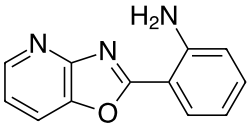

The titled compound was prepared according to procedure A2 using 2-amino-3-hydroxy pyridine (2.23 g, 20.25 mmol) and anthranillic acid (2.78 g, 20.25 mmol) to give 2-oxazolo[4,5-*b*]pyridin-2-yl-aniline as yellow crystals (0.50 g, 12 %).

mp = 186 – 188 ^{o}C (lit 182-183 ^{o}C [66] , IR $_{vmax}$ (cm^{-1}, solid): 761, 1253, 1407, 3303, 3395, ^{1}H NMR ($CDCl_3$) δ: 6.30 (s, 2H), 6.74-6.81 (m, 2H), 7.28 (m, 2H), 7.82 (d, *J* = 8.1,1H), 8.04 (d, *J* = 8.1, 1H), 8.51 (d, *J* = 5.1, 1H).^{13}C NMR ($CDCl_3$) δ: 107.5, 116.6, 116.8, 117.8, 119.9, 128.7, 131.5, 133.7, 141.8, 146.3, 149.0, 165.8.

5.3.3 Synthesis of 2-Oxazolo[4,5-*b*]pyridin-4-yl)aniline (105)

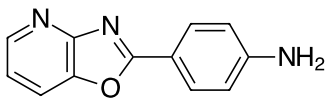

The titled compound was prepared according to procedure A2 using 2-amino-3-hydroxypyridine (1.00 g, 9.08 mmol) and *para*-aminobenzoic acid (1.25 g, 9.08 mmol) to give 2-oxazolo[4,5-*b*]pyridin-4-yl-aniline as a brown solid (400 mg, 20 %).

mp > 230 ^{o} C (lit. 262 C^{o} [66]) , IR $_{vmax}$ (cm^{-1}, solid): 798, 1266, 1300, 1406, 1450, 3322, 3490, ^{1}H NMR 4.50 (s, 2 H), 6.68 (dd, *J* = 6.9, 2.1 Hz, 2H), 7.07 (dd, *J* = 8.1, 4.8 Hz, 1H), 7.36 (dd, *J* = 7.8, 1.5 Hz, 1H), 7.80 (m, 3H).

5.3.4 Synthesis of 2-(2-Chloro-3-nitrophenyl)oxazolo[4,5-*b*]pyridine (106)

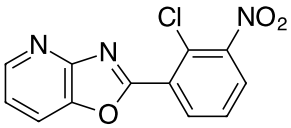

The titled compound was prepared according to procedure A1 from 2-amino-3-hydroxy-pyridine (0.55 g, 4.99 mmol) and 2-chloro-3-nitrobenzoic acid (1.01 g, 4.99 mmol) to give 2-(2-chloro-3-nitrophenyl)oxazolo[4,5-*b*]pyridine as a pale-yellow solid (0.83 g, 60 %).

mp = 220, IR $_{vmax}$ (cm^{-1}, solid): 782, 1263, 1406, 1524, 3086, ^{1}H NMR ($CDCl_3$) δ: 7.24 (dd, *J* = 8.4, 5.1 Hz, 1H), 7.61 (t, *J* = 8.1 Hz, 1H), 7.94 (m, 2H), 8.43 (dd, *J* = 7.8, 1.5 Hz, 1H), 8.68 (dd, *J* = 4.8, 1.5 Hz, 1H).

5.3.5 2-(4-Chloro-3-nitrophenyl)oxazolo[4,5-*b*]pyridine (107)

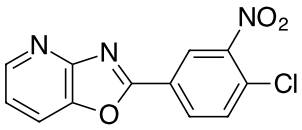

The titled compound was prepared according to the procedure A1 from 2-amino-3-hydroxypyridine (1.00 g, 9.08 mmol) and 4-chloro-3-nitrobenzoic acid (1.83 g, 9.08 mmol) to give 2-(4-chloro-3-nitrophenyl)oxazolo[4,5-*b*]pyridine as a grey solid (1.73 g, 6.28 mmol, 70 %)

mp = 220 ^{o}C, IR $_{vmax}$ (cm^{-1}, solid): 663, 725, 782, 793, 902, 1044, 1257, 1346, 1401, 1523, 1615, 3085, 3360, 3440, ^{1}H NMR ($CDCl_3$) δ 7.44 (dd, *J* = 8.2, 4.8 Hz, 1H), 7.80 (d, *J* = 8.8 Hz, 1H), 8.02 (dd, *J* = 8.2, 1.5 Hz, 1H), 8.34 (dd, *J* = 8.8, 2.7 Hz, 1H), 8.70 (d, *J* = 4.8 Hz, 1H), 9.16 (d, *J* = 2.7 Hz, 1H).

5.3.6 2-(2-Methyl-5-nitrophenyl)oxazolo[4,5-*b*]pyridine (101)

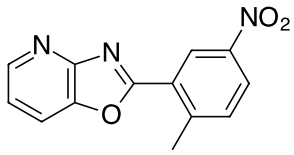

The titled compound was prepared according to the procedure A1 using 2-amino-3-hydroxypyridine (1.00 g, 9.08 mmol) and 2-methyl-5-nitro- benzoic acid (1.65 g, 9.08 mmol) to give 1.95g of 2-(2-methyl-5-nitrophenyl)oxazolo[4,5-*b*]pyridine (1.91 g, 82%).

mp = 123-125 ^{o}C, IR $_{vmax}$ (cm^{-1}, solid): 783, 1257, 1344, 1511, ^{1}H NMR ($CDCl_3$) δ: 2.95 (s, CH_3), 7.40 (m, 1H), 7.57 (d, *J* = 8.4, 1H), 7.98 (dd, *J* = 9.9, 1.5, 1H), 7.28 (d, *J* = 8.4, 1H), 8.65 (d, *J* = 4.8, 1H), 9.01 (s, 1H).

5.3.7 synthesis of 2-Chloro-3-(oxazolo[4,5-*b*]pyridin-2-yl)aniline (110)

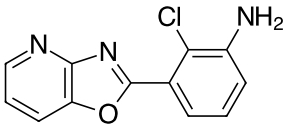

The nitro derivative **106** (0.40 g, 1.45 mmol) was reduced by heating with iron powder (4.35 mmol) and concentrated hydrochloric acid (20.3 mmol) in refluxing ethanol (5 ml) for five h. The reaction mixture was cooled and made alkaline with saturated sodium bicarbonate solution. The aqueous phase was extracted with ethyl acetate (3 x 30 mL) and the extract was dried with sodium sulfate, filtered and evaporated to give the title compound as a brown solid (236 mg, 66 %).

mp = 88-90 C^{o}, IR $_{vmax}$ (cm^{-1}, solid): 778, 1270, 1408, 1601, 3196, 3366;^{1}H NMR δ ($CDCl_3$): 4.50 (bs, 2H) 6.97 (d, *J* = 6.9 Hz, 1H), 7.35-7.19 (m, 2H), 7.70 (d, *J* =7.5 Hz, 1H), 7.89 (d, *J* = 8.1 Hz, 1H), 8.60 (s, 1H), HRMS: M^{+} predicted for $C_{12}H_8N_3OCl$ 245.0355, found 245.0354, LRMS m/z (EI+): 245 (M^{+}, 100), 209 (M^{+}- Cl, 10).

5.3.8 Synthesis of 2-Chloro-5-(oxazolo[4,5-*b*]pyridin-2-yl)aniline (111)

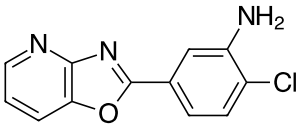

The nitro derivative **107** (0.725 mmol) was reduced according to the procedure used to prepare **110** to give the title compound, 4-Chloro-5-(oxazolo[4,5-*b*]pyridin-2-yl)aniline as a pale yellow solid (110 mg, 61 %).

mp = 88-90 ^{o} C, IR $_{vmax}$ (cm^{-1}, solid): 794, 1262, 1408, 3324, 3412, ^{1}H NMR δ ($CDCl_3$): 4.25 (bs, 2H), 7.30 (dd, *J* = 8.1, 5.1 Hz, 1H), 7.41 (d, *J* = 8.1 Hz, 1H), 7.62 (dd, *J* = 8.1, 1.8 Hz, 1H), 7.74 (d, *J* = 2.1 Hz, 1H), 7.85 (d, *J* = 8.1 Hz, 1H), 8.59 (d, *J* = 4.8 Hz, 1H).

^{13}C NMR δ ($CDCl_3$): 114.9, 118.4, 118.5, 120.4, 123.7, 125.9, 130.3, 143.4, 143.7, 146.9, 156.5, 165.4, HRMS: M^+ for $C_{12}H_8N_3O_1Cl_1$ 245.0355; found 245.0356, MS m/z (EI+): 245 (M^+, 100), 210 (M^+- Cl, 6).

5.3.9 Synthesis 4-methyl-3-(oxazolo[4,5-*b*]pyridin-2-yl)aniline (112)

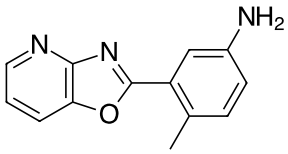

The nitro derivative **101** (1.00 g, 4.44 mmol) was reduced according to the procedure used to prepare **110** but was refluxed for 6 h to give 4-Methyl-3-(oxazolo[4,5-*b*]pyridin-2-yl)aniline (537 mg, 54 %).

mp > 230 C^o, ^{o} C, IR $_{vmax}$ (cm^{-1}, solid): 794, 1262, 1408, 3324, 3412, ^{1}H NMR ($CDCl_3$) δ 2.95 (s, 3H), 6.77 (d, *J* = 8.1 Hz, 1H), 7.11 (d, *J* = 8.1 Hz, 1H), 7.27 (t, 2H) 7.57 (s, 2H), 7.83 (d, *J* = 8.1 Hz, 1H), 8.55 (dd, *J* = 4.9 Hz, 1H), CNMR ($CDCl_3$) δ 20.1, 116.2, 118.2, 119.2, 120.1, 125.8, 129.8, 133.1, 142.6, 144.7, 146.6,156.5, 166.40, HRMS: M^+ for $C_{13}H_{11}N_3O$ 305.0800 m/z; found 305.0801 m/z, LRMS m/z (EI+): 305 (M^+, 100).

5.3.10 *N*-(3-(Oxazolo[4,5-*b*]pyridin-2-yl)phenyl)furan-2-carboxamide (113)

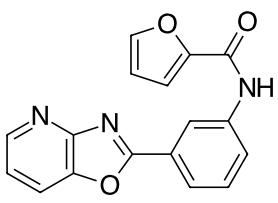

The title compound was prepared according to general procedure A3 using amine **103 (**250 mg, 1.18 mmol) and 2 furoic acid (0.16 g, 1.42 mmol) to give the crude sample that was purified by flash chromatography (silica: eluent 100% ethyl acetate) to yield *N*-(3-(Oxazolo[4,5-*b*]pyridin-2-yl)phenyl)furan-3-carboxamide as a pale-white solid (0.3 g, 83 %).

mp > 230 C^o, IR $_{vmax}$ (cm^{-1}, thin film): 774, 1264, 1650, 3287,^{1}H NMR δ ($CDCl_3$/ DMSO-d_6): 6.24 (dd, *J* = 3.3, 1.5 Hz, 1H), 6.99 (m, 2H) 7.17 (t, *J* = 8.1 Hz, 1H), 7.28

(d, *J* = 8.7 Hz, 1H), 7.58 (dd, *J* = 8.1, 1.2 Hz, 1H), 7.71 (ddd, 12.9, 7.5, 1.2 Hz, 2H), 8.20 (d, *J* = 4.2 Hz, 1H), 8.38 (s, 1H), 9.55 (s, 1H), ^{13}C NMR δ: 112.2, 115.15, 118.46, 119.7, 120.4, 123.4, 124.4, 126.7, 129.6, 139.3, 143.1, 144.9, 146.6, 147.7, 156.1, 156.9, 165.3, HRMS: M^+ for $C_{17}H_{11}N_3O_3$, predicted 305.0800; found 305.0802, MS m/z (EI+): 276 (10), 305 (M^+, 52), 95 (100).

5.3.11 Synthesis of *N*-(3-Oxazolo [4, 5-*b*] pyridine-2-yl)phenylfuran-3-carboxamide (114)

The title compound was prepared according to general procedure A3 from compound

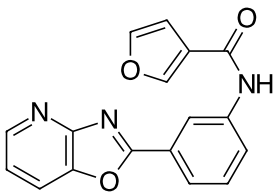

103 (100 mg, 0.47 mmol) and 3-furoic acid (63.68 mg, 0.57 mmol to yield the crude product which was purified by flash chromatography (silica gel, eluent: 100% ethyl acetate) to yield the title compound as an off-white solid (110.0 mg, 360.32 mmol, 76 %).

mp > 230 ^{o}C, IR $_{vmax}$ (cm^{-1}, thin film): 782, 1260, 1410, 1535, 1676, 3300; ^{1}H NMR δ ($CDCl_3$): 6.83 (d, *J* = 3.6 Hz, 1H) 7.29 (t, *J* = 4.8 Hz, 1H), 7.50-7.45 (m, 2H), 7.82 (dd, *J* = 8.1, 3.6 Hz, 1H), 8.00 (m, 2H), 8.15 (d, *J* = 0.9 Hz, 1H), 8.28 (s, 1H), 8.45 (s, 1H), 8.54 (d, *J* = 5.1 Hz, 1H); ^{13}C NMR δ ($CDCl_3$): 108.7, 118.6, 119.7, 120.5, 123.0, 124.1, 124.5, 127.2, 130.1, 138.8, 143.4, 144.3, 145.8, 146.9, 156.4, 161.3, 165.4; LRMS: M^+ for $C_{17}H_{11}N_3O_3$ predicted 305.0800, found 305.0801, MS m/z (EI+): 305 (M^+, 20), 95 (100).

5.3.12 *N*-(2-(Oxazolo[4,5-*b*]pyridine-2-yl)phenyl)furan-2-carboxamide (115)

The titled compound was prepared according to procedure A5 using aniline **104** (200 mg, 0.95 mmol and 2-furoyl chloride (2 eq, 0.18 ml, 1.89 mmol to give the crude product which was purified by flash chromatography (silica: eluent 100% ethyl acetate) to yield the title compound (0.17 g, 59 %).

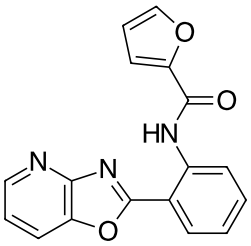

mp > 230 ^{o}C, IR $_{vmax}$ (cm^{-1}, solid): 744, 1259, 1263, 1691; ^{1}H NMR ($CDCl_3$) δ: 6.60 (dd, *J* = 3.6, 1.8, 1H), 7.25 (m, 1H), 7.35-7.42 (m, 3H), 7.597 (t, *J* = 8.1, 1H), 7.75 (s, 1H), 7.9 (d, *J* = 8.1, 1H), 8.24 (d, *J* = 8.1, 1H), 8.62 (d, *J* = 4.8, 1H), 8.97 (d, *J* = 8.4, 1H).^{13}C NMR ($CDCl_3$) δ: 112.51, 112.57, 115.5, 118.6, 120.9, 121.0, 123.4, 128.6, 134.2, 139.8, 141.2, 145.9, 147.2, 148.3, 155.3, 157.4, 164.6; HRMS: M^+ for $C_{17}H_{11}N_3O_3$, predicted 305.0800, found 305.0796, MS m/z (EI+): 305 (M^+, 100), 95 (50).

5.3.13 Synthesis of *N*-(2-(Oxazolo[4,5-*b*]pyridine-2-yl)phenyl)furan-3-carboxamide (116)

The titled compound was prepared according to procedure A5 using aniline **104** (200 mg, 0.95 mmol) and 3-furoyl chloride (2.4 eq, 296.6 mg, 2.27 mmol) to give the crude product which was purified by flash chromatography (silica: eluent 40 % ethyl acetate in hexane) to yield the titled compound as an off-white solid (37.60 mg, 13 %).

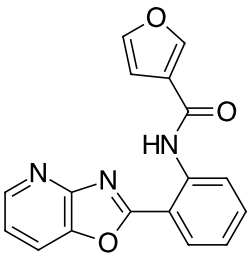

mp = 188-190 C^{o} ^{1}H NMR: 7.21 (m, 2H), 7.39 (dd, *J* = 8.1, 5.1, 1H), 7.58 (m, 2 H), 7.9 (d, *J* = 8.1, 1H), 8.26 (d, *J* = 8.1, 1H), 8.34 (s, 1H), 8.64 (d, *J* = 5.1, 1H), 9.00 (d, *J*

= 8.4, 1H) 12.40 (s, 1H). ^{13}C NMR: 108.8, 112.1, 118.7, 120.7, 121.0, 123.2, 124.0, 128.5,134.3, 140.2, 141.8, 144.4, 146.4, 147.2, 155.0, 161.7, 164.7. HRMS: M^+ for $C_{17}H_{11}N_3O_3$, predicted 305.0800, found 305.0806, MS m/z (EI+): 305 (M^+, 62), 95 (100), 288 (20), 277 (17), 264 (35), 249 (29), 248 (13).

5.3.14 Synthesis of *N*-(4-(Oxazolo[4,5-*b*]pyridine-2-yl)phenyl)furan-2-carboxamide (117)

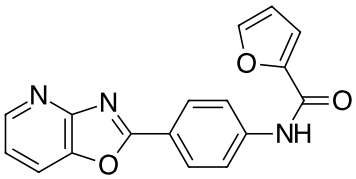

The titled compound was prepared according to procedure A4 using aniline **105** (200mg, 0.95 mmol) and 2-furoyl chloride (0.20 ml, 2.03 mmol) to give the crude product which was purified by flash chromatography (silica: eluent 100% ethyl acetate) to yield the title compound (0.17 g, 59 %).

Mp = 200 - 202 ^{o} C, IR $_{vmax}$ (cm^{-1}, solid): 748, 1245, 1679, 3253. ^{1}H NMR δ ($CDCl_3$): 6.39 (dd, *J* = 3.6, 1.8 Hz, 1H), 6.52 (d, *J* = 5.4 Hz, 1H), 7.08 (d, *J* = 3.6 Hz, 1H),7.24 - 7.4 (m, 2H), 7.47 (d, *J* = 7.8 Hz, 1H), 7.59 (d, *J* = 12.3 Hz, 1H), 7.72 (d, *J* = 8.7, 1H), 7.83 (m, 1H), 8.27 (dd, *J* = 4.8, 1.5 Hz, 1H), 8.34 (s, 1H); HRMS: M^+ for $C_{17}H_{11}N_3O_3$, predicted 305.0800, found 305.0804, MS m/z (EI+): 305 (M^+, 50), 95 (100).

5.3.15 Synthesis of *N*-(2-Chloro-3-(oxazolo[4,5-*b*]pyridin-2-yl)phenyl)furan-2-carboxamide (118)

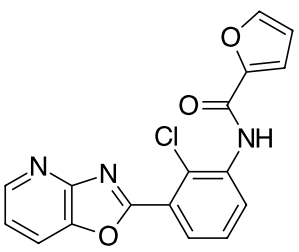

The titled compound was prepared according to procedure A4 using the amine **(110)** (0.2 g, 0.814 mmol) and 2-furoyl chloride (2 eq, 0.16 ml) to give the crude product, which

was purified by flash chromatography (silica, eluent: gradient elution from 50% EtOAc/Hexanes to 5 % MeOH in EtOAc) to give *N*-(2-chloro-3-(oxazolo[4,5-*b*]pyridin-2-yl)phenyl)furan-2-carboxamide as a pale-brown solid (0.15 g, 54%).

Mp = 210 - 212 ^{o}C, IR $_{vmax}$ (cm^{-1}, solid): 765, 1266, 1405, 1518,1685, 3403, ^{1}H NMR δ ($CDCl_3$): 6.6 (dd, *J*= 3.6, 1.8 Hz, 1H), 7.31 (d, *J* = 4.5 Hz, 1H), 7.37 (*J*= 8.1, 4.8 Hz, 1H), 7.49 (t, *J* = 8.4 Hz, 1H), 7.60 (d, *J* = 2.7 Hz, 1H), 7.96 (ddd, *J*= 14.4, 8.1, 1.5 Hz, 2H), 8.64 (dd, *J*= 4.8, 1.5 Hz, 1H), 8.78 (dd, *J* = 8.4, 1.5 Hz, 1H), 9.02 (s, 1H), ^{13}C NMR δ ($CDCl_3$): 113.1, 116.4, 118.8, 121.0, 122.6, 124.5, 126.1, 127.2, 127.9, 136.3, 144.2, 145.2, 147.3, 147.5, 155.9, 156.3, 163.5. HRMS:M^{+} for C17H10N3O3Cl, predicted 339.0410, found 339.0414, LRMS m/z (EI+): 339 (M^{+}, 3), 304 (M^{+}- Cl, 100), 95 (55).

5.3.16 Synthesis of *N*-(2-Chloro-5-(oxazolo[4,5-*b*]pyridin-2-yl)phenyl)furan-2-carboxamid (119)

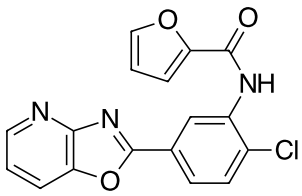

The titled compound was prepared according to procedure A4 using aniline **111** (200 mg, 0.814 mmol) and 2-furoyl chloride (0.16 ml, 1.63 mmol) to give the crude product which was purified by flash chromatography (silica: Eluent 60% ethyl acetate in hexane) to yield *N*-(2-chloro-5-(oxazolo[4,5-*b*]pyridin-2-yl)phenyl)furan-2-carboxamide as a pale-brown solid (0.13 g, 47%).

Mp = 210 - 212 ^{o}C, IR $_{vmax}$ (cm^{-1}, solid): 756, 1263, 1405, 1526, 1688, 3403, ^{1}H NMR ($CDCl_3$) δ 6.60 (dd, *J* = 3.6, 1.8 Hz, 1H), 7.33 (d, *J* =4.2 Hz, 2H), 7.58 (d, *J* = 8.4 Hz, 2H), 7.88 (dd, *J* = 8.1, 1.5 Hz, 1H), 8.09 (dd, *J* =8.4, 1.8 Hz, 1H), 8.57 (dd, *J* = 4.8, 1.2 Hz, 1H), 8.79 (s, 1H), 9.45 (d, *J* = 1.8 Hz, 1H), ^{13}C NMR δ ($CDCl_3$) δ

112.6, 113.1, 116.5, 118.7, 120.2, 120.6, 124.7, 126.3, 127.0, 135.1, 143.4, 145.1, 146.8, 147.1, 156.1, 156.3, 164.7, HRMS: M^+ for $C_{17}H_{10}N_3O_3Cl$, predicted 339.0410 found 339.0414, MS m/z (EI+): 304 (M^+- Cl], 100), 339 (M^+, 4), 95 (70).

5.3.17 Synthesis of *N*-(4-Methyl-3-(oxazolo[4,5-*b*]pyridin-2-yl)phenyl)furan-2-carboxamide (120)

The titled compound was prepared according to procedure A4 using aniline **112** (200 mg, 0.8879 mmol) and excess of 2-furoyl chloride (0.33 ml, 3.34 mmol) to give the crude sample which was purified by flash chromatography (silica: eluent 60 ethyl acetate in hexane) to yield *N*-(4-Methyl-3-(oxazolo[4,5-*b*]pyridin-2-yl)phenyl)furan-2-carboxamide as a pale brown solid (0.12 g, 42 % yield).

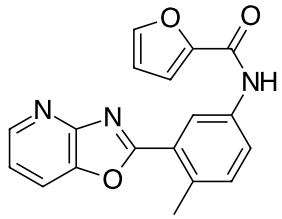

mp = 210-212, ^{o}C, IR $_{vmax}$ (cm^{-1}, solid): 779, 1259, 1408, 1522, 1649, 3278, ^{1}H NMR ($CDCl_3$) δ 2.66 (s, 3H), 6.55 (dd, *J* = 3.60, 1.5, 1H), 7.28 -7.36 (m, 2H), 7.52 (m, 2H), ,7.79-7.90 (m, 2H), 8.30 (s, 1H), 8.55 (m, 2H); ^{13}C NMR ($CDCl_3$) δ 20.1, 112.9, 115.8, 118.6, 120.5, 121.2, 123.5, 125.8, 133.0, 135.8, 136.3, 142.7, 144.6, 146.6, 146.86, 147.7, 156.3, 165.5, HRMS (M^+): predicted for $C_{18}H_{13}N_3O_3$ 319.0956; found 319.0962, MS m/z (EI+): 319 (M^+, 55), 95 (100).

5.3.18 Synthesis of 3-(1H-Imidazo[4,5-*b*]pyridine-yl)aniline (122)

The titled compound was prepared according to procedure A2 using 2,3-diaminopyridine (0.99 g, 9.07 mmol) and *m*-aminobenzoic acid (1.24 g, 9.07 mmol) to give the crude aniline as a tan solid (1.62 g, 84 %) and was used without further purification.

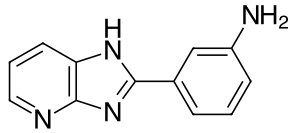

mp > 230 ^{o}C, IR $_{vmax}$ (cm^{-1}, solid): 770, 1267, 1414, 1473, 1596, 3303, 3465, ;^{1}H NMR δ (DMSO): 5.05 (bs, 2H), 6.71 (d, *J* = 7.6 Hz, 1H), 7.19 (m, 3H), 7.33 (m, 1H), 7.46 (s, 1H), 7.95 (bs, 1H), 8.29 (bs, 1H);^{13}C NMR δ (DMSO): 154.0, 149.8, 144.2, 136.2, 130.8, 130.1, 126.6, 119.7, 118.6, 116.9, 114.9, 112.7.

5.3.19 Synthesis of *N*-(3-(1H-Imidazo[4,5-*b*] pyridin-2-yl)phenyl)furan-2-carboxamide (123)

The titled compound was prepared according to procedure A5 using the crude aniline

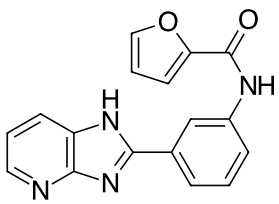

(122) (200 mg, 0.95 mmol) and 2-furoyl chloride (1.2 eq, 1.14 mmol, 0.11 mL) to give the crude product which was purified by flash chromatography (silica gel: eluent: gradient elution 1 - 2% MeOH in EtOAc) to give the title compound as a white solid (140 mg, 0.46 mmol, 48 %).

mp > 230 ^{o}C, IR $_{vmax}$ (cm^{-1}, solid):762, 1261, 1407, 1597, 1692, 3103, 3296; ^{1}H NMR δ ($CDCl_3$/DMSO): 6.34 (m, 1H), 6.95 (dd, *J* = 7.8, 4.8 Hz, 1H), 7.07 (d, *J* = 3.5 Hz, 1H), 7.25 (m, 1H), 7.37 (m, 1H), 7.77 (m, 3H), 8.10 (bs, 1H), 8.18 (s,1H), 9.33 (s, 1H). ^{13}C NMR δ ($CDCl_3$/DMSO): 112.3, 115.2, 118.2, 118.9, 122.6, 122.9, 129.6, 130.5, 138.7, 144.1, 144.8, 147.8, 153.1, 156.8; (three carbons missing or overlapped); HRMS: M^+ for $C_{17}H_{12}N_2O_2$, predicted 304.0960, found 304.0949, Ms m/s (EI+): 305 (M^+, 50), 237 (100), 212 (40), 194 (80).

5.3.20 Synthesis of *N*-(3-(1*H*-Imidazo[4,5-*b*]pyridin-2-yl)phenyl)furan-3-carboxamide (124)

The titled compound was prepared according to the general procedure A5 using

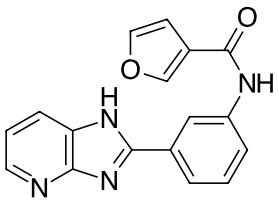

aniline derivative **122** (200 mg, 0.95 mmol) and 3-furoyl chloride (149.0 mg, 1.14 mmol) to give the crude product which was purified by flash chromatography (Silica gel: eluent: gradient elution 100% EtOAc to 2% MeOH in EtOAc to give the title compound as a white solid (0.13 g, 44 %).

mp > 230 ^{o}C, IR $_{vmax}$ (cm^{-1}, solid): 797, 1261, 1441, 1649, 3064, 3290, ^{1}H NMR δ ($CDCl_3$): 7.04 (dd, *J* = 1.8, 0.9 Hz, 1H), 7.27 (dd, *J* = 8.1, 5.1 Hz, 2H), 7.54 (t, *J* = 7.8 Hz, 1H), 7.80 (d, *J* = 1.5 Hz , 1H), 7.9 (dd, *J* = 8.1, 1.8 Hz, 1H), 8.05 (dd, *J* = 8.1, 1.2 Hz, 1H), 8.36 (m, 2H), 8.63 (s, 1H), 10.15 (s, 1H), ^{13}C NMR δ ($CDCl_3$/DMSO): 109.9, 118.9, 119.5, 122.4, 123.0, 123.5, ,130.1, 130.7, 140.2, 144.4, 145.0, 146.8, 161.3 (four carbons missing or overlapped); HRMS: M^+ for $C_{17}H_{13}N_4O_2$, predicted 305.1033, found 305.1031 , Ms m/s (EI+): 305 ([M+H]$^+$, 100), 306 (25), 237 ([M+Na]$^+$, 40).

5.3.21 Preparation of starting material 5-bromo-2-amino-3-hydroxy pyridine (132)

The titled compound **(132)** was prepared by the procedure reported by the previously reported method [79,81].

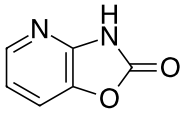

2-Amino-3-hyroxypyridine (5.5 g, 50 mmol) was dissolved in THF (100 mL) and 1,1-carbonyldiimidazole (CDI) 12.15 g (1.5 eq, 75 mmol) and refluxed for 7 h. The reaction mixture evaporated and the residue

dissolved in dichloromethane (100 ml) and the organic layer washed with 2 N NaOH (5 x100 mL). The combined aqueous layer were cooled with an ice bath and acidified to pH 5-6 with 2 N HCL. The resulting precipitate was collected by filtration and washed with water and dried to give (23.04 g, 99%) oxazolo[4,5-b]pyridine-2-(3H)-one **(130)**.

mp = 211-212^{o} (lit. m.p. 212-214 [110]), IR $_{vmax}$ (cm^{-1}, solid): 1782, 3099-2900, HNMR (DMSO- *d*6): 4.03 (bs, 1H), 7.04 (dd, *J* = 7.8, 5.4, 1H), 7.5 (d, *J* = 8.1, 1H), 7.9 (d, *J* = 5.5 Hz, 1H); ^{13}C NMR (DMSO- *d*6): 116.6, 118.5, 138.1, 143.0, 146.9, 154.2.

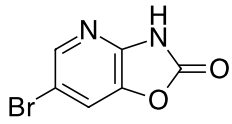

To a solution of oxazolo[4,5-*b*]pyridine-2-(3H)-one **130** (6 g, 44.11 mmol) in DMF (45 mL) was added bromine dropwise (2.5 ml, 48.53 mmol) and the solution stirred at rt. for 1.5 h. The reaction mixture was poured into crushed ice and water and the solid collected, washed with water, and dried to afford (9.50 g, 98%) of 6-bromooxazolo[4,5-*b*]pyridine-2(*3H*)-one **(131)**.

mp > 230 C^{o} (lit. mp = 234 C^{o} [81]) ^{o} IR $_{vmax}$ (cm^{-1}, solid) 1781, 3077-2800, 1610 ^{1}H NMR (DMSO-d6): 7.98 (d, *J* = 2.1, 1H), 8.15 (d, *J* = 2.1, 1H), 12.3 (bs, 1H). ^{13}C NMR (DMSO-d6): 112.5, 119.6, 138.6, 143.5, 146.2, 153.8.

6-Bromooxazolo[4,5-*b*]pyridine-2(*3H*)-one **131** (5.2g, 24.19 mmol) was hydrolysed by refluxing in 70 ml of 10% aqueous NaOH. The reaction mixture was cooled under ice bath and was acidified with 6 N HCL added to pH 7-8 and the precipitate was collected by vacuum filtration and dried in vacuum desiccator to give 5-bromo-2-amino-3-hydroxy pyridine (3 g, 65 %).

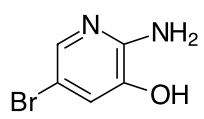

mp > 230 °C (lit. mp > 250 °C [68]); IR $_{vmax}$ (cm^{-1}, solid): 3100-3440, 3340 and 3438 ^{1}H NMR (DMSO-d6): 5.7 (s, 2H), 6.93 (s, 1H), 7.44 (s, 1H); ^{13}C NMR (d_6-DMSO): 105.2, 120.9, 137.2, 141.5, 150.6.

5.3.22 Synthesis of 6-Bromo-[4,5-*b*]oxazolopyridine-2-yl)-phenylamine (135)

The titled compound was prepared according to procedure A2 using 2-amino-3-hydroxy-5-bromopyridine (1.50 g, 7.94 mmol) and *m*-aminobenzoic acid (1.09g, 7.94 mmol) but was heated for 20 h to afford the crude product as a grey solid (1.21 g, 53%).

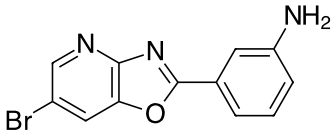

mp = 220-223 C°, IR $_{vmax}$ (cm^{-1}, solid): 1263, 3342, 3440, ^{1}H NMR δ ($CDCl_3$): 6.89 (dd, J = 8.1, 1.5 Hz, 1H), 7.29 (m, 2H), 7.60 (m, 2H), 7.98 (d, J = 2.1 Hz, 2H), 8.59 (d, J = 2.1Hz, 1H). ^{13}C NMR δ ($CDCl_3$): 113.8, 115.6, 117.6, 119.4, 121.2, 126.6, 130.0, 143.0, 147.6, 147.9, 154.6, 165.6. HRMS: M^+ for $C_{12}H_8BrN_3O$, predicted 288.9855, found 288.9855, LRMS m/z (EI+): 289 (Br^{81}, M^+, 100), 287 (Br^{79}, M^+, 98).

5.3.23 Synthesis of 6-Bromo([4,5-*b*]oxazolopyridine-2-yl)-phenyl-2-carboxamide (136)

The titled compound was prepared according to procedure A3 using the amine **135** (0.098 g, 0.338 mmol) and 2-furoic acid (1.2 eq, 45 mg, 0.405 mmol) to afford the crude product, which was purified by flash chromatography (silica gel: eluent 15 % ethyl acetate in dichloromethane) to give title compound as a pale-yellow solid (78 mg, 60%).

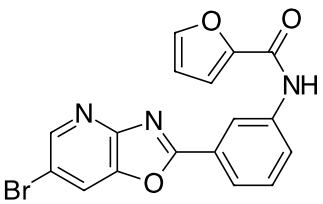

mp > 230 ^{o} C, IR $_{vmax}$ (cm^{-1}, solid): 1264, 1664, 3306, ^{1}H NMR ($CDCl_3$): 6.60 (dd, J = 3.6, 1.8, 1H), 7.30 (d, J = 4.2 Hz, 1H), 7.55 (m, 2H), 8.03 (m, 3 H), 8.30 (s, 1H), 8.50 (d, J = 1.8, 1H), 8.64 (d, J = 2.1, 1H); ^{13}C NMR ($CDCl_3$): 113.0, 116.1, 119.3, 121.4, 124.2, 124.4, 127.0, 130.3, 138.5, 143.5, 144.8, 147.6, 148.2, 155.2, 156.4, 165.9. (one carbon missing or overlapped). HRMS: M^+ for $C_{17}H_{10}BrN_3O_3$, predicted 382.9905, found 382.9907, LRMS m/z (EI+) $[M+H]^+$ 384 (Br^{79}, 13), 386 (Br^{81}, 10) ; $[M+Na]^+$ 406 (Br^{79}, 96), 408 (Br^{81}, 100); $[2M+Na]^+$ 789 (Br^{79}, 6), 791 (Br^{79}, 15), 793 (Br^{81}, 8).

5.3.24 Synthesis of 6-bromo([4,5-*b*]oxazolopyridine-2-yl)-phenyl-3-carboxamide (137)

The titled compound was prepared using procedure A3 using **135** (800 mg, 2.76 mmol) and 3-furoic acid (1.3 eq, 370 mg, 3.31 mmol) to afford the crude product **137** as a brown solid (784.2 mg, 74 %). Compound was used without further purification.

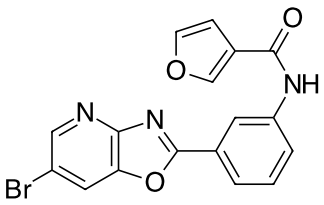

mp > 230 C^{o}, IR $_{vmax}$ (cm^{-1}, solid): 1646, 3284. ^{1}H NMR ($CDCl_3$): 7.59 (m, 2H), 7.80 (s, 1H), 7.90 (d, J = 6, 1H), 8.04 (m, 2H), 8.13 (s, 1H), 8.59 (d, J = 1.2, 1H), 8.67 (s, 1H), 10.31 (s, 1H). HRMS: M^+ for $C_{17}H_{10}N_3O_3$, predicted 382.9905, found 382.9904, LRMS m/z (EI+): 406 m/z [M+Na, Br^{79}], (100), 408 m/z [M+Na, Br^{81}], (100), 384 [M+H, Br^{79}]$^+$, (15), 386 m/z [M^+H, Br^{81}]$^+$, (15).

5.3.25 Synthesis of 6-Phenyl-([4,5-*b*]oxazolopyridine-2-yl)-phenyl-2-carboxamide (138)

The titled compound was prepared according to procedure A6 using 6-bromo([4,5-*b*]oxazolopyridine-2- yl)-phenyl-2-carboxamide **(136)** (1 eq, 30 mg, 0.0781 mmol) and phenylboronic acid (3.3 eq, 31.42 mg, 0.2577 mmol) to afford the title compound as a pale-yellow solid (26 mg, 90%).

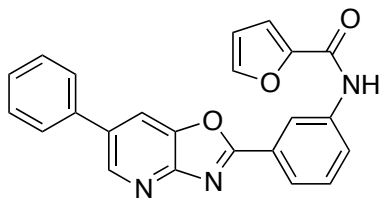

mp > 230 C^{o}, IR $_{vmax}$ (cm^{-1}, solid): 1260, 1649, 3219, ^{1}H NMR ($CDCl_3$): 6.60 (dd, *J* = 3.6, 1.8 Hz, 1H), 7.30 (d, *J* = 7.2 Hz, 1H), 7.44-7.56 (m, 5H), 7.65 (m, 2H), 8.04 (d, *J* = 9 Hz, 2H), 8.10 (d, *J* = 8.1 Hz, 1H), 8.31 (s, 1H), 8.54 (s, 1H), 8.56 (s, 1H); ^{13}C NMR ($CDCl_3$): 113.0, 115.6, 116.1, 116.8, 119.3, 124.0, 124.3,127.4, 127.8, 128.5, 129.5, 129.9, 130.3, 137.9, 138.4, 144.8, 146.3, 147.6, 155.7, 156.4, 165.7; HRMS: M^+ for $C_{23}H_{15}N_3O_3$, predicted 381.1113, found 381.1123, LRMS m/z (EI+): M^+, 382 (66), 404 ([M^+Na]$^+$, (100)].

5.3.26 6-Chlorophenyl-([4,5-*b*]oxazolopyridine-2-yl)-phenyl-2-carboxamide (139)

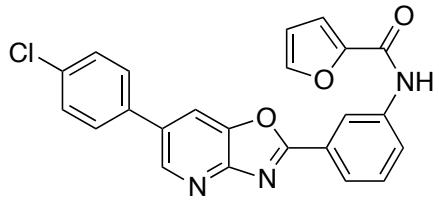

The title compound was prepared according to procedure A6 using using 6-bromo([4,5-*b*]oxazolopyridine-2- yl)-phenyl-2-carboxamide **136** (30 mg, 0.7809 mmol) and (4-chlorophenyl)boronic acid (40 mg, 0.2577 mmol) to offord 6-chlorophenyl-([4,5-*b*]oxazolopyridine-2-yl)-phenyl-2-carboxamide as a pale-yellow solid (22 mg, 69%).

mp > 230 C^{o}, IR $_{vmax}$ (cm^{-1}, solid): 1262, 1650, 3240; ^{1}H NMR (CDCl3): 6.60 (dd, *J* = 5.1, 1.5 Hz, 1H), 7.31 (dd, *J* = 3.3, 0.6 Hz, 1H), 7.60-7.48 (m, 6H), 8.01 (m, 2H), 8.14 (d, *J* = 7.8 Hz, 1H) 8.26 (s, 1H), 8.56 (s, 1H), 8.79 (bs, 1H); HRMS: M^{+}Na for $C_{23}H_{14}ClN_3O_3$, predicted 438.0616, found 438.0623, MS m/z (EI+): 438 (M^{+}Na, 100), 440 (30), 439 (26).

5.3.27 Synthesis of 6-(4-Methoxyphenyl)-([4,5-*b*]oxazolopyridine-2-yl)-phenyl-2-carboxamide (140)

The title compound was prepared according to procedure A6 using **136** (30 mg, 0.0783 mmol) and (4-methoxyphenyl)boronic acid (39 mg, 0.257 mmol) to give the title compound as a pale-yellow solid (11 mg, 33%)

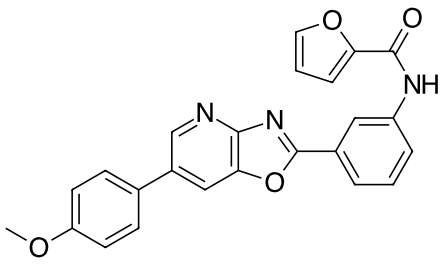

mp > 230 C^{o}, IR $_{vmax}$ (cm^{-1}, solid): 1260, 1649, 3290. ^{1}H NMR ($CDCl_3$): 3.89 (s, 3H), 6.60 (dd, *J* = 3.3,1.8 Hz, 1H), 7.05 (d, *J* = 8.7 Hz, 2H), 7.30 (dd, *J* = 3.6, 0.6 Hz, 1H), 7.56 (m, 5H), 7.98 (d, *J* = 2.0 Hz, 1H), 8.12 (m, 1H), 8.28 (bs, 1H), 8.52 (s, 1H), 8.78 (d, *J* = 2.0 Hz, 1H). ^{13}C NMR ($CDCl_3$): 55.7, 113.0, 114.9, 116.1, 116.3, 119.1, 123.8, 124.3, 127.6, 128.9, 130.3, 134.5, 138.4, 143.4, 144.7, 146.0, 147.6, 155.2, 156.4, 160.1, 165.4HRMS: M^{+} for $C_{17}H_{10}BrN_3O_3$, predicted 412.1292, found 412.1292, LRMS m/z (EI+): [M^{+}, 412 (53), 434 ([M^{+}Na]$^{+}$, 20), 242 (100).

5.3.28 6-(*o*-Aminophenyl-([4,5-*b*]oxazolopyridine-2-yl)-phenyl-2-carboxamide (141)

The titled compound was prepared according to procedure A6 using **136** (40 mg, 0.1028 mmol) and (2-aminophenyl)boronic acid (78 mg, 0.3551 mmol) to afford the crude product which was purified by flash chromatography (silica: eluent 60 % ethyl acetate in hexane) and 6-(o-aminophenyl-([4,5-*b*]oxazolopyridine-2-yl)-phenyl-2-carboxamide was obtained as a an off-white solid (22 mg, 53 %).

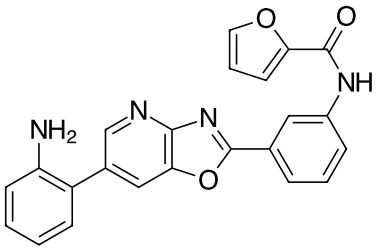

mp > 230 C^{o}, IR $_{vmax}$ (cm^{-1}, solid): 1263, 1654, 2940, 3346, 3415. ^{1}H NMR ($CDCl_3$): 4.00 (bs, 2H), 6.58 (dd, *J* = 3.6, 1.8, 1H), 6.86 (m, 2H), 7.15-7.29 (m, 3H), 7.55 (m, 2H), 7.98-8.11 (m, 3H), 8.30 (s, 1H), 8.50 (s, 1H), 8.66 (s, 1H). ^{13}C NMR (CDCl3): 113.02, 116.058, 116.30, 119.03, 119.26, 119.28, 123.53, 124.02, 124.31, 127.43, 129.80, 130.24, 131.19, 132.79, 138.47, 143.47, 144.21, 144.76, 147.66, 147.78, 155.51, 156.45, 165.72. HRMS: $M^{+}Na$ for $C_{24}H_{17}N_3O_3$, predicted 419.1115, found 419.1125, LRMS m/z (EI+): 419 $[M^{+}Na]^{+}$, (100), 397 $[M+H]^{+}$, (90).

5.3.29 6-Phenyl-([4,5-*b*]oxazolopyridine-2-yl)-phenyl-3-carboxamide (143)

The titled compound was prepared according to procedure A6 using **137** (30 mg, 0.0771 mmol) and phenylboronic acid (37 mg, 0.3083 mmol) to afford the titled compound as a white-off solid (14 mg, 48 %).

mp > 230 C^{o}, IR $_{vmax}$ (cm^{-1}, solid): 1665, 3238, ^{1}H NMR ($CDCl_3$): 6.95 (dd, *J* = 2,4, 0.6 Hz, 1H), 7.22-7.48 (m, 5H), 7.60 (d, *J* = 7.8 Hz,

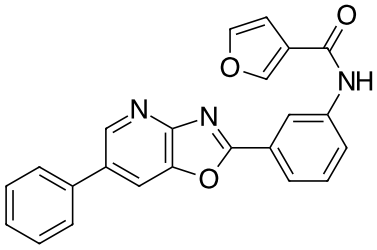

1H), 7.75 (m, 3H), 7.92 (m, 1H), 8.05 (m, 1H), 8.25 (s, 1H), 8.70 (m, 1H), 9.97 (s, 1H);^{13}C NMR ($CDCl_3$): 109.741, 116.93, 119.74, 123.21, 123.43, 124.53, 126.91, 127.66, 127.77, 128.51, 129.55, 129.87, 130.34, 134.076, 134.51, 137.69, 143.78, 143.91, 145.87, 161.44, 165.98. HRMS: M^+ for $C_{23}H_{15}N_3O_3$, predicted 382.1186, found 382.1184 , MS m/z (EI+): 382 ($[M^+H]^+$, 100), 383 (25).

5.3.30 6-(*m*-Methoxyphenyl-([4,5-*b*]oxazolopyridine-2-yl)-phenyl-3-carboxamide (144)

The titled compound was prepared according to procedure A6 using **137** (33 mg, 0.0856 mmol) and (*m*-methoxyphenyl)boronic acid (46 mg, 0.3027 mmol) to afford the titled compound as a pale-yellow solid (23 mg, 60 %).

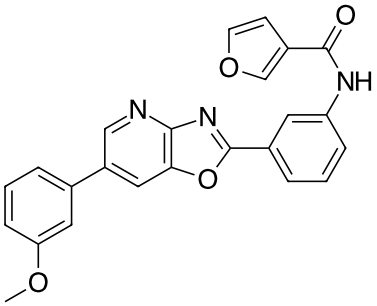

mp > 230 C^o, IR $_{vmax}$ (cm^{-1}, solid): 1260, 1598, 1650, 3284, ^{1}H NMR ($CDCl_3$): 3.88 (s, 3H), 6.83 (s, 1H), 6.99 (d, J = 1.2, 1H), 7.16 (m, 2H), 7.44 (m, 4H), 7.80 (m, 1H) , 8.05 (m, 3H), 8.42 (s, 1H), 8.77 (s, 1H). HRMS: M^+ for $C_{24}H_{17}N_3O_3$, predicted 412.1292, found 412.1300 , LCMS m/z (EI+): 412 (M^+, 100), 413 (30).

5.3.31 6-(*p*-Chlorophenyl-([4,5-*b*]oxazolopyridine-2-yl)-phenyl-3-carboxamide (145)

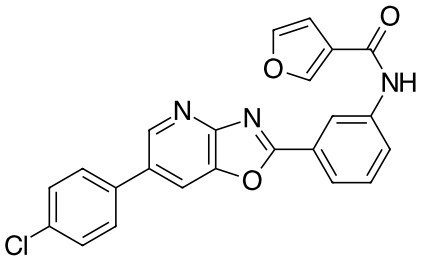

The titled compound was prepared according to procedure A6 using **137** (30 mg, 0.077 mmol) and (*m*-chlorophenyl)boronic acid (42 mg, 0.269 mmol) to afford the title compound as a pale-yellow solid (15 mg, 47 %).

mp > 230 C^{o}, ^{1}H NMR ($CDCl_3$): 6.50 (s, 2H) 7.39 (m, 5H), 7.74 (d, J = 6.3, 2H), (m, 3H), 8.60 (m, 1H), 9.16 (s, 1H). ^{13}C NMR ($CDCl_3$): 109.26, 117.04, 119.87, 123.20, 123.81, 124.88, 126.67, 128.01, 128.04, 128.95, 129.39, 129.71, 130.00, 135.87, 136.64, 136.85, 138.43, 139.68, 143.92, 145.43, 146.02, (one carbon missing or overlapped), HRMS: $M^{+}Na$ for $C_{23}H_{14}ClN_3O_3$, predicted 438.0639, found 438.0636, MS m/z (EI+): 438 ($[M^{+}Na]^{+}$, 100).

CHAPTER 6: References

(1) Ferrins, L.; Rahmani, R.; Sykes, M. L.; Jones, A.; Avery, V. M.; Teston, E.; Almohaywi, B.; Yin, J.; Smith, J.; Hyland, C.; White, K. L.; Ryan, E.; AU - Campbell, M.; Charman, S. A.; Kaiser, M.; Baell, J. B. European journal of medicinal chemistry 2013, 66, 450-465.

(2) Renslo, A. R.; McKerrow, J. H. Nature chemical biology 2006, 2, 701-710.

(3) Balasegaram, M.; Balasegaram, S.; Malvy, D.; Millet, P. PLoS neglected tropical diseases 2008, 2, e234.

(4) Williams, D. A.; Foye, W. O.; Lemke, T. L. *Foye's principles of medicinal chemistry*; Lippincott Williams & Wilkins, 2006.

(5) Bacchi, C. J.; Jacobs, R. T.; Yarlett, N. In *Trypanosomatid Diseases*; Wiley-VCH Verlag GmbH & Co. KGaA: 2013, p 515-529.

(6) Ferrins, L.; Rahmani, R.; Baell, J. B. Future medicinal chemistry 2013, 5, 1801-1841.

(7) Jacobs, T.; Nare, B.; Phillips, A. Current Topics in Med. Chem. 2011, 11, 1255-1274.

(8) Vickerman, K. British Medical Bulletin 1985, 41, 105-114.

(9) Sheader, K.; Vaughan, S.; Minchin, J.; Hughes, K.; Gull, K.; Rudenko, G. Proceedings of the National Academy of Sciences of the United States of America 2005, 102, 8716-8721.

(10) Brun, R.; Blum, J.; Chappuis, F.; Burri, C. The Lancet 2010, 375, 148-159.

(11) Foye, W. O.; Lemke, T. L.; Williams, D. A. *Foye's principles of medicinal chemistry*; Lippincott Williams & Wilkins, 2008.

(12) Jacobs, R. T.; Ding, C. Annu. Reports in Med. Chem. 2010, 45.

(13) Baral, T. N.; Magez, S.; Stijlemans, B.; Conrath, K.; Vanhollebeke, B.; Pays, E.; Muyldermans, S.; De Baetselier, P. Nature medicine 2006, 12, 580-584.

(14) Pearson, R. D.; Hewlett, E. L. Annals of internal medicine 1985, 103, 782-786.

(15) Priotto, G.; Kasparian, S.; Mutombo, W.; Ngouama, D.; Ghorashian, S.; Arnold, U.; Ghabri, S.; Baudin, E.; Buard, V.; Kazadi-Kyanza, S.; Ilunga, M.; Mutangala, W.; Pohlig, G.; Schmid, C.; Karunakara, U.; Torreele, E.; Kande, V. The Lancet 2009, 374, 56-64.

(16) Paliwal, S. K.; Verma, A. N.; Paliwal, S. Scientia pharmaceutica 2011, 79, 389.

(17) Bakunova, S. M.; Bakunov, S. A.; Patrick, D. A.; Kumar, E. S.; Ohemeng, K. A.; Bridges, A. S.; Wenzler, T.; Barszcz, T.; Kilgore Jones, S.; Werbovetz, K. A. Journal of medicinal chemistry 2009, 52, 2016-2035.

(18) Donkor, I. O.; Huang, T. L.; Tao, B.; Rattendi, D.; Lane, S.; Vargas, M.; Goldberg, B.; Bacchi, C. Journal of Medicinal Chemistry 2003, 46, 1041-1048.

(19) Bakunova, S. M.; Bakunov, S. A.; Wenzler, T.; Barszcz, T.; Werbovetz, K. A.; Brun, R.; Tidwell, R. R. Journal of medicinal chemistry 2009, 52, 4657-4667.

(20) Paine, M. F.; Wang, M. Z.; Generaux, C. N.; Boykin, D. W.; Wilson, W. D.; De Koning, H. P.; Olson, C. A.; Pohlig, G.; Burri, C.; Brun, R. Current opinion in investigational drugs (London, England: 2000) 2010, 11, 876-883.

(21) Meanwell, N. Journal of Medicinal Chemistry 2011, 54, 2529-2591.

(22) Wenzler, T.; Boykin, D. W.; Ismail, M. A.; Hall, J. E.; Tidwell, R. R.; Brun, R. Antimicrob. agents and chemotherap. 2009, 53, 4185-4192.

(23) Gonzalez, J. L.; Stephens, C. E.; Wenzler, T.; Brun, R.; Tanious, F. A.; Wilson, W. D.; Barszcz, T.; Werbovetz, K. A.; Boykin, D. W. European journal of medicinal chemistry 2007, 42, 552-557.

(24) Patrick, D. A.; Bakunov, S. A.; Bakunova, S. M.; Kumar, E. S.; Lombardy, R. J.; Jones, S. K.; Bridges, A. S.; Zhirnov, O.; Hall, J. E.; Wenzler, T. Journal of medicinal chemistry 2007, 50, 2468-2485.

(25) Bakunov, S. A.; Bakunova, S. M.; Wenzler, T.; Ghebru, M.; Werbovetz, K. A.; Brun, R.; Tidwell, R. R. Journal of medicinal chemistry 2009, 53, 254-272.

(26) Gillingwater, K.; Kumar, A.; Anbazhagan, M.; Boykin, D. W.; Tidwell, R. R.; Brun, R. Antimicrobial agents and chemotherapy 2009, 53, 5074-5079.

(27) Patrick, D. A.; Bakunov, S. A.; Bakunova, S. M.; Jones, S. K.; Wenzler, T.; Barszcz, T.; Kumar, A.; Boykin, D. W.; Werbovetz, K. A.; Brun, R. European journal of medicinal chemistry 2013, 67, 310-324.

(28) Wilkinson, S. R.; Bot, C.; Kelly, J. M.; Hall, B. S. Current topics in medicinal chemistry 2011, 11, 2072-2084.

(29) Bot, C.; Hall, B. S.; Alvarez, G.; Di Maio, R.; Gonzalez, M.; Cerecetto, H.; Wilkinson, S. R. Antimicrobial agents and chemotherapy 2013, 57, 1638-1647.

(30) Torreele, E.; Trunz, B. B.; Tweats, D.; Kaiser, M.; Brun, R.; Mazue, G.; Bray, M. A.; Pecoul, B. PLoS neglected tropical diseases 2010, 4, e923.

(31) DNDi In

(32) Sokolova, A. Y.; Wyllie, S.; Patterson, S.; Oza, S. L.; Read, K. D.; Fairlamb, A. H. Antimicrobial agents and chemotherapy 2010, 54, 2893-2900.

(33) Trunz, B. B.; Jedrysiak, R.; Tweats, D.; Brun, R.; Kaiser, M.; Suwinski, J.; Torreele, E. European journal of medicinal chemistry 2011, 46, 1524-1535.

(34) Hwang, J. Y.; Smithson, D.; Connelly, M.; Maier, J.; Zhu, F.; Guy, K. R. Bioorganic & medicinal chemistry letters 2010, 20, 149-152.

(35) Ding, D.; Zhao, Y.; Meng, Q.; Xie, D.; Nare, B.; Chen, D.; Bacchi, C. J.; Yarlett, N.; Zhang, Y.-K.; Hernandez, V.; Xia, Y.; Freund, Y.; Abdulla, M.; Ang, K.-H.; Ratnam, J.; McKerrow, J. H.; Jacobs, R. T.; Zhou, H.; Plattner, J. J. ACS Medicinal Chemistry Letters 2010, 1, 165-169.

(36) Jacobs, R. T.; Plattner, J. J.; Nare, B.; Wring, S. A.; Chen, D.; Freund, Y.; Gaukel, E. G.; Orr, M. D.; Perales, J. B.; Jenks, M.; Noe, R. A.; Sligar, J. M.; Zhang, Y. K.; Bacchi, C. J.; Yarlett, N.; Don, R. Future medicinal chemistry 2011, 3, 1259-1278.

(37) Nare, B.; Wring, S.; Bacchi, C.; Beaudet, B.; Bowling, T.; Brun, R.; Chen, D.; Ding, C.; Freund, Y.; Gaukel, E.; Hussain, A.; Jarnagin, K.; Jenks, M.; Kaiser, M.; Mercer, L.; Mejia, E.; Noe, A.; Orr, M.; Parham, R.; Plattner, J.; Randolph, R.; Rattendi, D.; Rewerts, C.; Sligar, J.; Yarlett, N.; Don, R.; Jacobs, R. Antimicrobial agents and chemotherapy 2010, 54, 4379-4388.

(38) Jacobs, R. T.; Nare, B.; Wring, S. A.; Orr, M. D.; Chen, D.; Sligar, J. M.; Jenks, M. X.; Noe, R. A.; Bowling, T. S.; Mercer, L. T. PLoS neglected tropical diseases 2011, 5, e1151.

(39) Hoet, S.; Opperdoes, F.; Brunc, R.; Quetin-Leclercq, J. The Royal Society of Chemistry 2004, 21, 353-364.

(40) Barker, R. H., Jr.; Liu, H.; Hirth, B.; Celatka, C. A.; Fitzpatrick, R.; Xiang, Y.; Willert, E. K.; Phillips, M. A.; Kaiser, M.; Bacchi, C. J.; Rodriguez, A.; Yarlett, N.; Klinger, J. D.; Sybertz, E. Antimicrobial agents and chemotherapy 2009, 53, 2052-2058.

(41) Deterding, A.; Dungey, F. A.; Thompson, K. A.; Steverding, D. Acta tropica 2005, 93, 311-316.

(42) Verlinde, C. L. M. J.; Hannaert, V. r.; Blonski, C.; Willson, M. l.; P√©ri√©, J. J.; Fothergill-Gilmore, L. A.; Opperdoes, F. R.; Gelb, M. H.; Hol, W. G. J.; Michels, P. A. M. Drug Resistance Updates 2001, 4, 50-65.

(43) Willson, M.; Lauth, N.; Perie, J.; Callens, M.; Opperdoes, F. R. Biochem. 1994, 33, 214-220.

(44) Lauth, N.; Alric, I.; Willson, M.; Perie, J. Phosphorus, Sulfur, and Silicon and the Related Elements 1993, 76, 155-158.

(45) Dardonville, C.; Rinaldi, E.; Barrett, M. P.; Brun, R.; Gilbert, I. H.; Hanau, S. Journal of medicinal chemistry 2004, 47, 3427-3437.

(46) Ruda, G. F.; Alibu, V. P.; Mitsos, C.; Bidet, O.; Kaiser, M.; Brun, R.; Barrett, M. P.; Gilbert, I. H. ChemMedChem 2007, 2, 1169-1180.

(47) Ruda, G. F.; Wong, P. E.; Alibu, V. P.; Norval, S.; Read, K. D.; Barrett, M. P.; Gilbert, I. H. J Med Chem 2010, 53, 6071-6078.

(48) Wierenga, R. K.; Swinkels, B.; Michels, P. A.; K Osinga, O. M.; J Van Beeumen, W. C. G.; J P Postma, P. B.; Opperdoes, F. R. EMBO J. 1987, 6, 215-221.

(49) Willson, M. l.; Callens, M.; Kuntz, D. A.; Perie, J.; Opperdoes, F. R. Molecular and Biochemical Parasitology 1993, 59, 201-210.

(50) Nowicki, M. W.; Tulloch, L. B.; Worralll, L.; McNae, I. W.; Hannaert, V.; Michels, P. A.; Fothergill-Gilmore, L. A.; Walkinshaw, M. D.; Turner, N. J. Bioorg Med Chem 2008, 16, 5050-5061.

(51) Vodnala, S. K.; Ferella, M.; Lunden-Miguel, H.; Betha, E.; van Reet, N.; Amin, D. N.; Oberg, B.; Andersson, B.; Kristensson, K.; Wigzell, H.; Rottenberg, M. E. PLoS neglected tropical diseases 2009, 3, e495.

(52) Ojo, K. K.; Gillespie, J. R.; Riechers, A. J.; Napuli, A. J.; Verlinde, C. L.; Buckner, F. S.; Gelb, M. H.; Domostoj, M. M.; Wells, S. J.; Scheer, A. Antimicrobial agents and chemotherapy 2008, 52, 3710-3717.

(53) Patel, G.; Karver, C. E.; Behera, R.; Guyett, P. J.; Sullenberger, C.; Edwards, P.; Roncal, N. E.; Mensa-Wilmot, K.; Pollastri, M. P. J Med Chem 2013, 56, 3820-3832.

(54) Sykes, M. L.; Baell, J. B.; Kaiser, M.; Chatelain, E.; Moawad, S. R.; Ganame, D.; Ioset, J. R.; Avery, V. M. PLoS neglected tropical diseases 2012, 6, e1896.

(55) Bemis, J. E.; Vu, C. B.; Xie, R.; Nunes, J. J.; Ng, P. Y.; Disch, J. S.; Milne, J. C.; Carney, D. P.; Lynch, A. V.; Jin, L. Bioorg. & med. chem. lett. 2009, 19, 2350-2353.

(56) Zheng, W. European journal of medicinal chemistry 2013, 59, 132-140.

(57) Garcia-Salcedo, J. A.; Gijun, P.; Nolan, D. P.; Tebabi, P.; Pays, E. The EMBO Journal 2003, 22, 5851-5862.

(58) Clark, R. L.; Pessolano, A. A.; Witzel, B.; Lanza, T.; Shen, T.; Van Arman, C. G.; Risley, E. A. Journal of Medicinal Chemistry 1978, 21, 1158-1162.

(59) Yalcin, I.; Oren, I.; Sener, E.; Akin, A.; Ucarturk, N. European journal of medicinal chemistry 1992, 27, 401-406.

(60) Yalcin, I.; Sener, E. International journal of pharmaceutics 1993, 98, 1-8.

(61) Sener, E.; Yalcin, I.; Sungur, E. Quantitative Structure Activity Relationships 1991, 10, 223-228.

(62) Jauhari, P.; Bhavani, A.; Varalwar, S.; Singhal, K.; Raj, P. Medicinal Chemistry Research 2008, 17, 412-424.

(63) Heuser, S.; Keenan, M.; Weichert, A. G. ChemInform 2006, 37.

(64) Townsend, L. B.; Wise, D. S. Parasitology Today 1990, 6, 107-112.

(65) Keurulainen, L.; Salin, O.; Siiskonen, A.; Kern, J. M.; Alvesalo, J.; Kiuru, P.; Maass, M.; Yli-Kauhaluoma, J.; Vuorela, P. Journal of Medicinal Chemistry 2010, 53, 7664-7674.

(66) Barni, E.; Pasquino, S.; Savarino, P.; Di Modica, G.; Giraudo, G. Dyes and Pigments 1985, 6, 1-12.

(67) Barni, E.; Pasquino, S.; Savarino, P.; Di Modica, G.; Giraudo, G. Dyes and Pigments 1985, 6, 1-12.

(68) Grumel, V.; M√©rour, J. Y.; Guillaumet, G. Heterocycles 2001, 55, 1329-1345.

(69) Eaton, P. E.; Carlson, G. R.; Lee, J. T. The Journal of Organic Chemistry 1973, 38, 4071-4073.

(70) Nunes, J., J.; Milne, J.; Bemis, J.; Xie, R.; Vu, C., B.; Ng, P., Yee; Disch, J. Benzimidazole Derivatives as Sirtuin Modulators 2007

(71) Mobinikhaledi, A.; Forughifar, N.; Shariatzadeh, S.; Fallah, M. Heterocyclic Communications 2006, 12, 427-430.

(72) Büttner, A.; Seifert, K.; Cottin, T.; Sarli, V.; Tzagkaroulaki, L.; Scholz, S.; Giannis, A. Bioorganic & Medicinal Chemistry 2009, 17, 4943-4954.

(73) Myllymaki, M. J.; Koskinen, A. M. P. Tetrahedron Letters 2007, 48, 2295-2298.

(74) Savarino, P.; Viscardi, G.; Barni, E.; Carpignano, R. Dyes and Pigments 1988, 9, 295-304.

(75) Vo, G. D.; Hartwig, J. F. Journal of the American Chemical Society 2009, 131, 11049-11061.

(76) O,Donnell, C. J.; Rogers, B. N.; Bronk, B. S.; Bryce, D. K.; Coe, J. W.; Cook, K. K.; Duplantier, A. J.; Evrard, E.; HajoÃÅs, M.; Hoffmann, W. E.; Hurst, R. S.; Maklad, N.; Mather, R. J.; McLean, S.; Nedza, F. M.; O,ÄôNeill, B. T.; Peng, L.; Qian, W.; Rottas, M. M.; Sands, S. B.; Schmidt, A. W.; Shrikhande, A. V.; Spracklin, D. K.; Wong, D. F.; Zhang, A.; Zhang, L. Journal of Medicinal Chemistry 2009, 53, 1222-1237.

(77) Mac, M.; Baran, W.; Uchacz, T.; Baran, B.; Suder, M.; Leoniewski, S. Journal of Photochemistry and Photobiology A: Chemistry 2007, 192, 188-196.

(78) Schareina, T.; Zapf, A.; Beller, M. Journal of Organometallic Chemistry 2004, 689, 4576-4583.

(79) Viaud, M. C.; Jamoneau, P.; Savelon, L.; Guillaumet, G. ChemInform 1995, 27, no-no.

(80) Daines, R. A.; Price, A. T. Preparation of quinoline, quinoxaline and naphthyridine derivatives as antibacterial agents WO2007016610A2, Glaxo Group Limited, UK . 2007

(81) Flouzat, C.; Bresson, Y.; Mattio, A.; Bonnet, J.; Guillaumet, G. Journal of Medicinal Chemistry 1993, 36, 497-503.

(82) Alt, K. O.; Christen, E.; Weis, C. D. Journal of Heterocyclic Chemistry 1975, 12, 775-778.

(83) Paushkin, S. V.; Naryshkin, N.; Welch, E.; Romfo, C. Treatment of spinal muscular atrophy by modifying splicing patterns of SMN2 mRNA WO2009151546A2, PTC Therapeutics, Inc., USA . 2009

(84) Tamagnan, G. D.; Alagille, D.; Da Costa, H. Preparation of amyloid binding compounds for therapeutic and imaging uses US20070258887A1, Molecular Neuroimaging, LLC, USA . 2007

(85) Wilde, R.; Welch, E.; Karp, G. M. Preparation of benzoxazoles for nonsense suppression WO2006044503A2, PTC Therapeutics, Inc., USA . 2006

(86) Yoon, N. M.; Gyoung, Y. S. The Journal of Organic Chemistry 1985, 50, 2443-2450.

(87) Kalgutkar, A. S.; Gardner, I.; Obach, R. S.; Shaffer, C. L.; Callegari, E.; Henne, K. R.; Mutlib, A. E.; Dalvie, D. K.; Lee, J. S.; Nakai, Y.; O'Donnell, J. P.; Boer, J.; Harriman, S. P. Current drug metabolism 2005, 6, 161-225.

(88) Tatipaka, H.; Gillespie, J. R.; Chatterjee, A. K.; Norcross, N. R.; Hulverson, M. A.; Ranade, R. M.; Nagendar, P.; Creason, S. A.; McQueen, J.; Duster, N. A.; Nagle, A.; Supek, F.; Molteni, V.; Wenzler, T.; Brun, R.; Glynne, R.; Buckner, F. S.; Gelb, M. H. Journal of Medicinal Chemistry 2013.

(89) Lima, L. M.; Barreiro, E. J. Current medicinal chemistry 2005, 12, 23-49.

(90) Gagnon, A.; Duplessis, M.; Alsabeh, P.; Barabé, F. The Journal of Organic Chemistry 2008, 73, 3604-3607.

(91) Wallace, D. J.; Chen, C.-y. Tetrahedron Letters 2002, 43, 6987-6990.

(92) Clayden, J.; Greeves, N.; Wareen, S.; Wothers, P. *ORGANIC CHEMISTRY* OUP Oxford 2000.

(93) Paul, F.; Patt, J.; Hartwig, J. F. Journal of the American Chemical Society 1994, 116, 5969-5970.

(94) O'Donnell, C. J. Journal of Medicinal Chemistry 2009, 53, 1222-1237.

(95) Jakszyn, P.; Agudo, A.; Ibanez, R.; Garcia-Closas, R.; Pera, G.; Amiano, P.; Gonzalez, C. A. The Journal of nutrition 2004, 134, 2011-2014.

(96) Pais, P.; Tanga, M. J.; Salmon, C. P.; Knize, M. G. Journal of agricultural and food chemistry 2000, 48, 1721-1726.

(97) Nguyen, T. M.; Novak, M. The Journal of organic chemistry 2007, 72, 4698-4706.

(98) Sugimura, T.; Wakabayashi, K.; Nakagama, H.; Nagao, M. Cancer science 2004, 95, 290-299.

(99) Turesky, R. J.; Le Marchand, L. Chemical research in toxicology 2011, 24, 1169-1214.

(100) Walters, D. G.; Young, P. J.; Agus, C.; Knize, M. G.; Boobis, A. R.; Gooderham, N. J.; Lake, B. G. Carcinogenesis 2004, 25, 1659-1669.

(101) Sugimura, T.; Wakabayashi, K.; Nakagama, H.; Nagao, M. Cancer Science 2004, 95, 290-299.

(102) Collins, C. J.; Bupp, J. E.; Tanga, M. J. Archive for orgnaic chemistry 2002, 2002, 90-96.

(103) Garrett, R.; Grisham, C. M. *Biochemistry* Granite Hill Publishers, 1995.

(104) Burma, S.; Chen, B. P.; Murphy, M.; Kurimasa, A.; Chen, D. J. Journal of Biological Chemistry 2001, 276, 42462-42467.

(105) Muslimovic, A.; Johansson, P.; Hammarsten, O. Current Topics in Ionizing Radiation Research. Rijeka: InTech 2012, 3-20.

(106) Foster, F. M.; Colin J. Traer; Abraham, S. M.; J., M. Journal of Cell Science 116, 3037-3040.

(107) Paull, T. T.; Rogakou, E. P.; Yamazaki, V.; Kirchgessner, C. U.; Gellert, M.; Bonner, W. M. Current Biology 2000, 10, 886-895.

(108) Liu, P.; Cheng, H.; Roberts, T. M.; Zhao, J. J. Nature reviews Drug discovery 2009, 8, 627-644.

(109) Still, W. C.; Kahn, M.; Mitra, A. The Journal of Organic Chemistry 1978, 43, 2923-2925.

(110) Flouzat, C.; Bresson, Y.; Mattio, A.; Bonnet, J.; Guillaumet, G. Journal of medicinal chemistry 1993, 36, 497-503.